Thesis

Electronic Structure and Chemical Properties of Endohedral Metallofullerenes

Shingo Okubo

Doctor of Philosophy

Department of Functional Molecular Science
School of Mathematical and Physical Science
The Graduate University for Advanced Studies

2002

Contents

Chapter 1
General introduction

1. 1. Endohedral Metallofullerenes

An endohedralmetallofullerene,a fullerene with a metal atom or atoms inside, is one of the most interesting molecules, which has novel chemical and physical properties.[1-3] There are a lot of reports, reviews, and books about this kind of molecules.[4-7] Now many attractive studies are in progress. The characteristic of the endohedral metallofullerene is that a reactive metal atom is protected by the carbon cage from the surrounding media. And the intra-molecular charge transfer form the internal metal atom to the carbon cage plays an important role to stabilize the metallofullerene molecule. Such a charge separated geometrical structure is analogous to a "super atom". The nature of the super atom can be chemically tuned by the combination of the metal with the fullerene cage. The enormous variety can be expected in terms of the central metal and of the fullerene cage.

1. 2. Production, extraction and isolation of endohedral metallofullerenes

Some endohedral metallofullerenes were soluble in organic solvents such as toluene, carbon disulfide (CS_2), and chlorinated benzenes. The soluble character of endohedral fullerenes makes the further investigations such as isolation or chemical experiments possible. For example, La@C_{82} is the first isolated endohedral fullerene, for which subsequent interests were mainly paid for this molecule.[8,9] Up to now, colored elements indicated in table 1-1 were encapsulated in the fullerene cage: Endohedral fullerenes of group 1 and group 15 were produced by the impact of ion beam to C_{60},[10-13] those of group 2, 3, and 4 were obtained by arc discharge or a laser ablation of a metal-carbon composite rod,[2,14] and those of group 18 were synthesized by the penetration of noble gas to C_{60} under high temperature - high pressure.[15] Extraction of endohedral metallofullerenes was mainly performed by the wet method, such as a soxlet extraction or refluxing with organic solvent. Solvents of toluene, CS_2, or chlorinated benzenes are used to the extraction of endohedral metallofullerenes.[16-18] The extraction yield of fullerenes and metallofullerenes depends on the solubility of these molecules.[19-21] High

efficiency of extraction under the anaerobic (oxygen free) or high pressure - high temperature method is known.[16,22-24] On the other hand, the large enhancement of metallofullerenes was given by extraction with pyridine and DMF (Dimethylformamide).[25-27] Especially aniline was only a solvent to extract metal-endohedral C_{60}.[25,26,28-31] Although the special ability in extraction of these solvents has been known from the early stage of metallofullerene study, there were no reports to explain a selective enrichment behavior of these solvents. A sublimation technique was also applied to extraction for the metallofullerene, which could not be extracted by solvents.[32,33]

Periodic table April. 2001.

	1	2	3	4	5	6	7	8	9	10	11	12	13	14	15	16	17	18
1	$_{1}$H																	$_{2}$He
2	$_{3}$Li	$_{4}$Be											$_{5}$B	$_{6}$C	$_{7}$N	$_{8}$O	$_{9}$F	$_{10}$Ne
3	$_{11}$Na	$_{12}$Mg											$_{13}$Al	$_{14}$Si	$_{15}$P	$_{16}$S	$_{17}$Cl	$_{18}$Ar
4	$_{19}$K	$_{20}$Ca	$_{21}$Sc	$_{22}$Ti	$_{23}$V	$_{24}$Cr	$_{25}$Mn	$_{26}$Fe	$_{27}$Co	$_{28}$Ni	$_{29}$Cu	$_{30}$Zn	$_{31}$Ga	$_{32}$Ge	$_{33}$As	$_{34}$Se	$_{35}$Br	$_{36}$Kr
5	$_{37}$Rb	$_{38}$Sr	$_{39}$Y	$_{40}$Zr	$_{41}$Nb	$_{42}$Mo	$_{43}$Tc	$_{44}$Ru	$_{45}$Rh	$_{46}$Pd	$_{47}$Ag	$_{48}$Cd	$_{49}$In	$_{50}$Sn	$_{51}$Sb	$_{52}$Te	$_{53}$I	$_{54}$Xe
6	$_{55}$Cs	$_{56}$Ba	57-71	$_{72}$Hf	$_{73}$Ta	$_{74}$W	$_{75}$Re	$_{76}$Os	$_{77}$Ir	$_{78}$Pt	$_{79}$Au	$_{80}$Hg	$_{81}$Tl	$_{82}$Pb	$_{83}$Bi	$_{84}$Po	$_{85}$At	$_{86}$Rn
7	$_{87}$Fr	$_{88}$Ra	89-103															

Lanthanoides	$_{57}$La	$_{58}$Ce	$_{59}$Pr	$_{60}$Nd	$_{61}$Pm	$_{62}$Sm	$_{63}$Eu	$_{64}$Gd	$_{65}$Tb	$_{66}$Dy	$_{67}$Ho	$_{68}$Er	$_{69}$Tm	$_{70}$Yb	$_{71}$Lu
Actinoides	$_{89}$Ac	$_{90}$Th	$_{91}$Pa	$_{92}$U	$_{93}$Np	$_{94}$Pu	$_{95}$Am	$_{96}$Cm	$_{97}$Bk	$_{98}$Cf	$_{99}$Es	$_{100}$Fm	$_{101}$Md	$_{102}$No	$_{103}$Lr

Table 1-1. Periodic table for Endohedral Fullerenes

The separation and the purification of endohedral fullerenes were performed by using the High-Performance Liquid Chromatography (HPLC) technique.[34-39] The parallel use of more than one type of column (two- or multi-stage method) and the peak-recycling technique were needed for the high purity. Table 1-2 shows the list of isolated endohedral metallofullerenes to date. The notation of I, II, III, etc. indicates the structural isomers.[40,41] This table is categorized by the number of encapsulated atoms, and clusters, such as Sc_3N and Sc_2C_2. Mono-metallo endohedrals are further categorized by the preferable oxidation state of encapsulated metal. Group 2 elements (Ca, Sr and Ba) and some lanthanoid (Sm, Eu, Tm, Yb) endohedrals prefer the

electronic structure of $M^{2+}@C_n^{2-}$.[42,43] Sc, Y, La and lanthanoid (Ce, Pr, Nd, may be Pm, Gd, Tb, Dy, Ho, Er and Lu) endohedrals prefer the electronic structure of $M^{3+}@C_n^{3-}$.[44,45] Hf and Ti were two of the transition metal encapsulated in fullerene cage, and it was suggested by the analysis of HPLC retention behavior that $Hf@C_{84}$ exhibited the electronic state of $Hf^{4+}@C_{84}^{4-}$. However, further confirmation should be needed. [46-48] For the case of "+3 type" metallofullerenes, isolation of mono-metallo-C_{82} is mainly reported to date. The reason is their exceptional stability and large content of $M@C_{82}$ in the soot extract.

Table 1-2. Isolated endohedral metallofullerenes

mono-metallo- +2 type	mono-metallo- +3 type	di-metallo-	tri-metallo-	cluster endohedrals
$Ca@C_{72}$[49]	$La@C_{82}$(I, II)[9,41]	$La_2@C_{80}$[50]	$Sc_3@C_{82}$[51]	$Sc_3N@C_{80}$[52]
$Ca@C_{74}$[49]	$La@C_{90}$(I-IV)[53]	$La_2@C_{72}$[54]	$Er_3@C_{74}$[55]	$Sc_3N@C_{68}$[56]
$Ca@C_{82}$(I-IV)[57]	$La@C_{86}$	$Sc_2@C_{74}$[58]		$Sc_3N@C_{78}$[59]
$Ca@C_{84}$(I, II)[57]	$Y@C_{82}$(I, II)[60]	$Sc_2@C_{76}$[58]		$Sc_2C_2@C_{84}$[61]
$Ca@C_{80}$[62]	$Sc@C_{82}$(I, II)[63]	$Sc_2@C_{82}$[58,64]		
$Sr@C_{82}$[42,65]	$Sc@C_{84}$[63]	$Sc_2@C_{84}$(I-III)[66]		
$Sr@C_{84}$[42,65]	$Ce@C_{82}$[67]	$Sc_2@C_{86}$(I, II)[64]		
$Sr@C_{80}$[62]	$Pr@C_{82}$ (I, II)[68,69]	$Y_2@C_{90}$[70]		
$Ba@C_{82}$[42,65]	$Nd@C_{82}$[71]	$Gd_2@C_{90}$[70]		
$Ba@C_{84}$[42,65]	$Gd@C_{82}$[72]	$Ce_2@C_{80}$[73]		
$Ba@C_{80}$[42]	$Tb@C_{82}$[74]	$Pr_2@C_{80}$[68]		
$Eu@C_{74}$[75]	$Dy@C_{82}$ (I, II)[76]	$Er_2@C_{82}$(I-III)[77,78]		
$Sm@C_{74}$[43]	$Ho@C_{82}$[44]	$Er_2@C_{84}$(I-III)[78]		
$Sm@C_{76}$ (I, II)[43]	$Er@C_{82}$ (I, II)[78]	$Er_2@C_{86}$(I-III)[55]		
$Sm@C_{78}$[43]	$Lu@C_{82}$[79]	$Er_2@C_{88}$(I-III)[55]		
$Sm@C_{80}$[43]	$Er@C_{84}$(I-III)[55]	$Er_2@C_{90}$(I-III)[55]		
$Sm@C_{82}$ (I-III)[43]	$Er@C_{86}$(I, II)[55]	$Er_2@C_{92}$(I-IV)[55]		
$Sm@C_{84}$ (I-III)[43]		$Er_2@C_{94}$(I, II)[55]		
$Tm@C_{82}$(I-III)[80]	$U@C_{82}$[81]	$Dy_2@C_{80}$[76]		
$Eu@C_{82}$[82]		$Dy_2@C_{82}$[76]		
$Yb@C_{82}$[82]		$Dy_2@C_{84}$(I-III)[76]		
		$Dy_2@C_{86}$(I, II)[76]		
$Eu@C_{60}$[83]	$Er@C_{60}$[84]	$Dy_2@C_{88}$(I, II)[76]		
		$Dy_2@C_{90}$(I-III)[76]		
		$Dy_2@C_{92}$(I-III)[76]		
		$Dy_2@C_{94}$(I, II)[76]		
		$Sc_2@C_{66}$[85]		
		$HoTm@C_{82}$(I-III)[86]		
	$Hf@C_{84}$[46]	$Ti_2@C_{80}$[47]		
		$Hf_2@C_{80}$[46]		

1. 3. Characterization of endohedral metallofullerenes

There are a lot of reports of the characterization of endohedral fullerenes. The main interests have been focused on the electronic and the geometrical structure of these molecules. The ESR spectroscopy was firstly applied to confirm the evidence of La@C_{82},[3,49] and then Sc@C_{82}, Y@C_{82}[50] and Sc_3@C_{82},[51] because of their paramagnetic nature. Its high sensitivity and high selectivity to paramagnetic species was useful to confirm the presence of the isomers of M_x@C_n (M= Sc, Y, and La, X= odd number).[16,52-59] On the other hand, the spectroscopic use of ESR revealed the electronic structure and the rotational dynamics of these molecules in solution.[60-73] The electronic structure of Y@C_{82} and La@C_{82} were suggested to be M^{3+}@C_{82}^{3-}, but there has been controversy as to whether Sc@C_{82} has a +2 or +3 charged state. The first report of the temperature dependent ESR study suggested the electronic structure of Sc^{2+}@C_{82}^{2-} because of about one order of magnitude larger hyperfine anisotropy than that of La@C_{82}.[60] However, different conclusion, the charge state of Sc^{3+}, was suggested from the analysis of quadrupole interaction for La@C_{82} and Sc@C_{82}.[62] The vibrational spectroscopy gave the information, such as carbon-carbon and metal-carbon vibrations. Similar vibrational structure of M@C_{82} (M=Y, La, Ce and Gd) was observed in IR and the Raman spectra.[8,74] The vibrational structures of Tm@C_{82} and Sc_2@C_{84} isomers were also discussed.[75,76] The high-energy spectroscopy, such as XPS (X-ray Photoelectron Spectroscopy), UPS (Ultraviolet Photoelectron Spectroscopy),[77-83] EXAFS (Extended X-ray Absorption Fine Structure),[84-86] EELS (Electron Energy Loss Spectroscopy),[47,87-90] gave the valuable information about the electronic environment of encapsulated metal atom(s).[91-93] The X-ray powder diffraction with the MEM-Reitvelt analysis gave the first evidence of the endohedral nature of an yttrium atom within a C_{82}, and this technique also proved the molecular structure of some endohedral fullerenes.[94-100] Theoretical calculations played an important role to predict the structure of endohedral metallofullerenes, because of experimental difficulties.[6,101-108] Recent calculations of M@C_{82},[109-114] M_2@C_{80},[115-117] and M_2@C_{84}[118-120] were in good agreement with the experimental results, but some disagreements still remain.[121] The chemical properties of endohedral fullerenes were also reported.[89,122-130] Difference of the chemical reactivity of endohedral fullerenes to that of hollow fullerenes was discussed with electrochemical investigations.[131,132] Nuclear magnetic

resonance (NMR) spectroscopy was applied to various endohedral fullerenes, such as $La_2@C_{80}$, $Sc_2@C_{84}$, $Sc_2C_2@C_{84}$, $Sc_2@C_{66}$, $Sc_3N@C_{80}$, $Sc_3N@C_{68}$, $Ca@C_{82}$, and $Tm@C_{82}$. ^{13}C- or multinuclear NMR revealed the symmetry of their cage and internal dynamics of endohedral atom(s).[133-142]An interesting case is $La@C_{82}$. [141,142] Ordinary, ^{13}C-NMR could not be applied because of its paramagnetic electronic structure of C_{82} cage. However ^{13}C- and ^{139}La-NMR were succeeded when $La@C_{82}$ mono-anion was prepared by electrochemical reduction, and the cage structures of C_{2v} symmetry and that of C_s were determined for the major and the minor isomer of $La@C_{82}$. Determination of the structures of fullerenes and endohedral fullerenes is one of the key information to understand the formation mechanism of these molecules. Early gas phase experiments have indicated the presence of numbers of metal-carbon clusters in vacuum.[143-149] But selected species were obtained in the soot extract. The isolated pentagon rule (IPR), a five-membered ring should be surrounded by five six-membered rings, is one of the most useful selection rules for considering the structure of fullerenes and endohedral fullerenes.[40] The numbers and intensities of ^{13}C-NMR lines for possible IPR isomers of C_n were summarized and this rule worked very well for hollow fullerenes.[150-153] For metallofullerenes, x-ray diffraction[96,98] and ^{13}C-NMR[141] study reported the C_{2v} symmetry of major isomer of $Sc@C_{82}$ and $La@C_{82}$, and C_s symmetry of the minor isomer of $La@C_{82}$.[142] These cage structures are different from most abundantly produced hollow C_{82} with C_2 symmetry.[152] Metallofullerenes with the cage size of 66 or 68 were reported as the non-IPR structure, which were proved by X-ray and ^{13}C-NMR measurements.[136,139] The electron transfer from metals to carbon cage gave an important factor for the stabilization of non-IPR fullerene cage. The reports of non-IPR fullerene cage with the endohedral metal might give a hint to understand the formation mechanism of fullerenes and metallofullerene. The formation mechanisms of fullerenes named “pentagon road”, model,[154] or the “ring stacking” model were proposed.[155,156] The suggestion of the C_{60} as a seed of $La@C_{82}$ was reported.[157] Another formation mechanism based on the reorientation of C-C bonds, called Stone-Wales transformation was proposed. The molecular dynamics simulation showed the formation of IPR-C_{60} structure from non-IPR C_{60} by annealing process.[158]

1. 4. Remained and newly subjected problems of metallofullerenes

Up to now, many kind of metallofullerene sample can be obtained in pure form by the conventional production and isolation protocol. And the methodology of the characterization has also been established. However, we can point out some unknown problems. The mono-metal endohedral fullerenes, M@C_n (n = even number) is a prototype for the investigation of interactions between internal metal atom and surrounding fullerene cage. And the systematic characterization of M@C_n will give the crucial information not only for understanding the remained questions to date but also for further investigations. Metallofullerenes with +3 type metal inside were the most frequently investigated species. And the preparation of few milligram of pure M@C_{82} is not so difficult to date. The property of M@C_{82} with respect to the internal atom was discussed in terms of the endohedral tuning of super atom. On the other hand, the discussion of the dependence on the cage structure is of a great interest in terms of framework tuning, however, this kind of research work has not been done for +3 type metallofullerenes. [43,64,90,159-161] Although the metallofullerenes with various size of the cage exist in an arc-burned soot, the number of available species is limited because of the difficulty in further treatment, such as the extraction and the purification processes.

In the extraction process, which is the first step treatment, the selection of the extraction solvent directly influences on the extraction yield of fullerenes and metallofullerenes. Solvents of CS_2 and chlorinated benzenes are favored for the extraction of fullerenes and metallofullerenes because of their large solubility. [16,18,52] In the soot extract by using these solvents, M@C_{82} is the most abundant metallofullerene species, and the content of M@C_n with the size except for 82 decreases. Interestingly, the species M@C_{60} and M@C_{70}, which are most abundant in the soot, are not extracted by above solvents. [2,14,154] On the other hand, the special ability in extraction of nitrogen-containing solvents, such as pyridine, DMF, and aniline, has been known from the early stage of metallofullerene study, but there were no reports to explain a selective enrichment behavior of these solvents. [23,25,27,29-31,37,162-165] One of the hints, which explain the special behavior of nitrogen containing solvents, may be hidden in the electrochemical investigation of fullerenes and metallofullerenes. For example, M@C_{60} can be soluble in organic solvent when electrochemical reduction was performed.[33]

The separation and the isolation of metallofullerenes are also performed in the solution phase. As indicated in previous section, the report of the purification of +3 type mono-metallofullerenes were limited to the cage size of 82, except for mono-Sc-, La- and Er- metallofullerenes. For the case of La-endohedral fullerenes, which are the most frequently investigated species, the report of the isolation was limited to the cage size of 82, 86 and 90.[9,41,159,166] And those with the size except for 82, 86, and 90 were not purified yet. We can point out two reasons why the systematic isolation and characterization of above metallofullerenes could not be reported. One is their small content in the soot extract. The second, which is the most important, is the miss-choice of HPLC eluent. The solvent of toluene has been commonly used as an HPLC eluent. However, the toluene has disadvantage in terms of its ability to store metallofullerenes under chemically stable condition.[57,128] By summarizing the previously reported experimental result, we can conclude that the consideration of the chemical interaction of metallofullerenes and organic solvents is necessary to perform the systematic isolation and characterization of the series of $M@C_n$s.

Recently, the interests are paid for the chemical and physical properties of metallofullerene ions. The chemical reactivity of $La@C_{82}$ with organic compounds was controlled by the electrochemical reduction and the oxidation of $La@C_{82}$-I.[167]

1. 5. Aim of this thesis

This thesis contains two aims, one is the construction of the methodology of the systematicthe separation and the characterization of metallofullerenes. For this purpose, a series of isomers of lanthanum endohedral fullerenes were investigated as the prototype of lanthanoid metallofullerenes. The second is the understanding the electronic structure of metallofullerene ions.

In chapter 2, the chemical interaction of endohedral fullerene with organic solvent was investigated. The efficient reduction of metallofullerenes by the solvation of pyridine, DMF and aniline was found and confirmed by Vis-NIR, ESR, and NMR spectroscopy. The special ability in extraction of these solvents has been known as described before. Our finding would give an explanation for the remarkable behavior of these solvents.

In chapter 3, the improvement of the separation method was performed to obtain the less-stable metallofullerene samples in high purity. The systematic separation of mono-lanthanum endohedral fullerene, La@C_n (n=76-90), was performed by replacing the commonly used toluene to chlorobenzene as a HPLC eluent. The separation and the characterization of new lanthanum endohedral fullerene isomers with the cage size of 76, 78, 80, 84, 86, and 88 were performed.

In chapter 4, the detailed electronic structure and the spin state of metallofuollerenes were investigated. The electronic structure of the series of La@C_n, (n=76-90) was discussed by the analysis of the temperature dependent ESR measurement. The isotropic and the anisotropic ESR parameters, such as the g- factor, the hyperfine coupling constant and the nuclear quadrupole coupling constant, were determined. The quantitative treatment of these parameters suggested the formal electronic structure of $La^{3+}@C_n^{3-}$ for all La@C_ns. The electronic structures of metallofullerene ions were also investigated by ESR spectroscopy. The spin state of the internal atom was monitored through the reduction and the oxidation process. For this purpose, Gd@C_{82}-I was chosen as an example because the unpaired electrons on the 4f-atomic orbital of Gd are the main origin of the ESR signal. For the case of Gd@C_{82}-I, the reduction and the oxidation occur at the fullerene cage. ESR measurement of $La_2@C_{80}$ anion was also performed. It is interesting to note that the excess electron lies on the internal La dimmer for the case of $La_2@C_{80}$ anion.

Chapter 2

Chemical Properties of Endohedral Metallofullerenes

(Contents in this chapter were submitted for publication.)

2. 1. Introduction

The chemical property of endohedral metallofullerenes is now a great interest. Preferable chemical and physical property can be achieved by introducing the functional group to fullerene cage. The basic chemical property is the interaction with solvent. Most frequently used solvent of toluene is believed as a good solvent for hollow fullerenes, such as C_{60} and C_{70}. However, some disadvantages of toluene were known in handling of metallofullerenes, such as the low solubility and the presence of unknown. In chapter 3, the use of chlorobenzene as a HPLC eluent gave highly efficient separation of less stable endohedral metallofullerenes. And the choice of solvent is important through the handling metallofullerenes. Various solvents have been used in the extraction of endohedral metallofullerenes from the raw soot produced by the arc-discharge method. The solvents of toluene, CS_2, and chlorinated benzenes have been used generally as an extraction solvent.[1,2] On the other hand, pyridine and dimethylformamide (DMF) were known to give effective enrichment of metallofullerenes in the extraction, and aniline is especially effective for endohedral metallo-C_{60}.[3-5] The specific affinity of these solvents with metallofullerenes may be attributed to the electronic interaction of the lone pair electron on nitrogen of the solvent with the π orbital of the metallofullerene's cage. However the exact nature of the interaction has not been clarified as yet.

In this chapter we present the evidence that anions of La@C_{82}-I, La@C_{82}-II, and La_2@C_{80} are easily produced with almost 100% yield by the solvation of pyridine and DMF. The formation of the La@C_{82}-I anion was confirmed by Vis-NIR, ESR and ^{13}C-NMR measurements, which gave almost identical spectra with those of the La@C_{82}-I anion reported before.[6,7] The reduction of La@C_{82}-II and La_2@C_{80} was also confirmed by ESR and Vis-NIR measurement. The electron spin resonance (ESR) and Vis-NIR spectra of La@C_{82}-I, La@C_{82}-II, and La_2@C_{80} dissolved in pyridine and DMF gave good agreements with those of the anion produced by electrochemical reduction. The

confirmation of the formation of anion was also performed by the reaction with chemical reduction reagent. It could be generally concluded that the solvation of pyridine, and DMF, and aniline leads to the efficient reduction of endohedral metallofullerenes. The reduction of C_{60} by the solvation of pyridine was also confirmed, but the efficiency was smaller than that for metallofullerenes. And the subsequent reaction of C_{60} anion radical with the pyridine molecule was observed. The evidence of the reduction of metallofullerenes gave an explanation of the strange extraction behavior of these solvents.

2. 2. Experimentals

An endohedral metallofullerene samples were prepared and separated according to the method reported before[8]. The sample purity of more than 95 % was confirmed by laser desorption time of flight mass (LD-TOF MASS, Kratos Kompact MALDI IV) and X-band ESR (Bruker ESP300E) measurements. Pyridine was distilled over CaH_2 under vacuum prior to use. Aniline was distilled, and DMF was used as purchased. Electrochemical-grade tetra-*n*-butylammonium perchlorate (TBAP), purchased from Wako, was recrystallized from absolute ethanol and dried under vacuum at 313 K prior to use. Or tetra-*n*-butylammonium perfluorate (TBAF) was used as purchased. Bulk controlled-potential electrolysis of the two isomers of $La@C_{82}$ was used to prepare the corresponding anion and cation using a potentiostat/galvanostat (BAS CW-50). Solutions containing $[La@C_{82}]^-$ and $[La_2@C_{80}]^-$ were obtained in ODCB/TCB (3:1) containing 0.2 M TBAP by setting the applied potential at 150 - 250 mV more negative or more positive than $E_{1/2}$ for the $La@C_{82}/[La@C_{82}]^-$ and $La_2@C_{80}$ /$[La_2@C_{80}]^-$ redox couple, respectively.[9,10] Chemical reduction was performed by mixing with DBU (1,8-diazabicycro[5,4,0]-7-undecene, Wako) in ODCB, which were used as purchased.[11] ^{13}C-NMR spectra were obtained at 125 MHz on a Bruker AVANCE500. Chemical shifts were expressed downfield of the signal for the carbon atom in CS_2 as an internal standard (δ = 195.0). The ^{139}La-NMR spectrum was measured at 300 K at 70.6 MHz on a Varian unity 500sw spectrometer. The ^{139}La chemical shift was calibrated with 0.6 M $LaCl_3/D_2O$ as an external reference (δ = 0). Vis-NIR spectra were recorded on Hitachi U-3500 spectrophotometer.

2. 3. Results

2. 3. 1. La@C_{82}-I

The La@C_{82}-I solution in CS_2, toluene, or chlorinated benzenes exhibited well-known octet ESR lines with a hyper-fine splitting of 1.15 gauss at ambient temperature. However, an addition of a large amount of pyridine to the solution caused vanishing of the ESR spectrum accompanied by a greenish color change of the solution. Figure 2-1(a) shows the Vis-NIR spectrum of La@C_{82}-I in CS_2, which changed to the line (c) in pyridine. And that in aniline (line (b)) looked like to the halfway of the spectra of CS_2 solution and of pyridine solution.

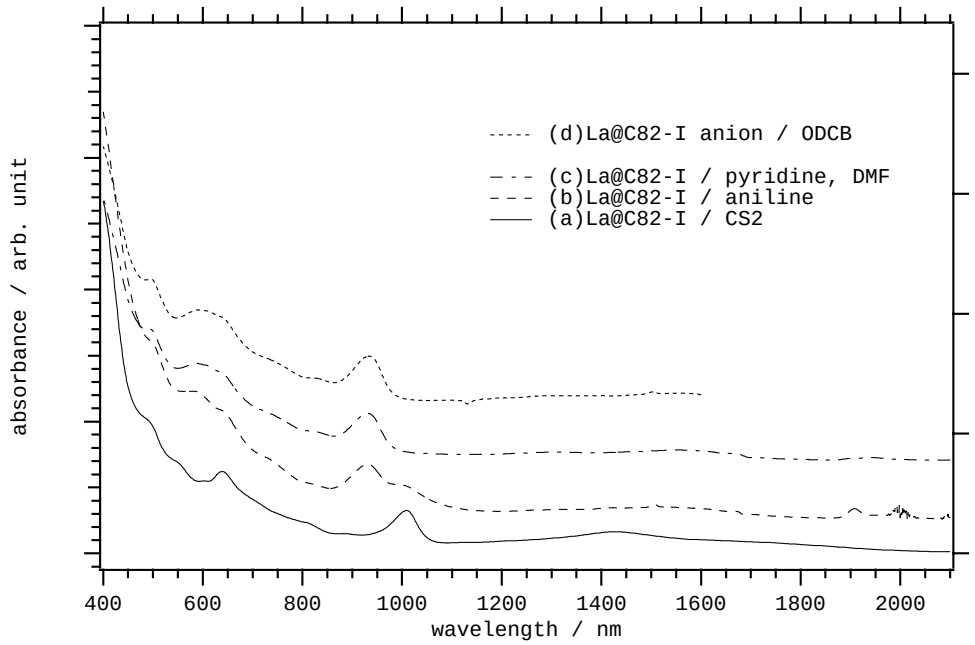

Figure 2-1. Vis-NIR spectra of La@C_{82}-I in (a) CS_2, (b) aniline, and (c) pyridine. Line (d) shows the electrochemically generated La@C_{82}-I anion in ODCB.

A series of solutions with different concentrations of pyridine were obtained by titrating the initial CS_2 solution with pyridine solution, as shown in Figure 2-2. We observed an increase (decrease) of the intensity of the band at 942 (1009) nm with an isosbestic point at around 970 nm (inset of Figure 2-2(a)). This indicates an equilibrium reaction between two forms. The vanishing of the ESR spectrum took place concurrently with the change of the Vis-NIR spectrum at the molar fraction of about 0.17 (figure 2-2(b)).

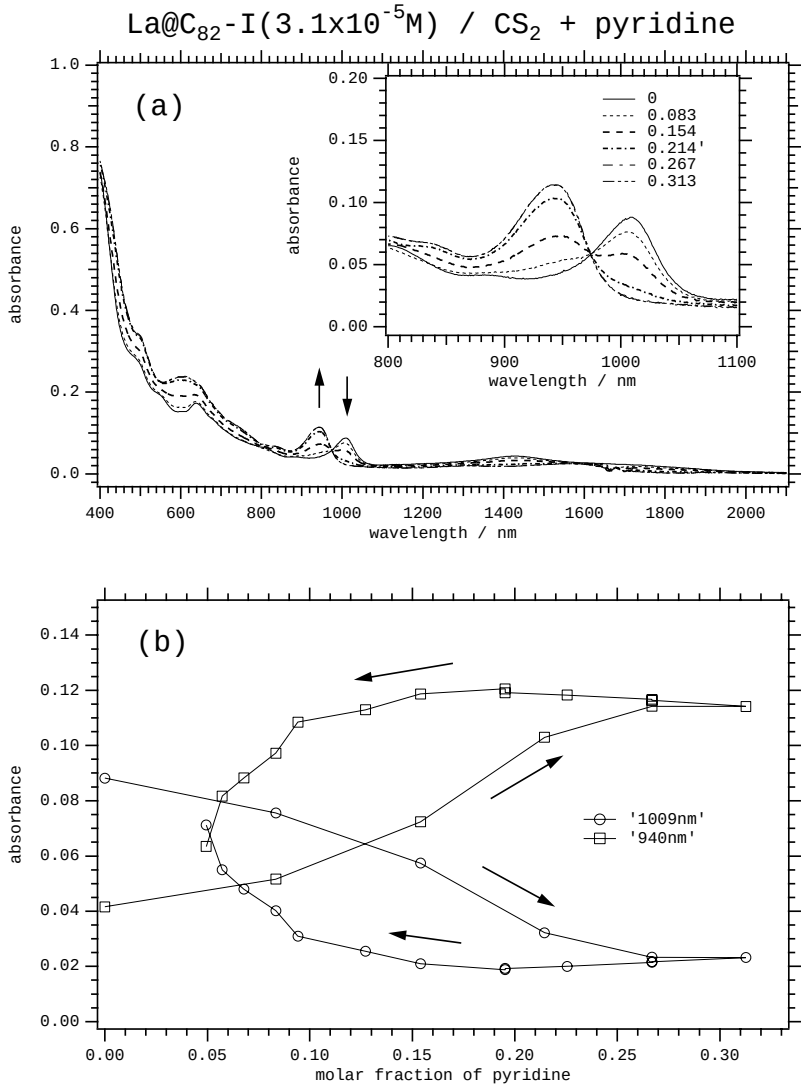

Figure 2-2. (a) Vis-NIR titration spectra of La@C_{82}-I in CS_2 and pyridine. (b) shows the intensity of characteristic absorption band versus molar fraction of pyridine in CS_2

The value of molar fraction at equilibrium was independent of the concentration of La@C_{82}-I. And most importantly the Vis-NIR spectrum of the final solution in the titration was identical with that of La@C_{82}-I anion obtained by electro-chemical reduction[6], as shown in Figure 2-1(d). The efficiency of the conversion could be calculated to be almost 100% from the estimation of both concentrations by using molar absorption coefficients (ε~6100 and ~9100 ($M^{-1}cm^{-1}$) for La@C_{82}-I and its anion, respectively). The spectral change took place in a reversed manner when the final solution of the forward titration was titrated back with CS_2 solutions. However the reverse change took place at a lower molar fraction (0.07) in the backward titration. This means that more amounts of CS_2 were needed for the reverse change. Figure 2-3 shows the time evolution of the ESR signal intensity of La@C_{82}-I. The signal intensity of La@C_{82}-I was decreasing and finally disappeared with the time after mixed with pyridine under absence of the light. The disappeared signal was recovered by "dry up - redissolve in vacuum" procedure. The second decreasing of the intensity of the ESR signal was investigated under presence of the light. Almost identical decay rate suggested that the photo induced reduction process could be neglected. Finally 73% of the signal intensity could be recovered when the sample tube was opened and resealed with 100% CS_2 solvent. The spectral change recorded for a solution obtained by titrating with DMF or 2,6-dimethylpyridine in a CS_2 solution gave an almost identical result. The Vis-NIR spectrum recorded for the final solution was identical with that of the La@C_{82}-I anion, and the ESR spectrum vanished at a molar fraction of 0.2.

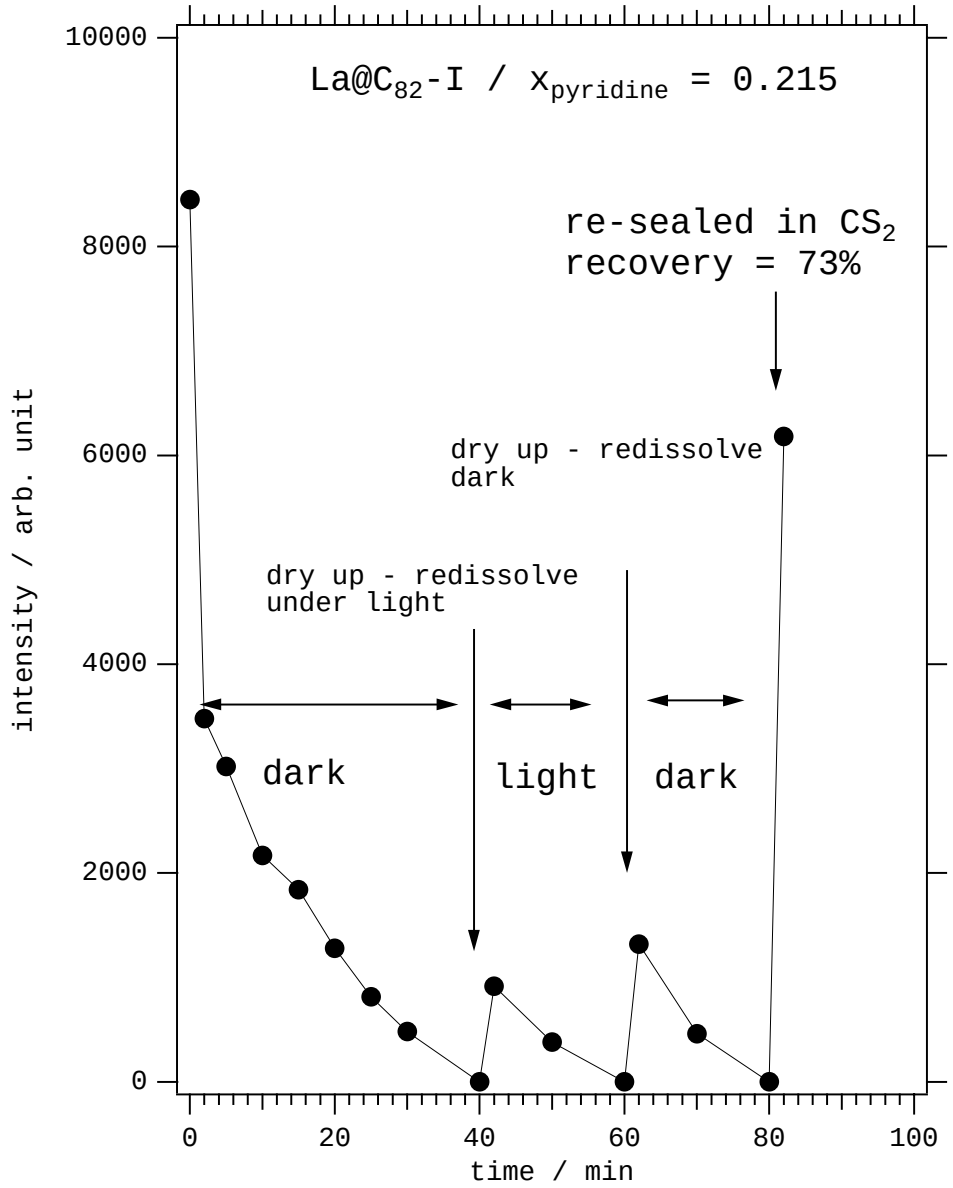

Figure 2-3. Time dependent ESR signal intensity of La@C_{82}-I in CS_2 and pyridine.

A clear ^{139}La-NMR line was recorded in the DMF-d_7 solution, as shown in the inset of Figure 2-4(a). The chemical shift of the ^{139}La-NMR line corresponded with that of the La@C_{82}-I anion reported before.[7] For the assignment the anion generated in DMF, ^{13}C-NMR spectrum was measured under same condition of electrochemically method in literature. After addition of electrolyte (TBAP) and removed DMF, the anion of La@C_{82} generated in DMF was dissolved in a mixture of CS_2 and acetone (1:1, vv). The spectrum is in good agreement with that prepared by electrochemical method.[7]

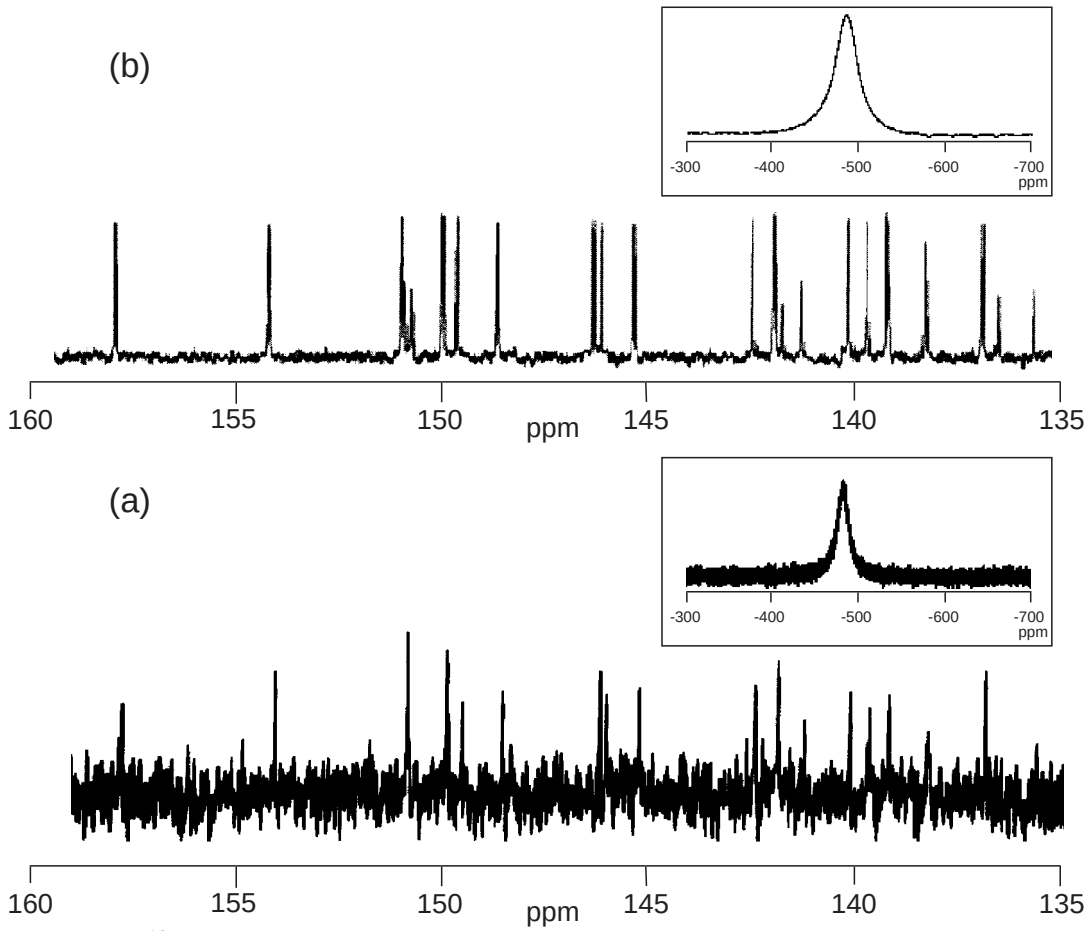

Figure 2-4. ^{13}C-NMR spectra of (a) La@C_{82}-I co-crystallized with TBAP in DMF, and (b) electrochemically generated La@C_{82}-I anion in CS_2: acetone (1:1 vv). Insets are corresponding ^{139}La-NMR spectra.

2. 3. 2. La@C_{82}-II

La@C_{82}-II in pyridine did not show any ESR signal. And figure 2-9 shows the Vis-NIR spectra of La@C_{82}-II in CS_2 and in pyridine. The spectrum in pyridine is again identical to that of electrochemically generated anion.

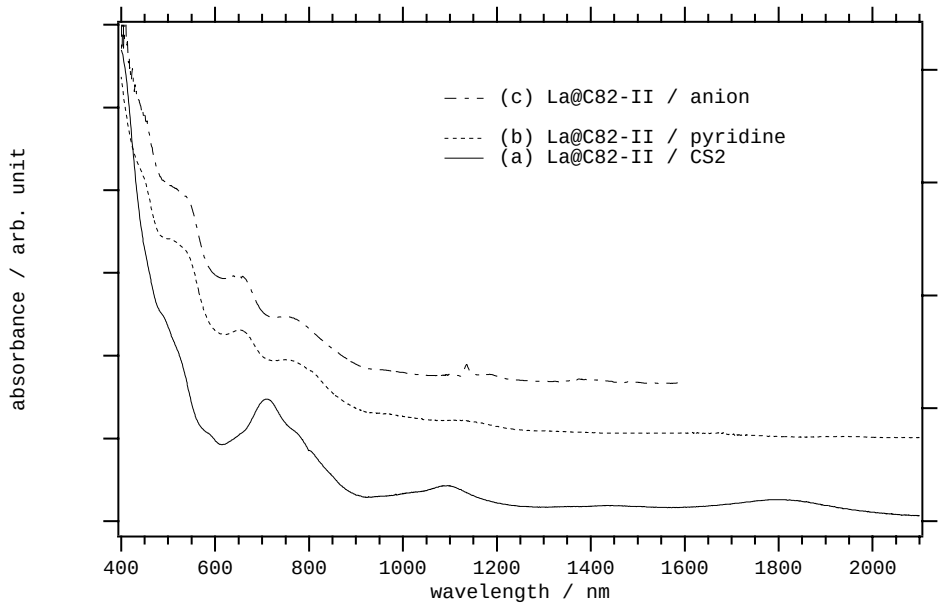

Figure 2-9. Vis-NIR spectra of La@C_{82}-II in (a) CS_2, (b) pyridine, and (c) electrochemically generated La@C_{82}-II anion in ODCB.

Figure 2-10 shows the Vis-NIR titration spectra of La@C_{82}-II. The absorption band at 707 nm in CS_2 solution decreased by adding the pyridine solution, and the absorption band at 660nm increased with isosbestic points at 689 and 765 nm. The spectrum of CS_2 solution completely changed to that of pyridine solution at the molar fraction of about 0.26.

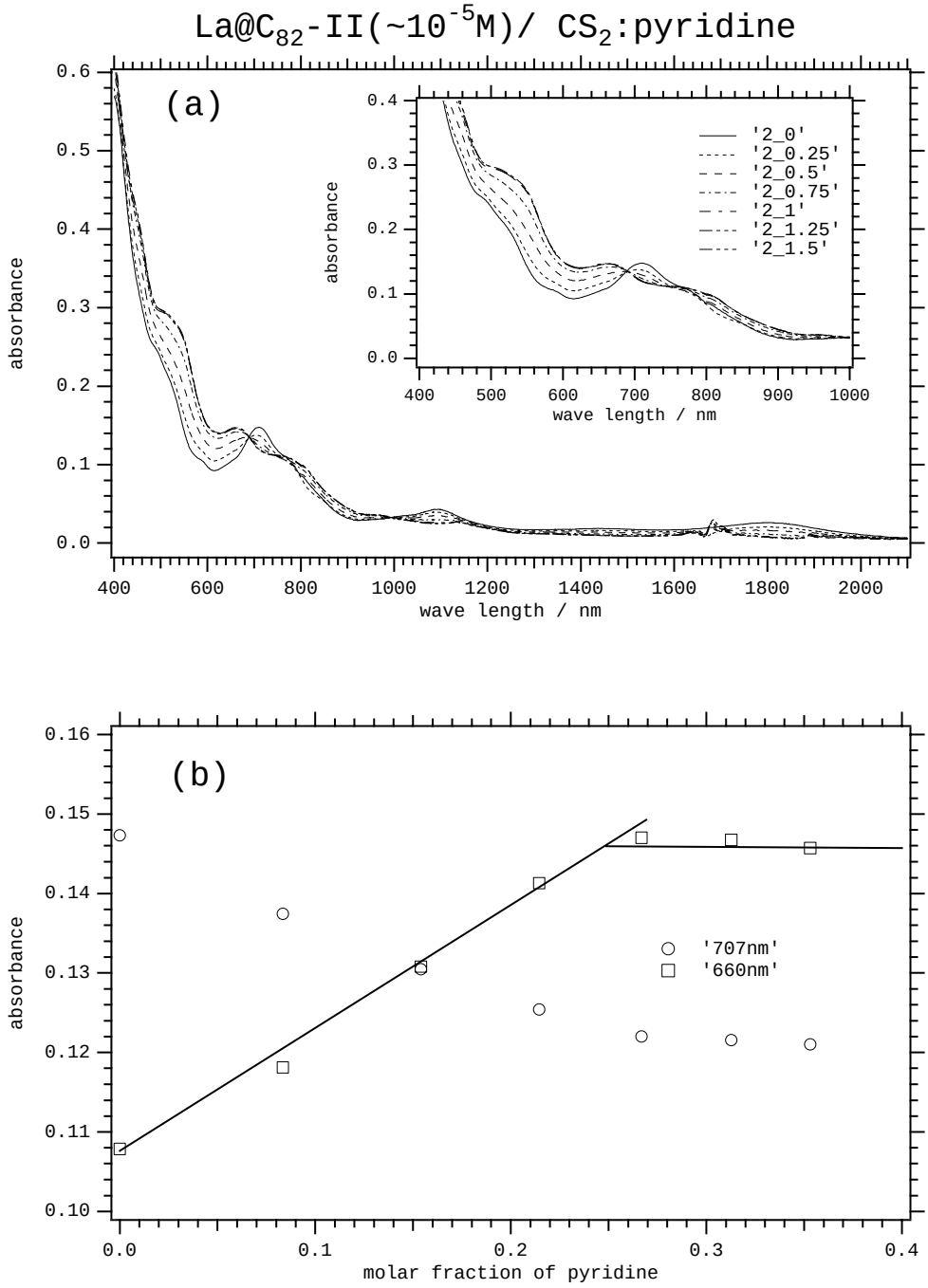

Figure 2-10. Vis-NIR titration spectra of La@C_{82}-II in CS_2 and pyridine. (b) shows the intensity of characteristic absorption band versus molar fraction of pyridine in CS_2

2. 3. 3. $La_2@C_{80}$

The vis-NIR spectrum of $La_2@C_{80}$ in pyridine showed the different absorption feature from that of chlorobenzene solution. The formation of the $La_2@C_{80}$ anion in pyridine was also proved by comparing the absorption spectrum with that of electrochemically generated anion, as in Figure 2-11.

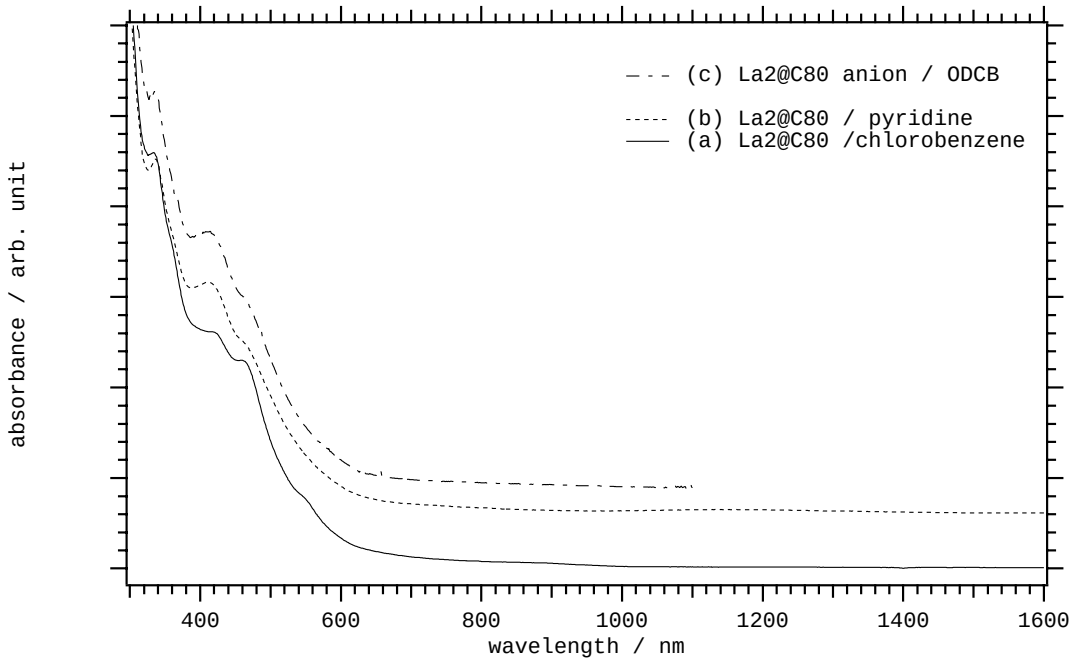

Figure 2-11. Vis-NIR spectra of $La_2@C_{80}$ in (a) chlorobenzene, and (b) pyridine. Line (c) shows the electrochemically generated $La_2@C_{80}$ anion in ODCB.

Figure 2-12 shows the X-band ESR spectrum of the $La_2@C_{80}$ in pyridine at 3K. The ESR spectrum of $La_2@C_{80}$ in pyridine appeared the widely spaced hyperfine structure. And further confirmation of the reduction of $La_2@C_{80}$ was given by the chemical reduction with DBU, which showed almost the same ESR spectrum as in Figure 2-12. The observed hyperfine coupling constant of $La_2@C_{80}$ anion (~360 gauss) is much larger than that of $La@C_{82}$-I (1.15 gauss) and is indicated the large spin density on the internal La dimmer. The detailed discussion of the electronic structure of $La_2@C_{80}$ anion will be discussed in the latter chapter.

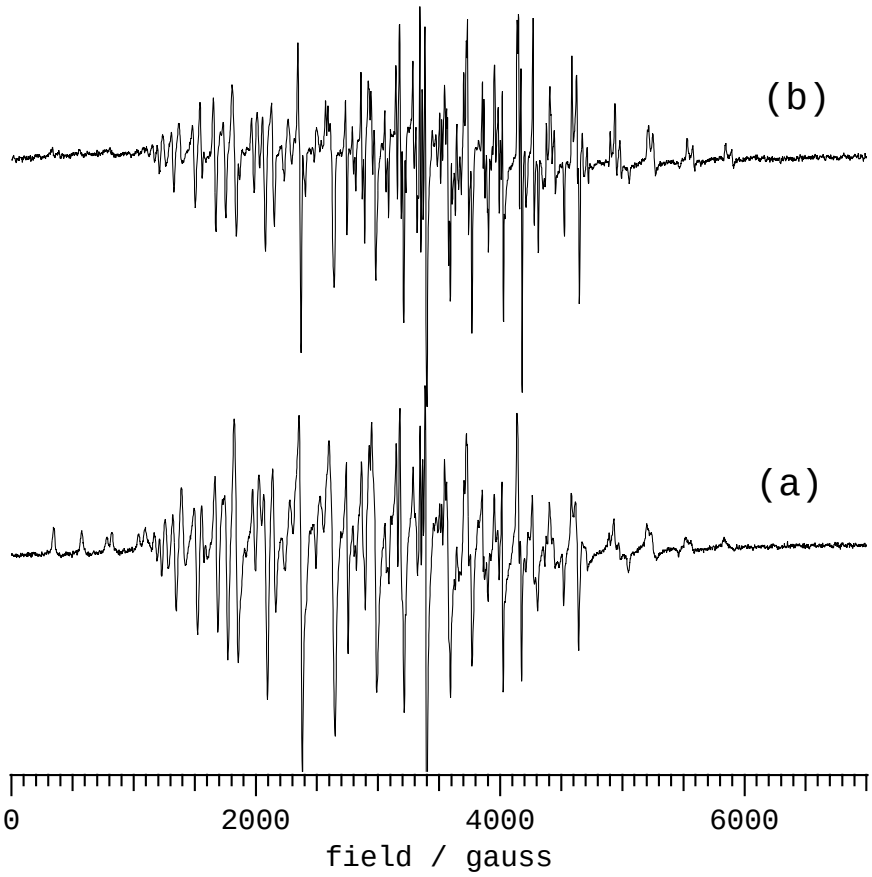

Figure 2-15. X- band ESR spectra of $La_2@C_{80}$ (a) in pyridine, and (b) with DBU in TCB and toluene. All spectra are measured at 3 K.

2. 4. Discussions

In the case of C_{60}, the charge transfer reactions with amines were well studied, and the ability of pyridine to act as a reducing agent was suggested.[12] However there was no report to explain why metallofullerenes could be enriched in the pyridine extract. We investigated the same spectroscopic measurement for C_{60} in pyridine to elucidate the process of the enrichment of metallofullerenes. The characteristic absorption band at 1075 nm for C_{60}^- was detected in pyridine solution, and an ESR signal due to C_{60}^- was obtained in pyridine at 3K. [13] However the formation yield of C_{60}^- was estimated to be less than 2% from the intensity of the absorption band.[14] Furthermore, the absorption band of C_{60}^- disappeared after 4 hour when C_{60} was dissolved in pyridine, and the most of C_{60} became insoluble precipitated after few weeks. The precipitate might be originated to the zwitterion, and the reaction of C_{60} with pyridine is very similar to that with DBU and TDAE.[11,15,16]

The spectral data obtained in former section gave the evidence of the red-ox equilibrium for fullerenes and metallofullerenes dissolved in pyridine (DMF). And the difference in reduction efficiency could be explained by the difference of their reduction potentials. One of the key-factor for the reduction by solvation of pyridine (DMF) is the exceptionally low reduction potential of metallofullerenes. As in Table 2-1, the first reduction potential of the isomers of La@C_{82} is much higher than that of C_{60}.[9] And the other factor is the polarity of the solvent. Table 2-2 shows the first reduction potentials of C_{60} in numbers of solvents.[17,18] The reduction potential of C_{60} was positively shifted in pyridine, DMF, and aniline than that in chlorobenzene, and the correlation with the dielectric constant ε was found. [19] Such a solvent dependence was also observed in the Vis-NIR and the ESR spectra of La@C_{82}-I. The half way changed spectra were observed in aniline and in N,N-dimethylaniline, and the incomplete spectral change was in good agreement with the ε of solvents. The results of the Vis-NIR titration experiments of the two isomers of La@C_{82} indicated that the equilibrium point was reached at a high molar concentration of pyridine (DMF), 2.8 M (2.6 M), which corresponding to an enormous molar ratio, i.e. 10000, to solute La@C_{82}-I (~10^{-4} M). Then to form a stable anion the reduction must be accompanied with the solvation of enough amount of pyridine (DMF). The solvation by the solvent with a higher ε makes

a much more polar environment around metallofullerenes and stabilizes their anion form.

However, the identification of the counter cation has not been succeeded in both ESR and vis-NIR. This may be explained by the instability of solvent cations, which immediatery react with other solvent molecules or unknown impurities. [20-23]

Table 2-1. Reduction potentials of $La@C_{82}$ and C_{60}in V in ODCB, Referenced to the reduction potential of the $Fc^{0/+}$ couple in 0.1M $TBAPF_6$.

Compd.	$^{red}E1$
$La@C_{82}$-I	-0.42
$La@C_{82}$-II	-0.47
$La_2@C_{80}$	-0.31
C_{60}	-1.12

Table 2-2. Reduction potentials of C_{60} in mV. Referenced to the reduction potential of the $Me_{10}Fc^{0/+}$ couple in 0.1M $TBAClO_4$. Dielectric constant s of solvents are also indicated.

solvent	$^{red}E1$	dielectric constant
PhCl	-573	5.6895
ODCB	-535	10.12
pyridine	-343	13.26
DMF	-312	38.25
aniline	-396	6.97
N,N-dimethylaniline	-547	4.9

Our results gave a possible explanation of the remarkable extraction behavior of these solvents. Scheme 2-1 shows the plausible mechanism of the reaction of C_{60} and metallofullerenes with pyridine. The reduction of fullerenes and endohedral fullerenes yields the dissociation of clusterized fullerenes by their electric repulsive force. Secondly, the fullerene cage would have closed shell electronic structure for both $M@C_{82}$ and $M_2@C_{80}$ anion. This is in analogous to the solution of the ionic compounds. The closed shell electronic structure of the cage of the metallofullerene anion is in contrast to that of the hollow fullerene anion, which has the open shell electronic structure on the cage. And the radical character of fullerene anion promotes the subsequent reaction with the counter ion or other solvent molecules.[11] Such a different solvation nature of the metallofullerene from that of hollow fullerene would be attributed to the super atom character of metallofullerenes.

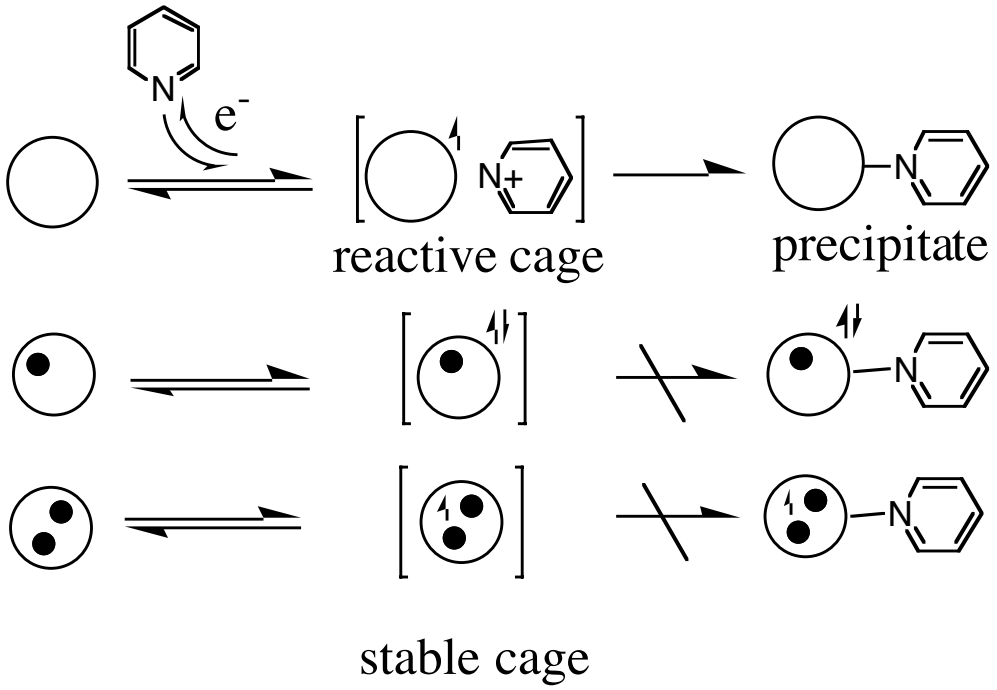

Scheme 2-1. Plausible mechanism of the reaction of fullerenes and metallofullerenes with pyridine.

The thought of the reductive solvation of pyridine to metallofullerenes suggest some applications. One is the improvement of the isolation technique of the separation of new types of fullerenes, which was not obtained by conventional method reported to date.

For example, Gd@C_{60} and C_{74}, which were not extracted by toluene, CS_2 and chlorinated benzenes, were extracted and separated by using the electrochemical reduction technique.[24] If our finding, reduction by solvation, would be applied to the isolation of these fullerenes without any electrochemical equipments. And other application is the control of the chemical reactivity of metallofullerenes. Drastic change in the chemical reaction, such as the rate, the path, and the product, may be expected.

2. 5. Conclusion

A chemical property of endohedral metallofullerenes was investigated. Highly efficient reduction of metallofullerenes by the solvation of pyridine, DMF and aniline was confirmed by spectroscopic measurements. Vis-NIR measurement revealed that almost 100% of metallofullerenes was reversibly reduced by solvation of pyridine and DMF. The ^{13}C-NMR of La@C_{82}-I was carried out without electrochemical reduction of the sample. The reversible reduction by solvation was also confirmed to La@C_{82}-II, and La_2@C_{80}. The high efficiency of the reduction of metallofullerenes was compared with the reported electrochemical data of C_{60}. The evidence of the reduction of metallofullerenes gave an explanation of the strange extraction behavior of these solvents. Our finding of the reduction by solvation will be applied for further investigations, such as the separation of the new family of fullerenes, and the control of the chemical reactivity of metallofullerenes.

Chapter 3

Separation and Characterization of ESR-Active Lanthanum Endohedral Fullerenes

(Contents of this chapter has been published in *New Diamond and Frontier Carbon Technology*, **2001**, *11*, 285-294)

3. 1. Introduction

Since the first large-scale production of endohedral metallofullerene, it has been of much interest to understand the structure as well as the chemical and physical properties of this new carbon-based material.[1] There exist a series of metallofullerenes (M_xC_n) in arc-generated soot. In the case of extracts of soot containing Sc, Y, and La, ESR spectra showed existence of numbers of ESR-active species.[2-4] For further investigation, we need to obtain the series of pure fullerenes. HPLC has been widely used to obtain pure fullerene samples. However, the one-step separation procedure is not sufficient to obtain high-purity samples of endohedral fullerenes. The two-stage HPLC method by serial use of two different columns is well known as a highly efficient separation technique for endohedral fullerenes. Toluene has been widely used as an eluent for the two-stage HPLC method because of its high resolving power. The separation of La@C_{82}-I, II and La@C_{90}-I, II, III, and IV with toluene has been reported.[5-9] However, toluene has a disadvantage in terms of its ability to store endohedral fullerenes under chemically stable condition. Compared with toluene, chlorobenzene can keep endohedral fullerenes stable. For example, ESR signals of La@C_{76} and La@C_{80}-II decreased after storage in toluene for a few days,[4] but we found that the signals remained visible even after storage for one month in chlorobenzene. This means that loss of an unstable endohedral fullerene may take place during the HPLC separation process that uses toluene. Because of this reason, some components of endohedral fullerenes have not been successfully separated by the two-stage HPLC method with toluene. The resolving power of chlorobenzene for the two-stage HPLC separation of endohedral fullerenes is lower than that of toluene.[10] However, the total yield by the separation with chlorobenzene was

much higher. In this study, full separation of topological isomers of each La@C_n component (n=76 to 90) was attempted, and all species of La@C_n with even number n from 76 to 90 were detected. Among them, La@C_{76}, La@C_{80}-I, II, La@C_{84}-I, II, La@C_{86}-II, and La@C_{88}-I, II, III were purified for the first time, La@C_{78} was partially purified, and their ESR and Vis-NIR absorption spectra were obtained.

3. 2. Experimental

Soot containing metallofullerenes was produced by DC arc discharge with electrodes made of La-carbide rod (15xl5x300 mm, 0.8 atom%, Toyo Tanso Co., Ltd.) at 500 A under He atmosphere (58-80 Torr). The produced soot was collected under anaerobic conditions and extracted by CS_2 and pyridine. The extracts were dissolved in chlorobenzene or trichlorobenzene (TCB) prior to HPLC separation. HPLC separation was performed by using the LC-908-C60 system (Japan Analytical Industries) and pentabromobenzyl column (Cosmosil 5PBB, 20 mm i.d., 250 mm length, Nacalai Tesque Co.) with chlorobenzene as eluent (flow rate of 12 ml/min), or 2-(pyrenyl) ethylsilylated silica column (Cosmosil 5PYE, 20 mm i.d., 250 mm length, Nacalai Tesque Co.) with chlorobenzene as eluent (flow rate of 6 ml/min). Recycled HPLC with PYE column was also used. A UV detector set at 330 nm was used in both HPLC procedures.

Sample isolation was confirmed by positive- and negative- LD-TOF mass spectrometry (Kompact MALDI IV, Kratos). ESR spectra were recorded using ESR spectrometer (Bruker ESP300E and E500) at room temperature. Samples were dissolved in CS_2, degassed by few times of freeze-pump-thaw cycle, and sealed in thin-walled quartz tubes. Absorption spectra in chlorobenzene solution were measured in a 10 mm quartz cell with UV-Vis-NIR spectrometer (U-3500, Hitachi).

3. 3.Results and Discussion

Figure 3-1. shows the mass spectrum of the CS_2 extract. These spectra indicated that C_{60}, C_{70}, and LaC_{82} were predominantly produced, together with LaC_{76}, LaC_{84} and LaC_{90}. In an ESR spectrum of the CS_2 solution of crude extract (figure 3-1b), four sets of octet signals were visible. However, many other octets due to trace amount (below the detection limit) of La@C_ns were likewise observed. These species in low amount

were detected in the HPLC chromatogram and their ESR spectra became observable with the progress of HPLC separation.

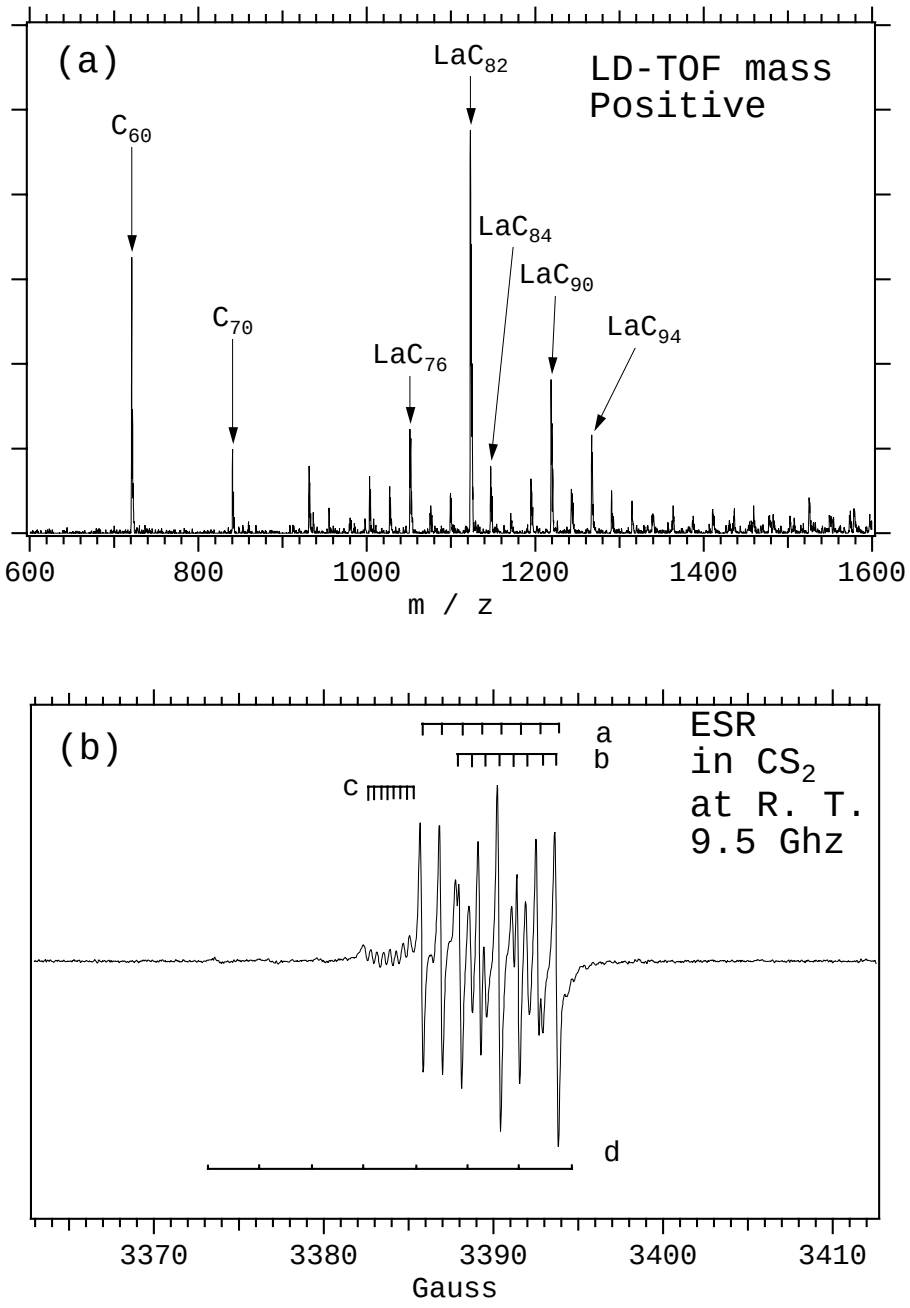

Figure 3-1. (a) Positive-ion LD-TOF mass spectrum and (b) ESR spectrum of the CS_2 extract of Lanthanum endohedral fullerenes.

On the other hand, the presence of metallofullerenes in the crude extract was highly enhanced by using more polar solvents such as pyridine and DMF (dimethyl formamide). In our experiment, pyridine was used as the solvent for second stage extraction. However, large amount of LaC_{80} and trace amounts of LaC_{76} and LaC_{78} was detected in the mass spectrum of the pyridine extract, but the corresponding ESR signals were not observed.

HPLC profiles of the CS_2 extract using PBB and PYE columns with chlorobenzene as eluent are shown in Figure 3-2. The use of chlorobenzene as eluent decreased the retention time of C_ns and La@C_ns compared to that when toluene was used, but showed better separation performance than that with TCB or CS_2.[11] The fractions separated by PBB and PYE columns were analyzed by mass and ESR measurements. The characteristic performance of PBB and PYE columns was confirmed by mass analysis, i.e., good separation in terms of molecular weight in PBB and that in terms of topological molecular structure using the PYE column. The ESR-active fractions were extracted after the retention times of 19.4 and 18.4 min, respectively. From a comparison of the mass and ESR spectra of the fractions separated by the PBB column, we could determine the number of isomers for each size of La@C_n, as tabulated in Table 3-1. These endohedral fullerenes were purified for the first time by the PBB-chlorobenzene combination. As mentioned in the Introduction, the well-balanced separation performance of chlorobenzene was reflected on the successful separation of less stable fractions.

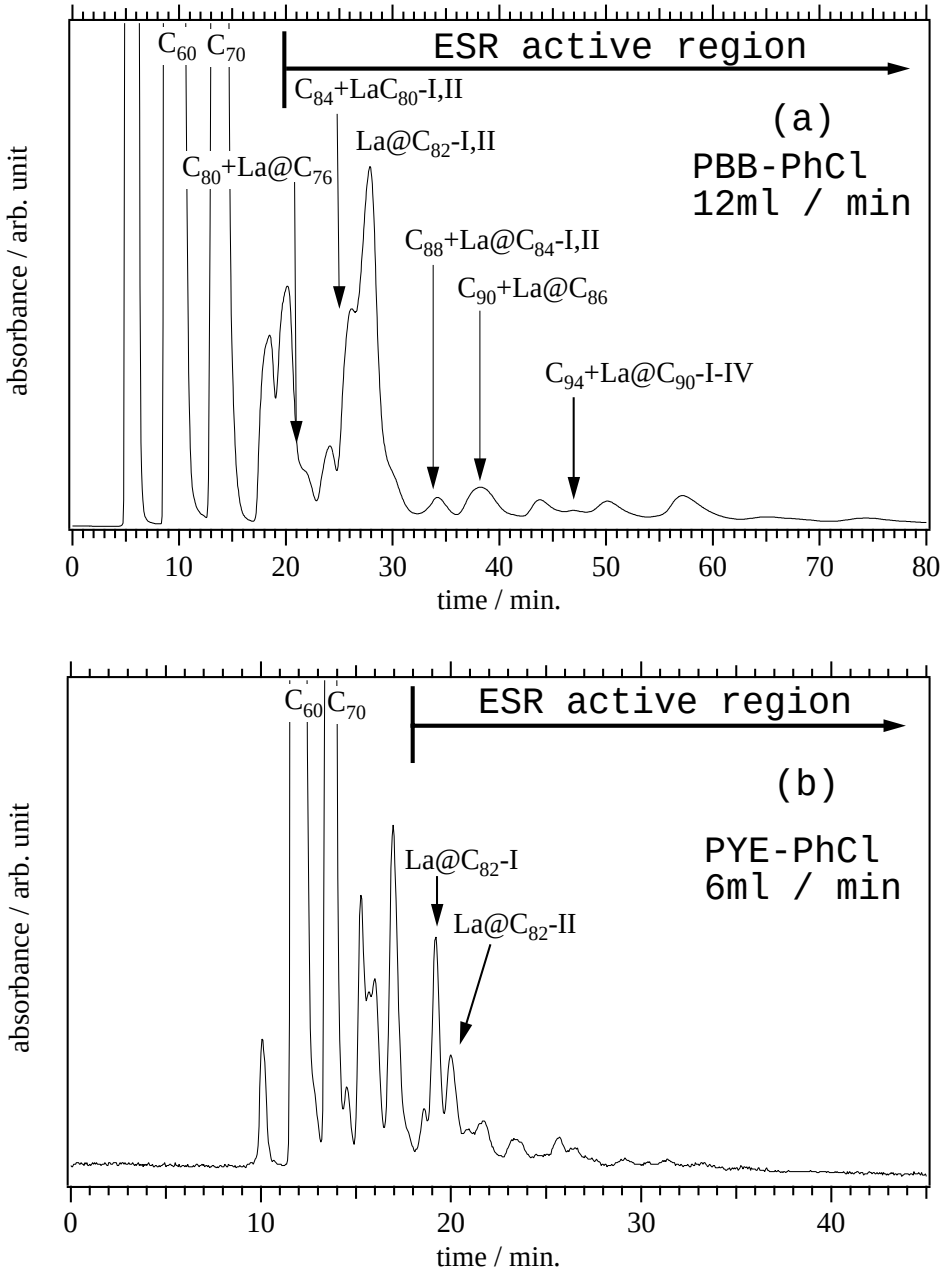

Figure 3-2. HPLC chromatograms of CS_2-extract of Lanthanum endohedral fullerenes using (a) PBB column and (b) PYE column with chlorobenzene as eluent.

Table 3-1. ESR parameters of La@C_n isomers

LaC_n	*g* value	hfc / Gauss
La@C_{76}	2.0044	0.388
La@C_{78}	2.0013	1.540
La@C_{80}-I	2.0010	2.405
La@C_{80}-II	2.0011	2.037
La@C_{82}-I	2.0008	1.150
La@C_{82}-II	2.0002	0.830
La@C_{84}-I	2.0012	1.380
La@C_{84}-II	2.0040	3.080
La@C_{86}-I	2.0010	1.632
La@C_{86}-II	2.0018	1.237
La@C_{88}-I	2.0023	1.545
La@C_{88}-II	1.9991	1.262
La@C_{88}-III	2.0017	0.582
La@C_{90}-I	2.0015	0.600
La@C_{90}-II	2.0013	0.600
La@C_{90}-III	2.0015	0.509
La@C_{90}-IV	2.0025	0.121

Based on this result, the crude extract was injected to PBB with chlorobenzene as eluent. Then the size-separated fraction was injected into the PYE column, again with chlorobenzene as eluent. Using this separation protocol, La@C_{76}, La@C_{78}, La@C_{80}-I, II, La@C_{84}-I, II, La@C_{86}-II, and La@C_{88}-I, II, III and La@C90-I, II, III, IV could be separated (see Appendix). The mass spectra of these materials were shown in Figure 3-3, 3-4, 3-5, 3-6, 3-7 and 3-8. The purity of La@C_{76}, La@C_{80}-I, II, La@C_{84}-I, II was higher than 90 %, and that of La@C_{78} was approximately 60 %. The ESR spectra are shown in Figure 3-9 (n=76-84) and in Figure 3-10 (n=86-90), with that of two isomers of La@C_{82} for comparison. Only one octet was observed in all spectra, indicating that the isomeric separation of La@C_ns was successful using this separation protocol. The Vis-NIR spectra of isomer-separated samples in chlorobenzene are shown in Figure 3-11, 3-12

and 3-13. All molecules show a large absorption band around the near-IR region, which originates from the unpaired electronic structure of the molecules. The observed absorption features are different for each other.

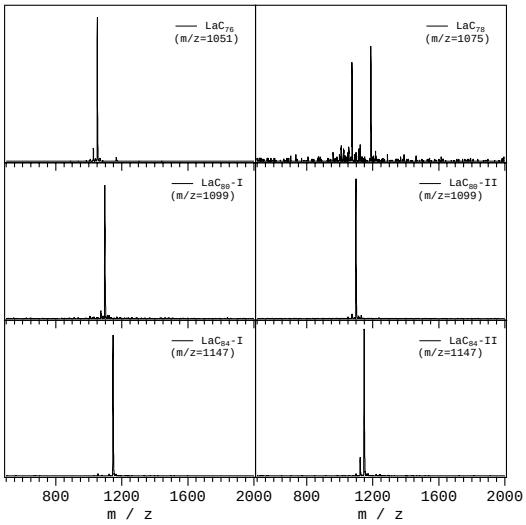

Figure 3-3. LD-TOF mass spectra of separated La@C_ns (La@C_{76}, La@C_{78}, La@C_{80}-I, La@C_{80}-II, La@C_{84}-I, and La@C_{84}-II). All spectra were obtained in the negative-linear mode.

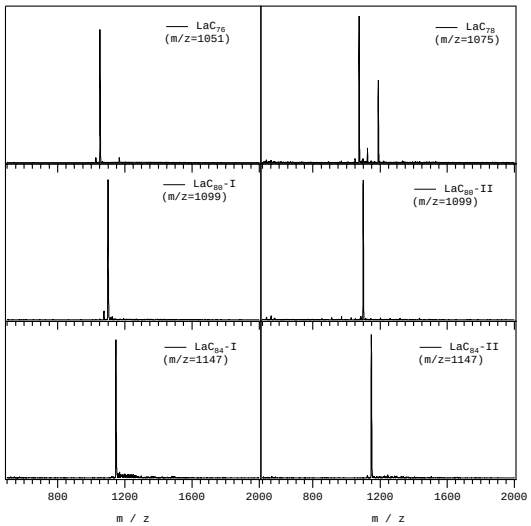

Figure 3-4. LD-TOF mass spectra of separated La@C_ns (La@C_{76}, La@C_{78}, La@C_{80}-I, La@C_{80}-II, La@C_{84}-I, and La@C_{84}-II). All spectra were obtained in the positive-linear mode.

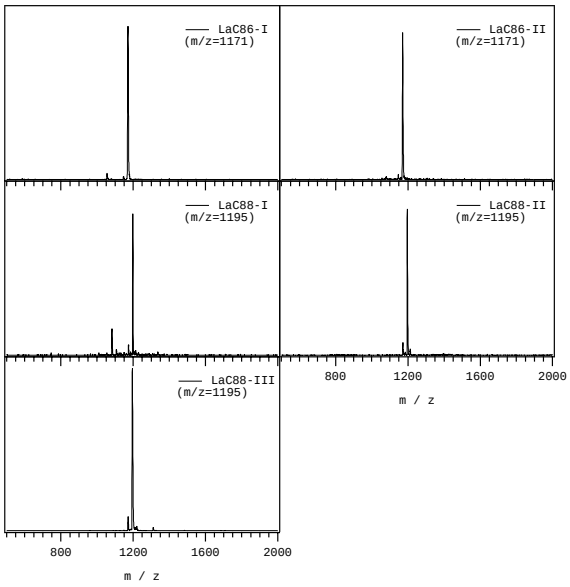

Figure 3-5. LD-TOF mass spectra of separated La@C_ns (La@C_{86}-I, La@C_{86}-II, La@C_{88}-I, La@C_{88}-II, and La@C_{88}-III). All spectra were obtained in the negative-linear mode.

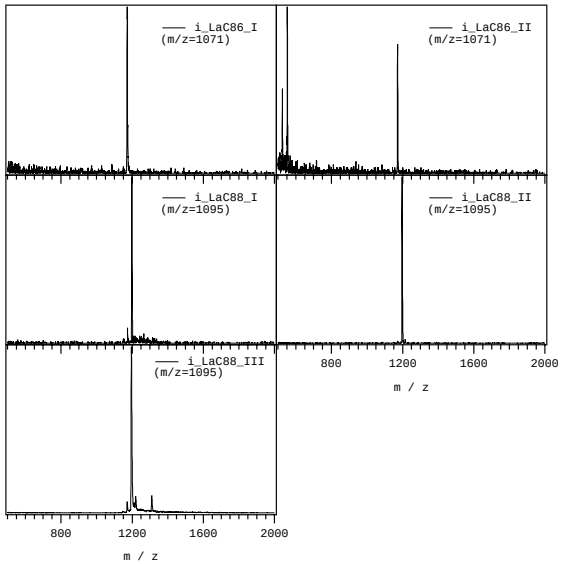

Figure 3-6. LD-TOF mass spectra of separated La@C_ns (La@C_{86}-I, La@C_{86}-II, La@C_{88}-I, La@C_{88}-II, and La@C_{88}-III). All spectra were obtained in the positive-linear mode.

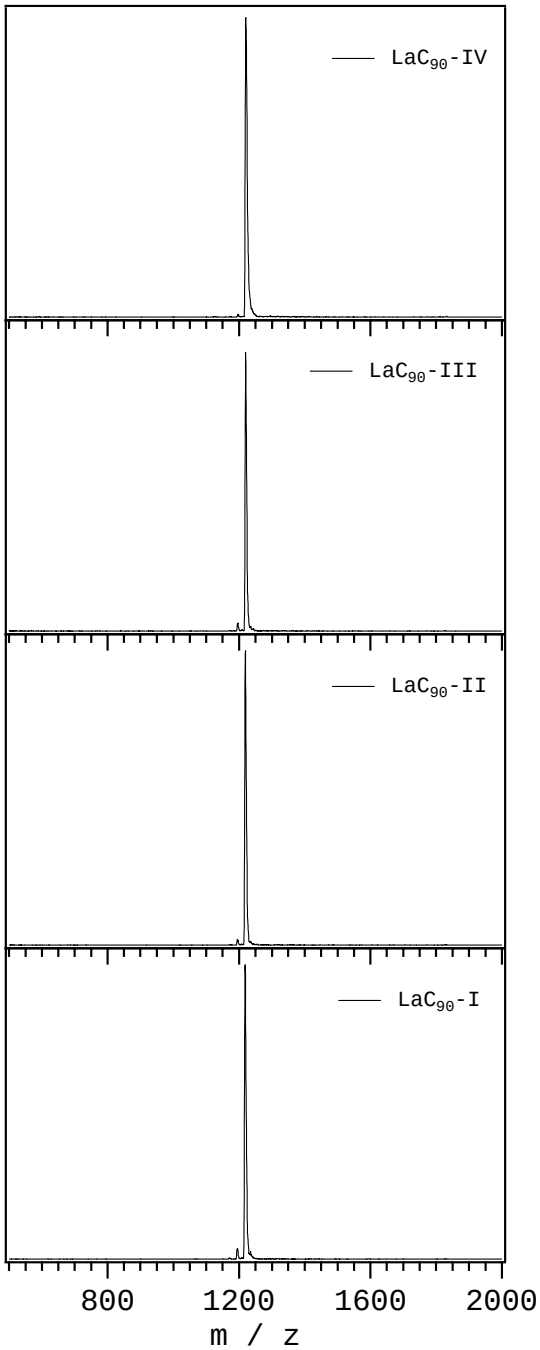

Figure 3-7. LD-TOF mass spectra of separated La@C_{90} isomers. All spectra were obtained in the negative-linear mode.

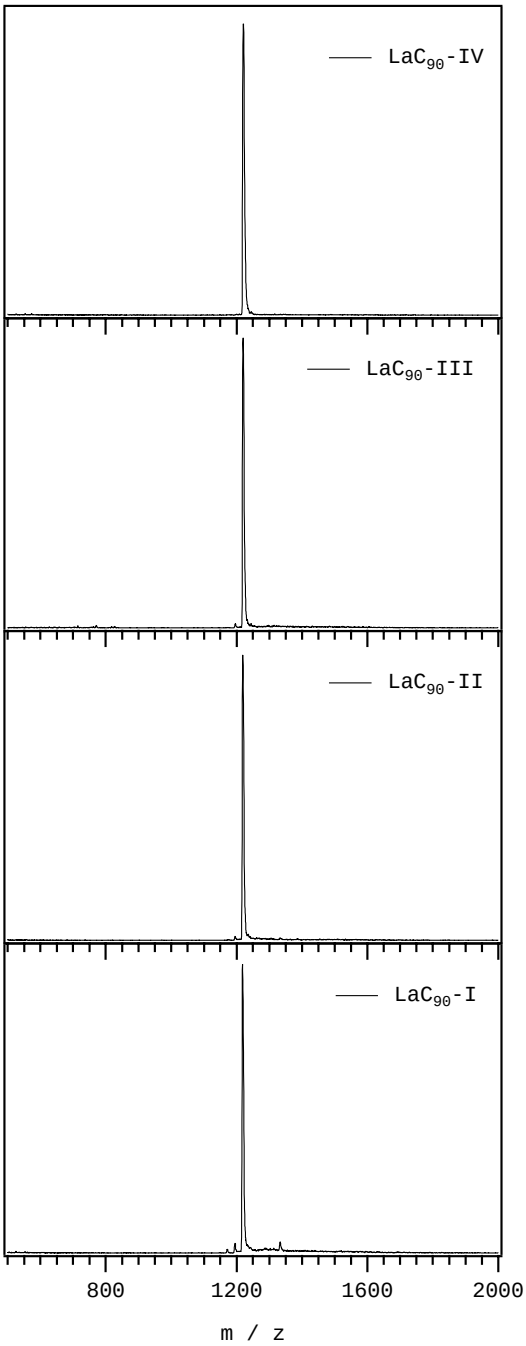

Figure 3-8. LD-TOF mass spectra of separated La@C_{90} isomers. All spectra were obtained in the positive-linear mode.

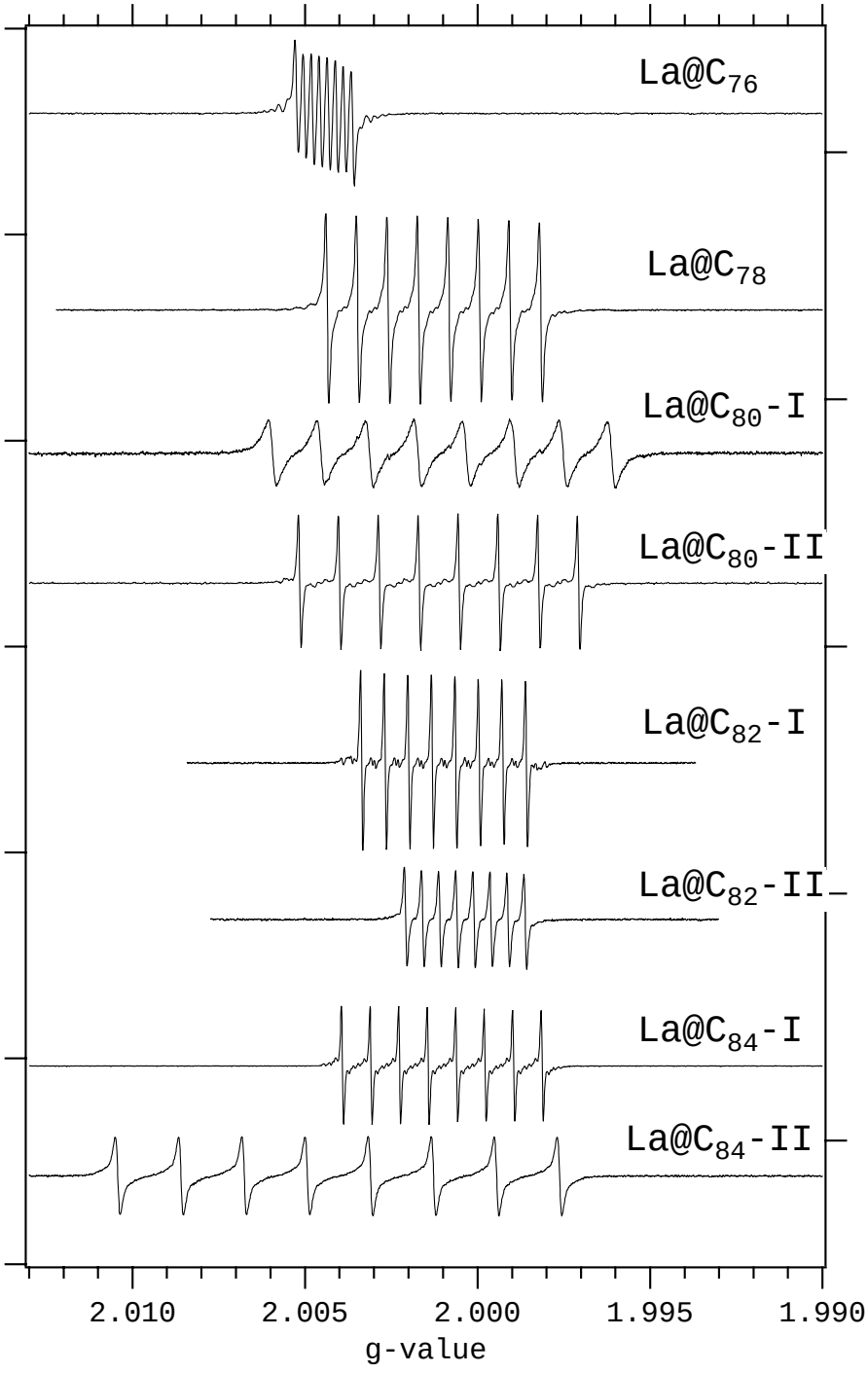

Figure 3-9. ESR spectra of La@C_{76}, La@C_{78}, La@C_{80}-I, La@C_{80}-II, La@C_{84}-I, and La@C_{84}-II. All spectra were measured at room temperature in CS_2.

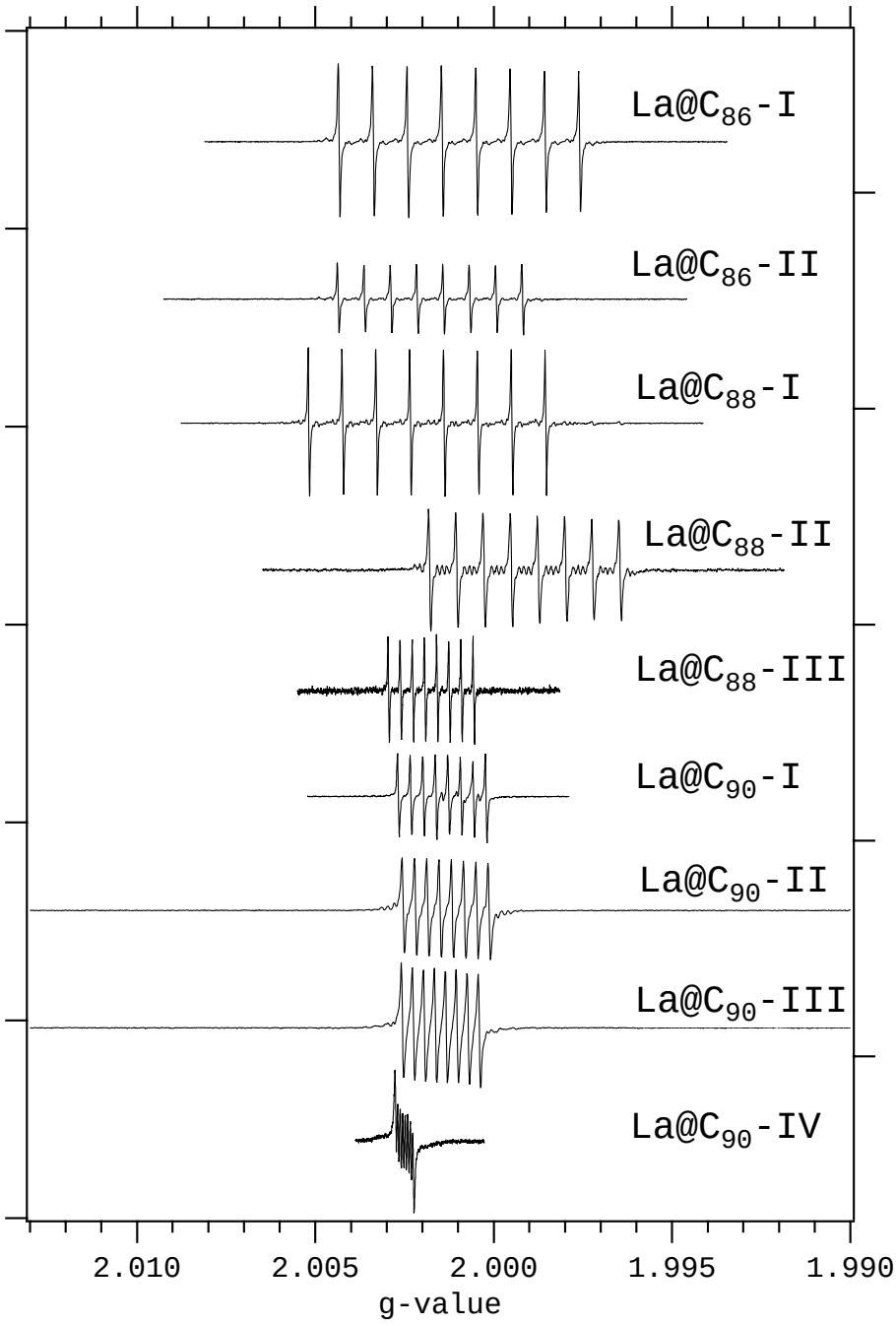

Figure 3-10. ESR spectra of La@C_{86}-I, La@C_{86}-II, La@C_{88}-I, La@C_{88}-II, La@C_{88}-III, La@C_{90}-I, La@C_{90}-II, La@C_{90}-III, and La@C_{90}-IV. All spectra were measured at room temperature in CS_2.

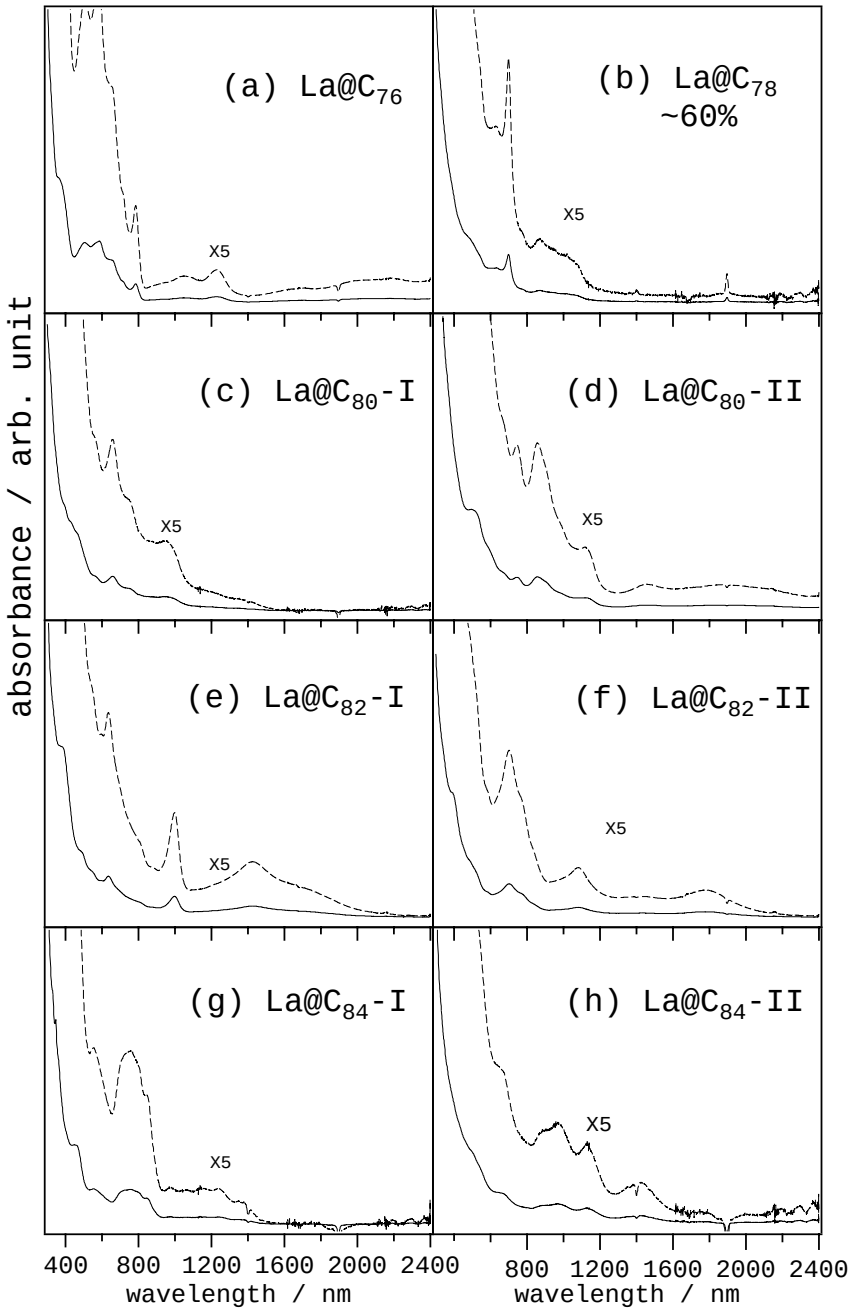

Figure 3-11. Vis - NIR absorption spectra from 300 to 2400 nm of (a) La@C_{76}, (b) La@C_{78}, (c) La@C_{80}-I, (d) La@C_{80}-II, (e) La@C_{82}-I, (f) La@C_{82}-II, (g) La@C_{84}-I, and (h) La@C_{84}-II. All spectra were measured at room temperature in chlorobenzene. Spectrum (b) corresponds to a mixture of 60% La@C_{78} and 40 % La_2@C_{76}.

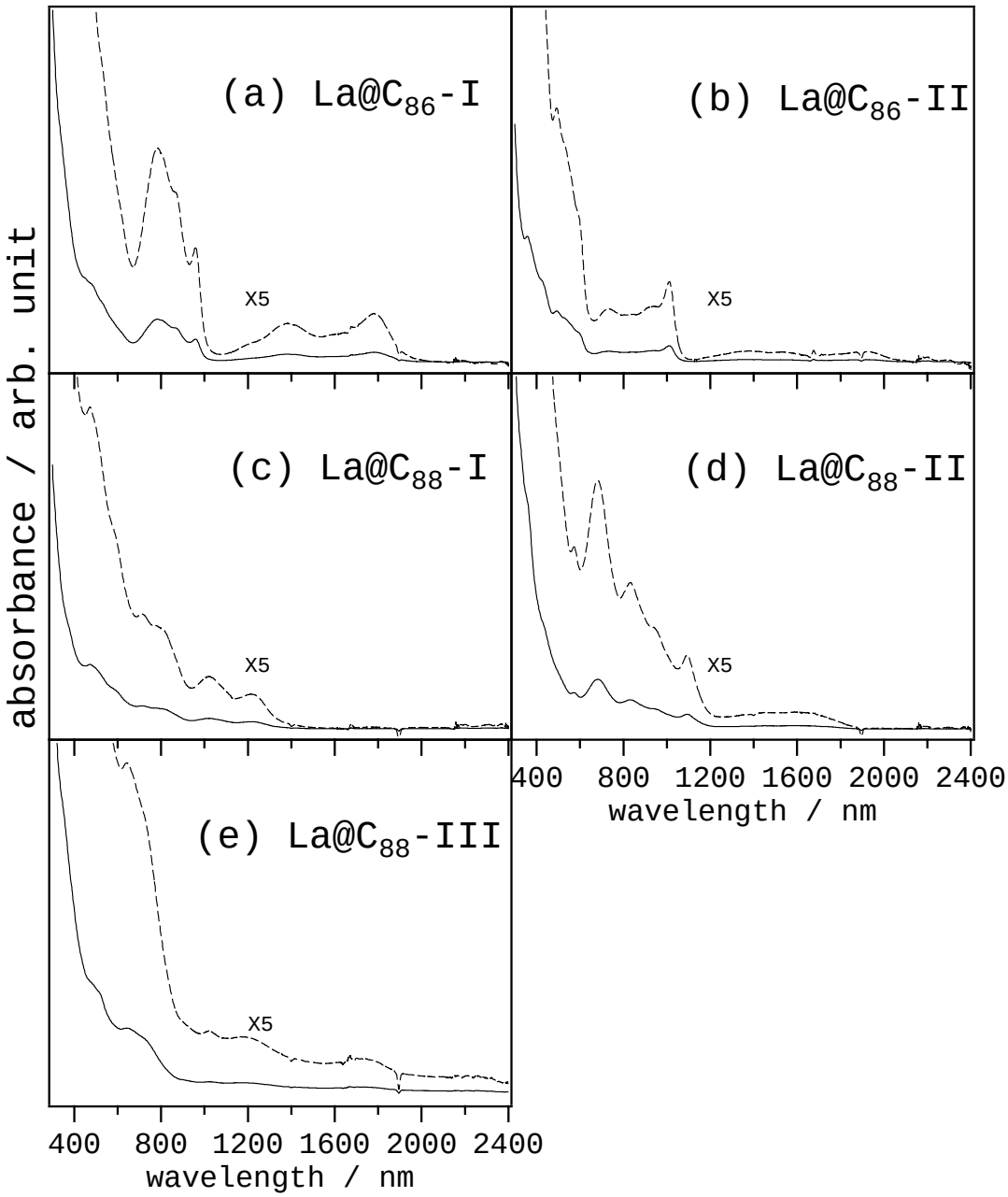

Figure 3-12. Vis - NIR absorption spectra from 300 to 2400 nm of (a) La@C_{86}-I, (b) La@C_{86}-II, (c) La@C_{88}-I, (d) La@C_{88}-II, (e) La@C_{88}-III. All spectra were measured at room temperature in chlorobenzene.

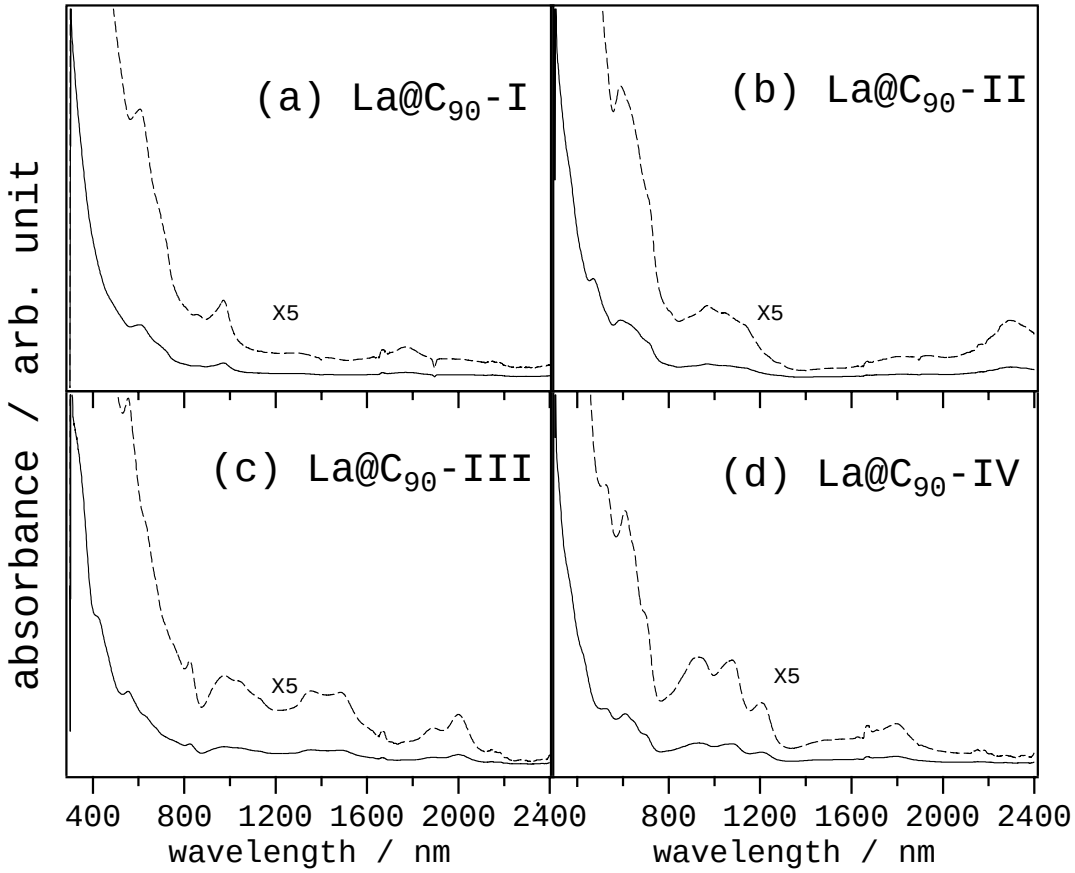

Figure 3-13. Vis - NIR absorption spectra from 300 to 2400 nm of (a) La@C_{90}-I, (b) La@C_{90}-II, (c) La@C_{90}-III, (d) La@C_{90}-IV.All spectra were measured at room temperature in chlorobenzene.

Previous studies have reported that the chromatographic retention of fullerenes and endohedral fullerenes exhibits some correlation with the polarizability and the number of pi-electrons on the fullerenes cage surface. [13,14] The logarithm of HPLC separation factor *k'* of C_ns and La@C_ns is plotted against the number of carbon atoms in PBB and PYE columns at room temperature, as shown in Figure 3-14. The separation factors of

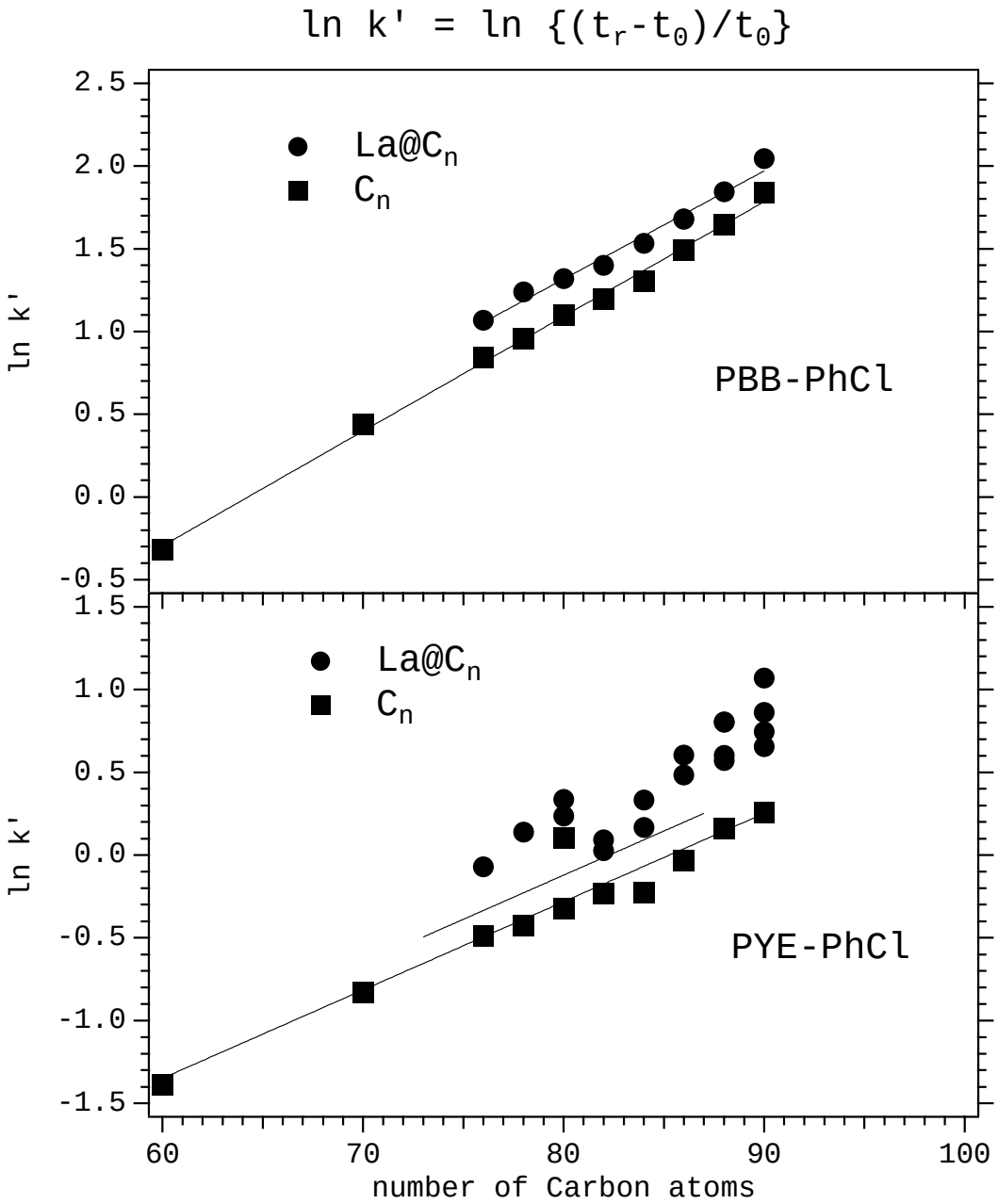

Figure 3-14. Logarithm of separation factor (k') versus number of carbon atoms of C_ns and La@C_ns in (a) PBB and (b) PYE columns with chlorobenzene as eluent. Lines in (a) and (b) are the linear fits for C_n and $C_{(n+3)}$.

the PBB phase for La@C_ns and C_ns showed a linear dependence on the number of carbon atoms but not on the isomeric structure of the fullerene cage. Such a linear fullerene size dependence of the separation factor of the PBB phase indicates that the retention mechanism of this solute-stationary phase system depends strongly on the number of π-electrons on the fullerenes cage surface. Stevenson et al. discussed the electronic structures of dimetallofullerenes species such as $La_2@C_{72}$ by analyzing the HPLC retention time on a PBB-CS_2 system, and estimated the electronic structure of $(La^{3+})_2@C_{72}^{6-}$.[13] The electronic structure of La@C_n could be regarded as $La^{3+}@C_n^{3-}$ in the same manner.

On the other hand, with the PYE phase, the separation factor of La@C_ns could not be easily described as $C_{(n+3)}$ (line in Figure 3-14 (b)). Such a large deviation of the separation factor of La@C_ns in PYE phase reflects the difference in dipole interaction of the PYE phase with La@C_ns with that of the PBB phase. Fuchs et al. analyzed the retention behavior of M@C_{82} (M=Y, La, Ce and Gd) in the PYE-toluene system, and estimated the effective dipole moment of M@C_{82}.[14] In the same manner, newly separated La@C_ns have larger dipole moments than La@C_{82}. This is consistent with the low solubility of these materials in nonpolar solvents such as toluene. We can expect a high solubility of La@C_ns in polar solvents such as pyridine, i.e., La@C_ns (n>78) were highly enriched in pyridine extract. However, La@C_{76}, La@C_{78}, and La@C_{80}, were not stable in pyridine. The exceptional instability of these molecules remains as an open question.

Some correlation between the HPLC elution behavior and the absorption spectrum of M@C_{82} has been reported in relation to the structure of the carbon cage and the oxidation state of the encapsulated metal atom(s).[14-17] Such similarity was also observed for the second (minor) isomers of La@C_{82} and Pr@C_{82}.[18] These lines of evidences indicate that the present separation procedure could be applied to Y and some lanthanoid metallofullerenes (Ce, Pr, Nd, Pm, Gd, Tb, Dy, Ho, Er, and Lu). Furthermore, absorption spectra of La@C_ns could be compared with these of M@C_ns, which will be obtained in the future.

The discussion of the electronic state of La@C_{82} has been based upon the results of ESR measurements, and the electronic state was subsequently described as $La^{3+}@C_{82}^{3-}$. This feature of a +3 oxidation state for the La metal with a -3 anion radical of the C_{82}

cage was deduced from the extraordinarily small isotropic hyperfine coupling (hfc) constant a_0 measured for the metal nucleus and a *g* factor similar to that of a C_{60}^{-} radical anion. The same order of magnitude of the hfc constant measured for La@C_n, compared with that of La@C_{82} (1.15 G for isomer I), and a *g* factor equal to approximately around 2 suggest that the electronic state of every La@C_n obtained can be described in terms of the same oxidation state of La^{3+} with a C_n^{3-} anion radical. More detailed discussion of the oxidation state of encapsulated La atom for each La@C_ns will be realized by conducting more ESR experiments. The topological cage structure is reflected by the specific values of the hfc constant and the *g* factor as well as the line width at room temperature. For example, the ESR spectrum at room temperature of La@C_{84}-II gives a_0=3.08 G with a line width (ΔHpp) of 0.231 G, in contrast to a_0=0.12 G and ΔHpp=0.05 G of La@C_{90}-IV. The difference in the parameter is also due to the spin dynamics of each topological isomer. In order to characterize the spin dynamics of each topological isomer, anisotropic components of hfc and g tensors and relaxation times T_1 and T_2 should to be measured. Measurements of the values of these parameters are in under way.

2. 4. Conclusion

ESR-active mono-lanthanofullerenes were separated by HPLC using chlorobenzene as eluent. The separation of La@C_n according to molecular weight was carried out by HPLC using PBB column. Further HPLC using a PYE column successfully separated La@C_{76}, La@C_{78}, topological isomers of La@C_{80}, La@C_{84}, La@C_{86}, La@C_{88}, and La@C_{90}. ESR and Absorption spectra of La@C_{76}, La@C_{78}, La@C_{80}-I, II, La@C_{84}-I, II, La@C_{86}-II, and La@C_{88}-I, II, III, were obtained for the first time. The confirmation of the purity of each ESR-active isomer La@C_n was realized by the combination of mass and ESR measurements. Some correlation between HPLC elution behavior and the absorption spectrum of M@C_{82} has been reported in relation to the structure of the fullerene cage and the oxidation state of the encapsulated metal atom(s).[14-18] From the analogous feature of the absorption spectrum of M@C_{82}, a similar elution behavior could be expected for Y and some lanthanoid metallofullerenes (Ce, Pr, Nd, Pm, Gd, Tb, Dy, Ho, Er, and Lu), and the present separation procedure could be applied.

3. 5. Appendix

Appendix 3A

2nd stage HPLC chromatogramn of La@Cn (n=76-90).

Figure 3A-1. 2nd stage HPLC chromatogramn of La@C_{76}.

Figure 3A-2. 2nd stage HPLC chromatogramn of La@C_{78}, La@C_{80}-I and II.

Figure 3A-3. 2nd stage HPLC chromatogramn of La@C_{82}-I and II.

Figure 3A-4. 2nd stage HPLC chromatogramn of La@C_{84}-I and II.

Figure 3A-5. 2nd stage HPLC chromatogramn of La@C_{86}-I and II.

Figure 3A-6. 2nd stage HPLC chromatogramn of La@C_{88}-I and II.

Figure 3A-7. 2nd stage HPLC chromatogramn of La@C_{90}-I, II, III and IV.

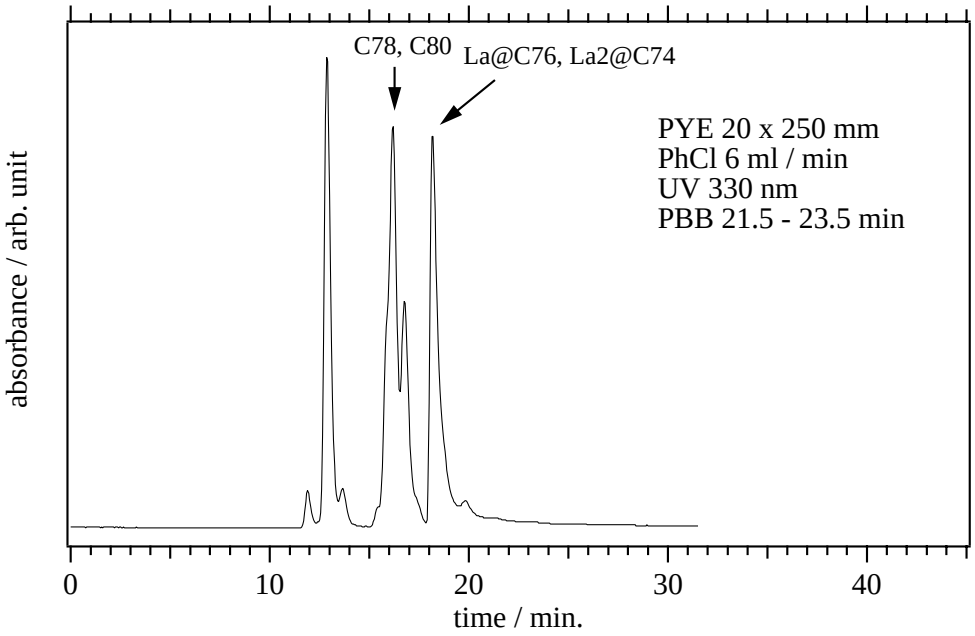

Figure 3A-1. 2nd stage HPLC chromatogramn of La@C_{76}.

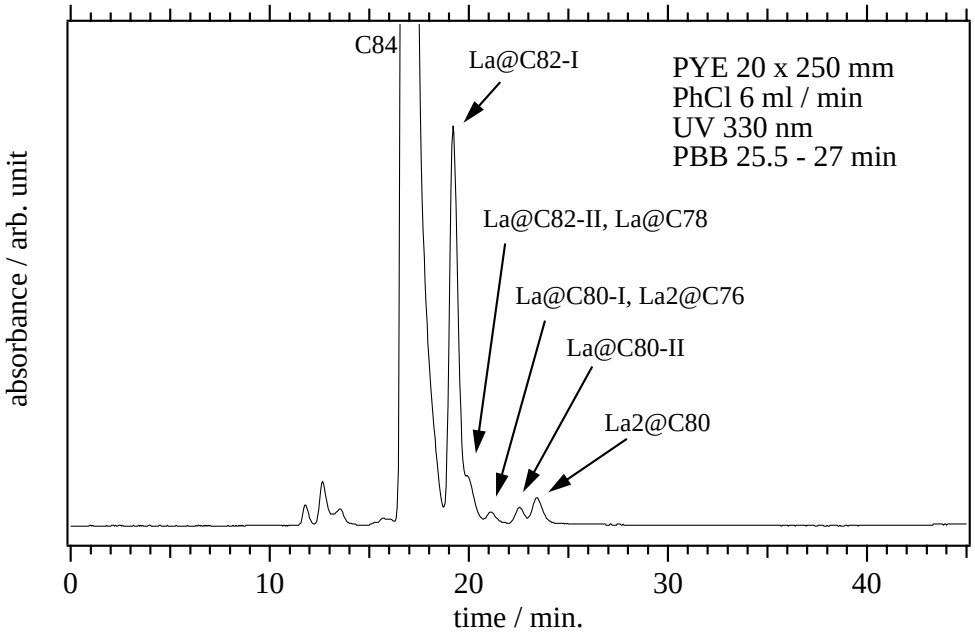

Figure 3A-2. 2nd stage HPLC chromatogramn of La@C_{78}, La@C_{80}-I and II.

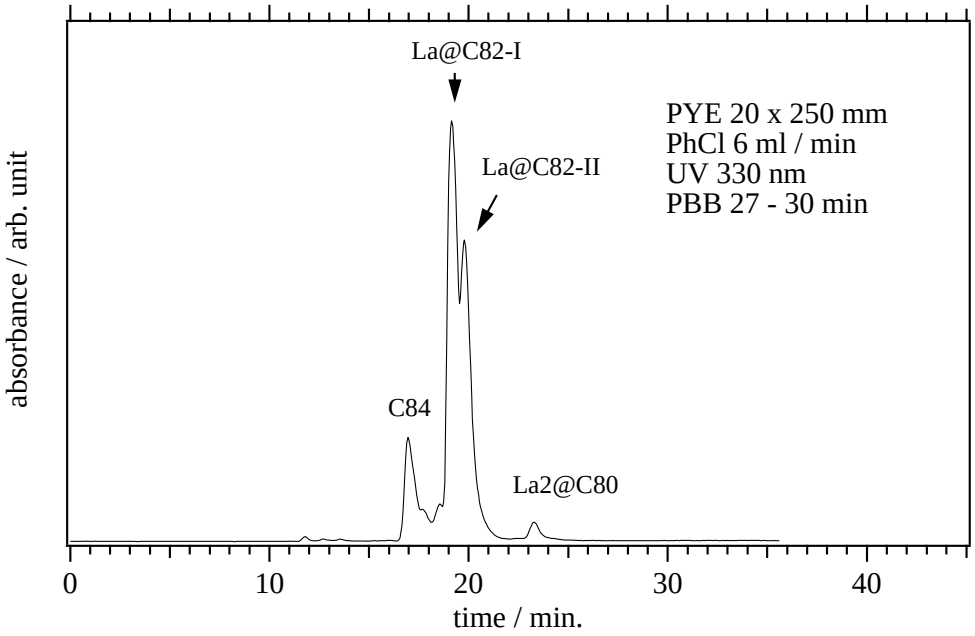

Figure 3A-3. 2nd stage HPLC chromatogramn of La@C_{82}-I and II.

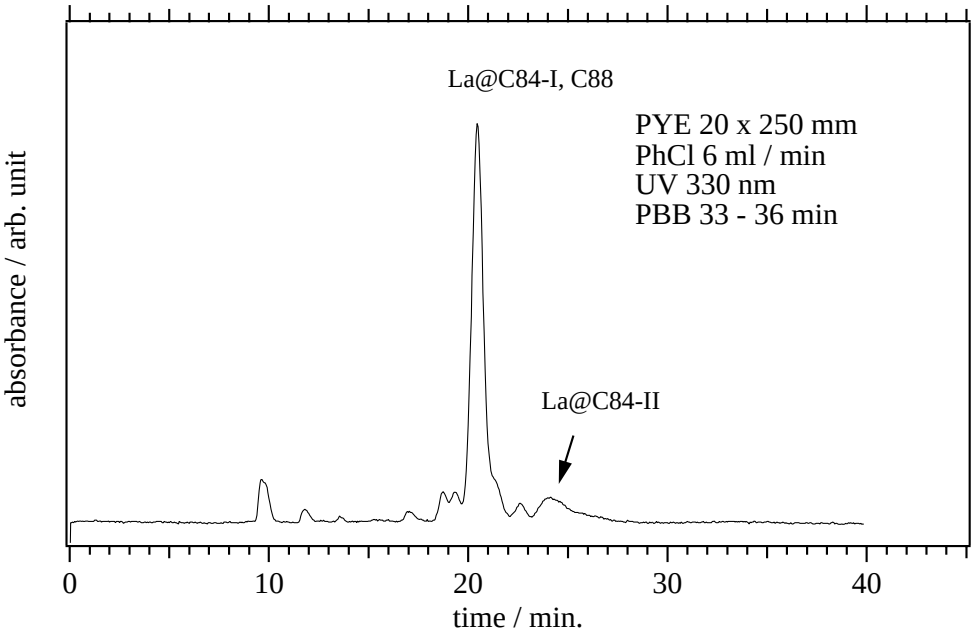

Figure 3A-4. 2nd stage HPLC chromatogramn of La@C_{84}-I and II.

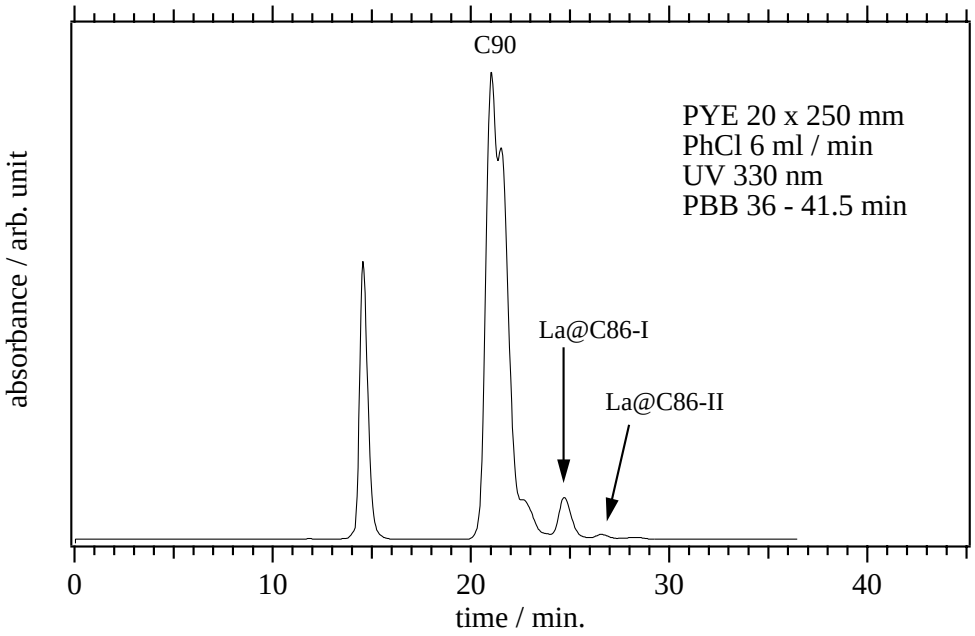

Figure 3A-5. 2nd stage HPLC chromatogramn of La@C_{86}-I and II.

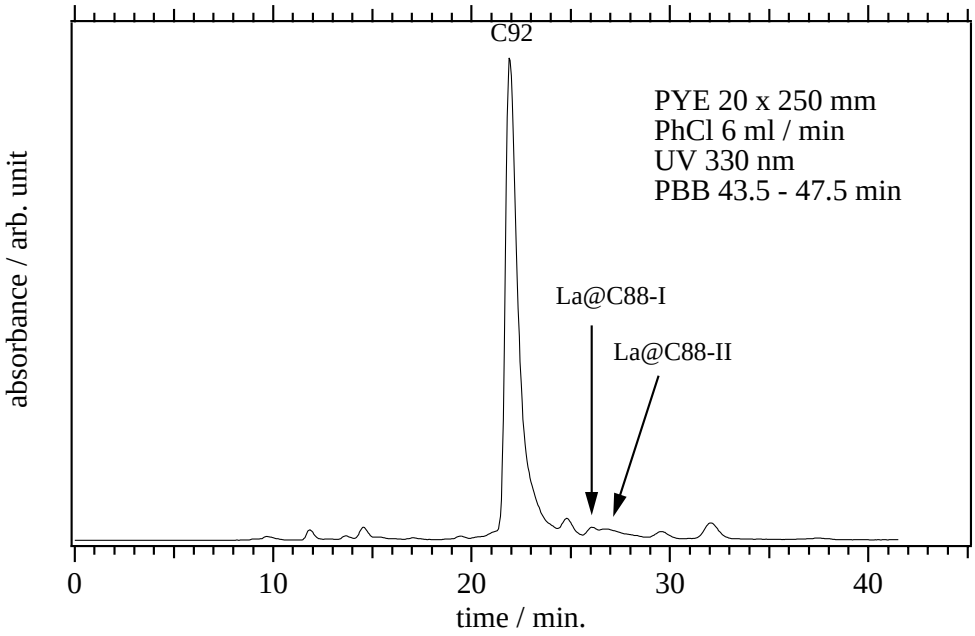

Figure 3A-6. 2nd stage HPLC chromatogramn of La@C_{88}-I and II.

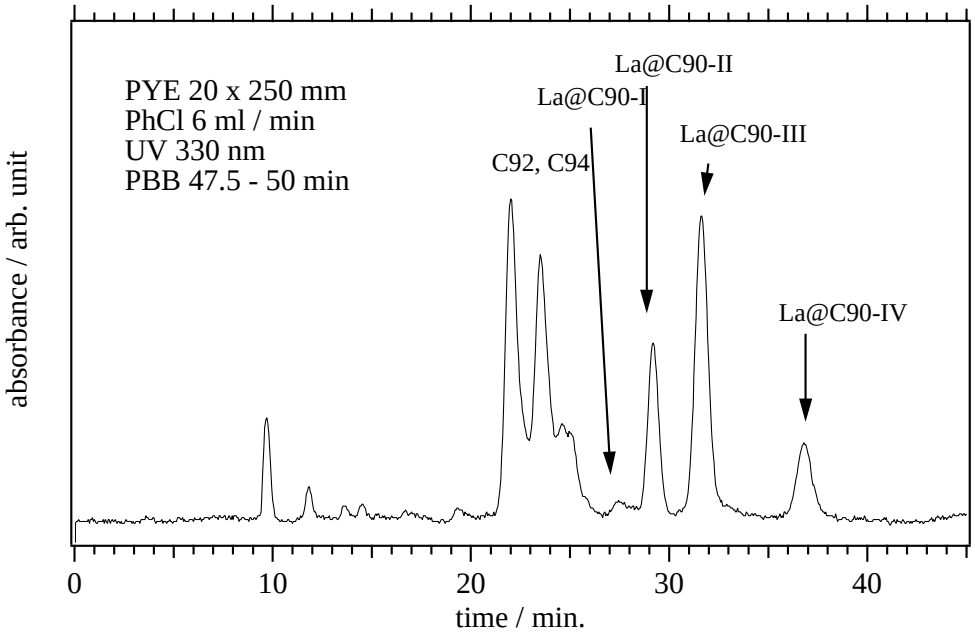

Figure 3A-7. 2nd stage HPLC chromatogramn of La@C_{90}-I, II, III and IV.

Chapter 4
Electronic Structures of Endohedral Metallofullerenes

4. 1. Introduction

Electromagnetic interaction of the outer cage with the encapsulated metal atom(s) is one of the interesting subject of the research of endohedral metallofullerenes, $M_x@C_n$ (M= Sc, Y, La and Lanthanides).[1] We can expect that the chemical and physical properties of metallofullerenes can be modulated by selecting the endohedral atom(s) and by changing the outer fullerene cage structure.[2-5] However, most of investigations were performed for $M@C_{82}$, which was the firstly observed and isolated species.[6-10] And especially $La@C_{82}$ was extensively investigated by using ESR spectroscopy.[11-17] The next interest is the cage structure dependence of these properties. The investigation of the other size of $M@C_n$ was limited because of their low abundance and especially of the low stability under atmosphere.[18-22] But our recent achievement on the separation technique made the characterization possible.

And the electronic structures of metallofullerene ions are the other interest. The change of the electronic structure toward the reduction and the oxidation opened the new direction of the metallofullrene chemistry. For example, the ^{13}C-NMR measurement of $La@C_{82}$ mono-anion could be performed because the electrochemical reduction quenches an unpaired electron on C_{82} cage.[23,24]

In this chapter, we investigated the systematic characterization of the series of La@Cns by using the temperature dependent ESR study in solution. The anisotropic parts of the ESR parameters such as the anisotropy of g factor (Δg), that of hyperfine coupling (hfc) tensor (Δa), and nuclear quadrupole interaction (NQI). The quantitative analysis of the isotropic and the anisotropic values was done to investigate the influence of the carbon cage structure upon the encapsulated La atom. As a result, it was found that the electronic structures of all $La@C_n$s was stabilized by the intramolecular charge transfer and described as $La^{3+}@C_n^{3-}$. Interesting feature such as the jumping among the Jahn-Teller distorted structures of carbon cage was suggested for $La@C_{80}$-I and $La@C_{84}$-II.

Furthermore, electronic structures of metallofullerene ions are also investigated by ESR spectroscopy. The W-band ESR of the anion and the cation of Gd@C82-I indicated that the oxidation state of an internal Gd ion was unchanged toward the reduction and the oxidation. In other word, The SOMO of Gd@C_{82}-I was the π-orbital of C_{82}. An interesting case is the anion of $La_2@C_{80}$, the excess electron lied on the internal La dimmer. In other ward, the LUMO of $La_2@C_{80}$ was derived from internal La dimmer. These conclusions of metallofullerene ions were consistent with previous theoretical calculations.

4. 2. ESR study of the series of isomer of La@C_n

4. 2. 1. Experimentals

The procedure of the production of the fullerene soot, the extraction, and the separation were reported elsewhere.[9,18,25] The soot containing La metallofullerenes was generated by the conventional arc discharge method. The series of the isomer of La@C_n, was separated by the 2-stage HPLC method using PBB and PYE with chlorobenzene eluent. Sample purity was checked by the laser desorption time of fright (LD-TOF) mass spectrometry and the ESR measurement, and the purity of more than 95 % was confirmed except for La@C_{78}. Samples for the ESR measurement were dissolved in CS_2, degassed by freeze-pump-thaw cycle, and sealed in thin wall quartz tube. ESR spectra were recorded by using Bruker ESP300E X-band spectrometer with liquid nitrogen temperature control unit. The measurements were done in the temperature range from 295 K to 161 K, that is the freezing point of CS_2. The field modulation frequency of 100 kHz with the microwave power less than 1 mW was used except for La@C_{90}-IV (the field modulation frequency of 25 kHz was used because of small hfc and linewidth).

4. 2. 2. Results and discussions

[Analysis of the ESR line width]

Figure 4-1 shows the temperature dependent ESR spectra of the two isomers of La@C_{84}, as an example, where the notations of isomer I, II, III and IV are the elution order in HPLC of PYE - chlorobenzene system.[25]. With lowering the temperature, minimum line width was observed at around 215 K, and the spectrum at 170 K showed

the fish bone like line pattern, which depend on the projection of the nuclear quantum number M_I. Furthermore, the minimum linewidth (the maximum intensity) was observed at the lowest magnetic field for La@C_{84}-I, but observed at the highest magnetic field for La@C_{84}-II. The specific spectral change could be interpreted by the rotational diffusion of a radical molecule in solution.[13,21,26]

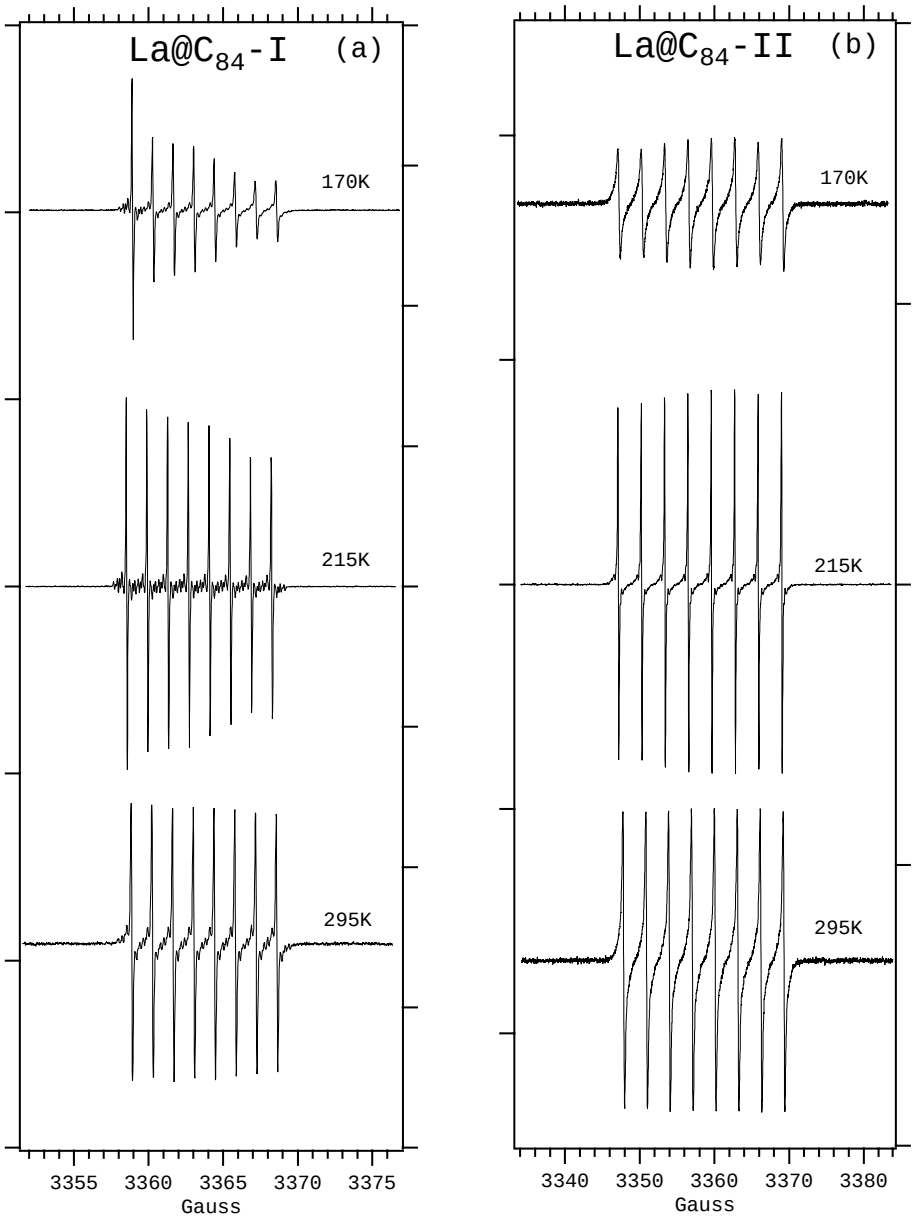

Figure 4-1. Temperature dependent ESR spectra of (a) La@C_{84}-I and (b) La@C_{84}-II in CS_2.

The line width at maximum slope ω_{msl} of the ESR spectrum was fitted to an expression of the form

$$\Delta\omega_{msl} = K_0 + K_1 M_I + K_2 M_I^2 + K_4 M_I^4 \qquad (1)$$

where coefficient K_i means;

$$K_0 = \frac{\hbar}{g_e \mu_B}\left\langle \begin{aligned} &\frac{1}{45}\left[\Delta g \frac{\mu_B B_0}{\hbar}\right]^2 \left\{4\tau_r + 3\frac{\tau_r}{1+(\omega_z\tau_r)^2}\right\} \\ &+\frac{1}{40}\left(\frac{2}{3}\Delta a\right)^2 I(I+1)\left\{3\tau_r + 7\frac{\tau_r}{1+(\omega_z\tau_r)^2}\right\} \\ &+\frac{3}{40}\left[\frac{eQV_{zz}}{I(2I-1)}\right]^2 I(I+1)\left[I(I+1)-1\right]\tau_r \end{aligned}\right\rangle$$

$$K_1 = \frac{\hbar}{g_e \mu_B}\frac{1}{15}\left[\Delta g \frac{\mu_B B_0}{\hbar}\right]\left(\frac{2}{3}\Delta a\right)\left\{4\tau_r + 3\frac{\tau_r}{1+(\omega_z\tau_r)^2}\right\} \qquad (2)$$

$$K_2 = \frac{\hbar}{g_e \mu_B}\left\langle \frac{1}{40}\left(\frac{2}{3}\Delta a\right)^2 \left\{5\tau_r - \frac{\tau_r}{1+(\omega_z\tau_r)^2}\right\} + \frac{3}{20}\left[\frac{eQV_{zz}}{I(2I-1)}\right]^2 I(I+1)\tau_r \right\rangle$$

$$K_4 = -\frac{\hbar}{g_e \mu_B}\frac{9}{40}\left[\frac{eQV_{zz}}{I(2I-1)}\right]^2 \tau_r$$

and

$$\tau_r = \left(\frac{n_C}{82}\right)^{\frac{3}{2}} \times \frac{14.5\times10^{-12}\exp(1350/T)}{T} + \left(\frac{n_C}{82}\right)\times\frac{8.1\times10^{-11}}{\sqrt{T}} \qquad (3)$$

here the parameters g_e, μ_B, ω_z, I, and M_I were the g-factor of the free electron, the Bohr magneton, the microwave frequency of measurement, the nuclear spin quantum number, and its projection.

The anisotropic parameters, Δg, Δa and $eQV_{zz}/I(2I-1)$ were estimated from linewidth coefficients, K_1, K_2 and K_4, respectively. The rotational correlation time τ_r was given by the analytical expression of eq. (3). Where the first term is the classical Stokes-Einstein term and the second denotes the "free rotator" correlation time.[13,21] The hybrid expression of the rotational correlation time τ_r was proposed by Rubsam et al. and well reproduced the hydrodynamics of metallofullerenes in solution.[13,21] We followed their expression of τ_r with including the fullerene size dependence with the symbol n_C which was the number of carbon atoms within a molecule. Figure 4-2 shows the temperature

dependences of linewidth coefficients K_1, K_2 and K_4 for two isomers of La@C_{84}, the marked point is the observed value and the solid line is the theoretical curve. The good agreement of the observed value with the theoretical curve, lines in figure 4-2, suggests the validity of the hybrid expression of τ_r given by eq. (3). Estimated anisotropic parameters, Δg, Δa and $eQV_{zz}/I(2I-1)$ for all molecules are tabulated in Table 4-1 with their isotropic components. The anisotropic parameters were plotted to the number of carbon atom in a molecule to clarify the dependence of each parameter on the cage size of molecule as in Figure 4-3.

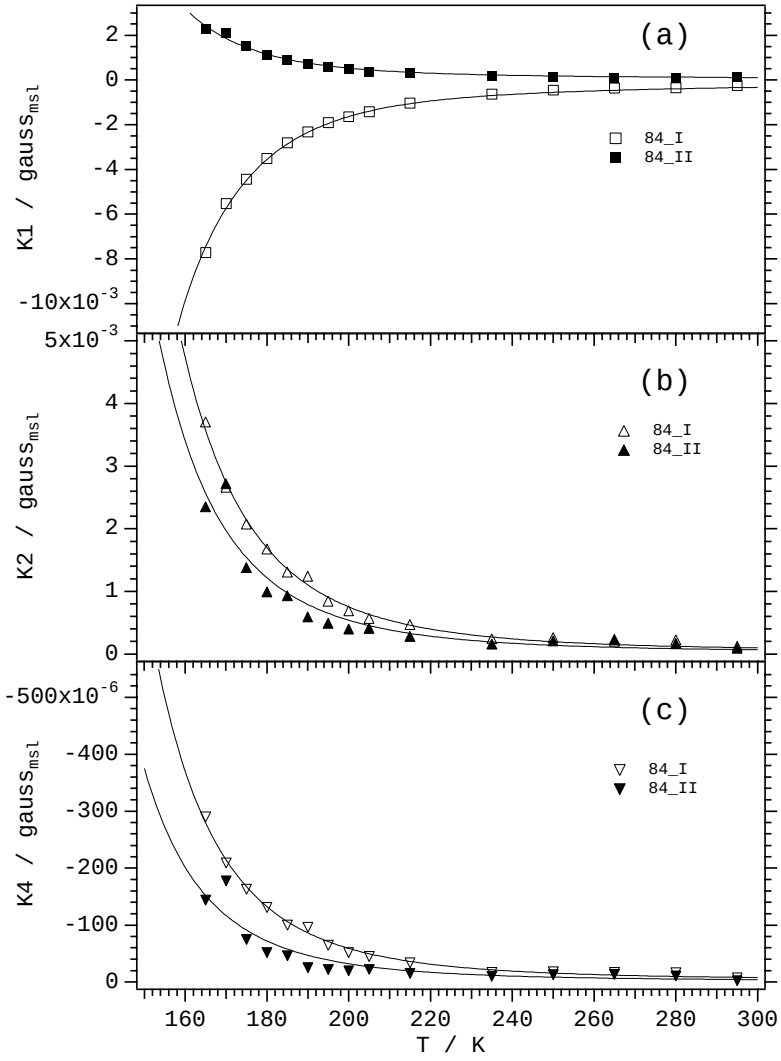

Figure 4-2. Temperature dependences of linewidth coefficients; (a) K_1, (b) K_2 and (c) K_4 of two isomers of La@C_{84} in CS_2. marked point: observed value, solid line: theoretical expression.

Table 4-1: ESR parameters of La@C_n isomers in CS_2

La@C_n	g_{iso}[a]	a_{iso} / Gauss[a]	Δg	Δa / MHz	eQVzz /I(2I-1) / MHz	ρ La-6s	ρ La-5d
La@C_{76}	2.0044	0.388	0.0039	1.76	1.20	0.0002	0.009
La@C_{78}	2.0013	1.540	-0.0009	3.78	0.69	0.0007	0.019
La@C_{80}-I	2.0010	2.405	0.0011	4.42	0.45	0.0011	0.022
La@C_{80}-II	2.0011	2.037	-0.0002	3.47	0.88	0.001	0.017
La@C_{82}-I	2.0008	1.150	-0.0062	4.89	1.71	0.0005	0.024
La@C_{82}-II	2.0002	0.830	-0.0027	4.87	1.82	0.0004	0.024
La@C_{84}-I	2.0012	1.380	-0.0040	5.21	1.70	0.0006	0.026
La@C_{84}-II	2.0040	3.080	0.0011	6.40	1.25	0.0014	0.032
La@C_{86}-I	2.0010	1.632	-0.0035	5.34	1.98	0.0008	0.026
La@C_{86}-II	2.0018	1.237	0.0010	2.14	3.38	0.0006	0.011
La@C_{88}-I	2.0018	1.545	-0.0015	3.08	1.77	0.0007	0.015
La@C_{88}-II	1.9991	1.262	-0.0111	6.43	3.00	0.0006	0.032
La@C_{88}-III	2.0017	0.582	0.0013	8.18	3.14	0.0003	0.040
La@C_{90}-I	2.0015	0.600	-0.0007	3.85	2.12	0.0003	0.019
La@C_{90}-II	2.0013	0.600	-0.0006	1.40	2.18	0.0003	0.007
La@C_{90}-III	2.0015	0.509	-0.0009	1.67	2.11	0.0002	0.008
La@C_{90}-IV	2.0025	0.121	-0.0025	1.71	3.39	$6x10^{-5}$	0.008

[a] data obtained at 295K

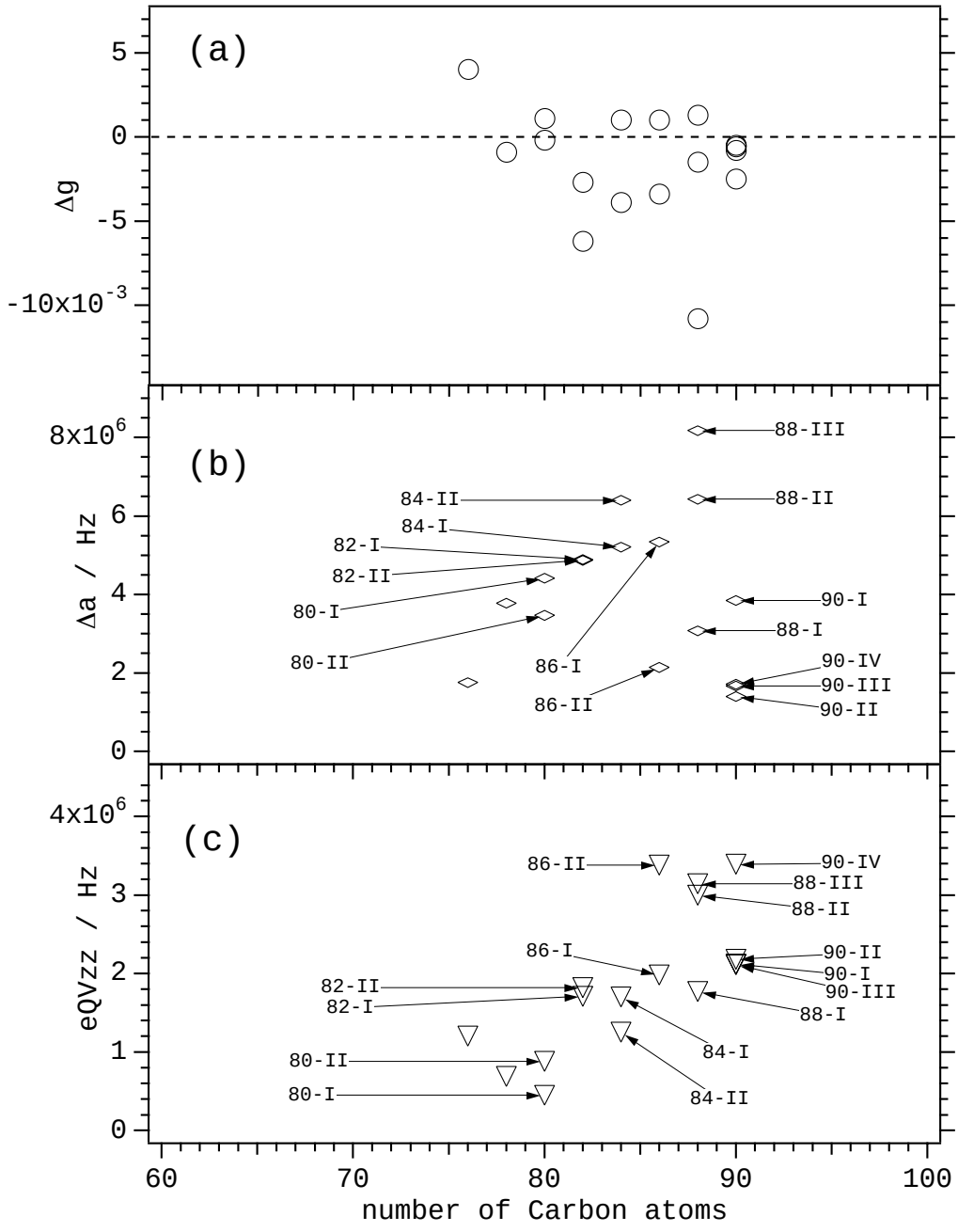

Figure 4-3. Anisotropic ESR parameters of La@C_n isomers versus fullerene size; (a) Δg, (b) Δa, and (c) eQVzz/I(2I-1).

[Hyperfine coupling constants]

The hyperfine term was originated from two types of interaction, the Fermi contact interaction and the dipolar interaction. The Fermi contact interaction is isotropic and its value relates to spin density on a nucleus. The dipolar interaction is due to the coupling of magnetic dipoles between an electron spin and a nuclear spin. The coupling is anisotropic, and is vanished by the averaging with a hydrodynamic rotation in solution during the time scale of ESR observation. Then the coupling is usually observed in solid sample or frozen solution. And in solution with high viscosity, the anisotropic coupling gives much effect on ESR spectra.

The spin densities ρ on 6s and $5d_z^2$ orbital of the La atom was estimated by comparing the value of isotropic and anisotropic part of hfc with the atomic data.[27] For the case of La@C_{82}-I, the a_{iso} of 1.15 gauss was compared with the atomic data of 2143.5 gauss, that is expected value of the unit spin density on 6s atomic orbital. And the spin density of 0.0005 on the 6s orbital of La atom was estimated. The anisotropic part Δa of 4.9 MHz was also compared with the atomic data of 237.1 MHz with the angular factor of (2/7) for the La $5d_z^2$ orbital. And the estimated spin density on this orbital is;

$$\frac{1}{3} \times 4.9 \Big/ \frac{2}{7} \times 237.1 = 0.024$$

where the factor of (1/3) comes from the normalization constant of the angular averaging. By combining the isotropic and the anisotropic contribution, we can estimate the total spin density of 0.0245 (~2.5 %) on an encapsulated La atom for the case of La@C_{82}-I, and the electronic structure of $La^{2.975+}@C_{82}^{2.975-}$ could be written.

We estimated the spin density on the La atom for all La@C_n. The isotropic hfc, a_{iso}, ranging from 0.12 gauss (La@C_{90}-IV) to 3.08 gauss (La@C_{84}-II), indicated the spin densities on 6s orbital from 0.00006 to 0.0014. And those on $5d_{zz}$ orbital from 0.007 (La@C_{90}-II) to 0.032 (La@C_{84}-II) was estimated from the anisotropy of hfc (Table 4-1). The total spin densities on encapsulated La atom from 0.007 (La@C_{90}-II) to 0.033 (La@C_{84}-II) were estimated. Although the total spin density varied with the size of carbon cage, the deviation was just minute. As a result it was concluded the electronic structure of all species could be described as $La^{3+}@C_n^{3}$.

The fullerene size dependence of Δa was crudely observed. The estimated value of Δa seemed to be increased with increase of the fullerene size from 76 to 84, but large scatter was observed from the size from 86 to 90. The reason of this relationship has not been clarified yet. Further investigations should be needed.

[*g* factors]

In our experiment, values of g_{iso} for La@C_ns were ranging from 1.9991 (La@C_{88}-II) to 2.0044 (La@C_{76}), which were close to the value of free electron, g_e = 2.0023. The sign of Δg, was estimated from the sign of the K_1 by assuming the positive sign of Δ*a*. And the estimated tensor components of g ($g_{\|}$ and $g_{\perp}$) were in good agreement with that observed in frozen toluene solution for the most of La@C_n (see appendix).

The isotropic g factors close to g_e indicated that all molecules could be assigned to the spin doublet state without any degeneracy. And this led appropriate figure of the electronic state with one radical spin on the π orbital of the fullerene cage. The deviation of the g-tensor from g_e could be explained by the second-order perturbation theory. The excited electronic configuration *m* mixed in the ground state *t* gives the deviation of the g-factor respect to g_e through the spin-orbit coupling constant ζ. The tensor component g_{pp} was expressed by;

$$g_{pp} - g_e = g_e \zeta \sum_{m \neq t} \frac{\left| \langle \psi_t | l_p | \psi_m \rangle \right|^2}{\varepsilon_t - \varepsilon_m} \qquad (4)$$

p = x, y, z

The sign of g_{pp}- g_e relate to the configuration of two electronic state and we could estimated from the type of excitation. The configuration of the type of electron gives the minus sign of g_{pp}- g_e, and that of hole promotion gives the positive sign. The deviation of $g_{\|}$ and $g_{\perp}$ dispersed around 2.0023 with both positive and negative sign. The feature is inherent to the electronic structure of La@C_ns. For example, La@C_{76} and La@C_{84}-II exhibited the larger value of the g-tensor than 2.0023 ($g_{\|}$ = 2.0071, $g_{\perp}$ = 2.0031 for La@C_{76} and $g_{\|}$ = 2.0047, $g_{\perp}$ = 2.0037 for La@C_{84}-II). The low-lying excited configuration must be that of the type of hole promotion.

[Nuclear quadrupole interaction]

Values of NQI roughly increased with increasing the fullerene cage size. The NQI is originated from the interaction between the nuclear quadrupole moment and the electronic field gradient (EFG) at the lanthanum nucleus. The EFG is originated from the outer valence shell electrons, the surrounding charge distribution, and the polarization effect of the inner closed shell electrons, which is caused by the surrounding non-spherical charge distribution. In our system the electronic structure was found to be $La^{3}+@C_n^{3-}$ for all $La@C_n$. This means that internal lanthanum ion has the closed shell electronic state as that of xenon. Then the contribution of outer valence shell electron at the encapsulated La atom could be neglected. Thus the modulation of the value of EFG could be attributed to the surrounding fullerene cage. The simple consideration indicated that the observed fullerene cage size dependence of the value of NQI suggests that the distance from encapsulated La ion to unpaired electron decreases with increasing the fullerene cage size, because of the $1/r^3$ dependence of the EFG. We estimated the nearest metal-carbon distance from the value of NQI with the reported nearest metal-carbon distance of 2.55 Å from X-ray diffraction study of $La@C_{82}$-I.[28] The 3.39 MHz of NQI, the maximum value in this study, corresponds to 2.03 Å for $La@C_{90}$-IV, and the minimum value of 0.45 MHz corresponds to 3.98 Å for $La@C_{80}$-I. The value for $La@C_{80}$-I is slightly smaller than the radius of C_{80} (4.10 Å). This indicates that La ion is in the center of C_{80} cage. And the result would suggest the highly symmetric cage structure, such as I_h, for $La@C_{80}$-I.

[Additional line broadening mechanism]

In the line width formula, term of K_0 has other components except for anisotropic *g*, *a*, and quadrupole interactions, such as spin-rotation, exchange and dipole-dipole interactions. For all $La@C_n$, values of K_0 showed the parabolatic temperature dependence. This indicates the presence of the spin-rotation interaction, which is proportional to $(\Delta g)^2$ and to T/τ. However, In all case, high temperature region of the linewidth coefficient K_0 could not be expressed by only adding spin-rotation contribution and constant value of about 0.027 gauss should be added to all temperature range. The constant term may be originated from unresolved ^{13}C-hyperfine couplings or inhomogeneity of the spectrometer, but the other term, which depends on T/τ, should be

remained. The interesting cases were fond for La@C_{80}-I and La@C_{84}-II. Relatively large M_I independent line width was observed at high temperature region. And spectra at 215 K, which correspond to the minimum linewidth, showed the less characteristic ^{13}C-hyperfine structure. The temperature dependences of linewidth coefficient K_0 for La@C_{80}-I, La@C_{82}-I and La@C_{84}-II are shown in Figure 4-4. For La@C_{80}-I and La@C_{84}-II, The increasing of the line width at high temperature is too large to be explained by spin-rotation interaction and disappearance of the ^{13}C-hyperfine structures could not be explained by mechanisms discussed above.

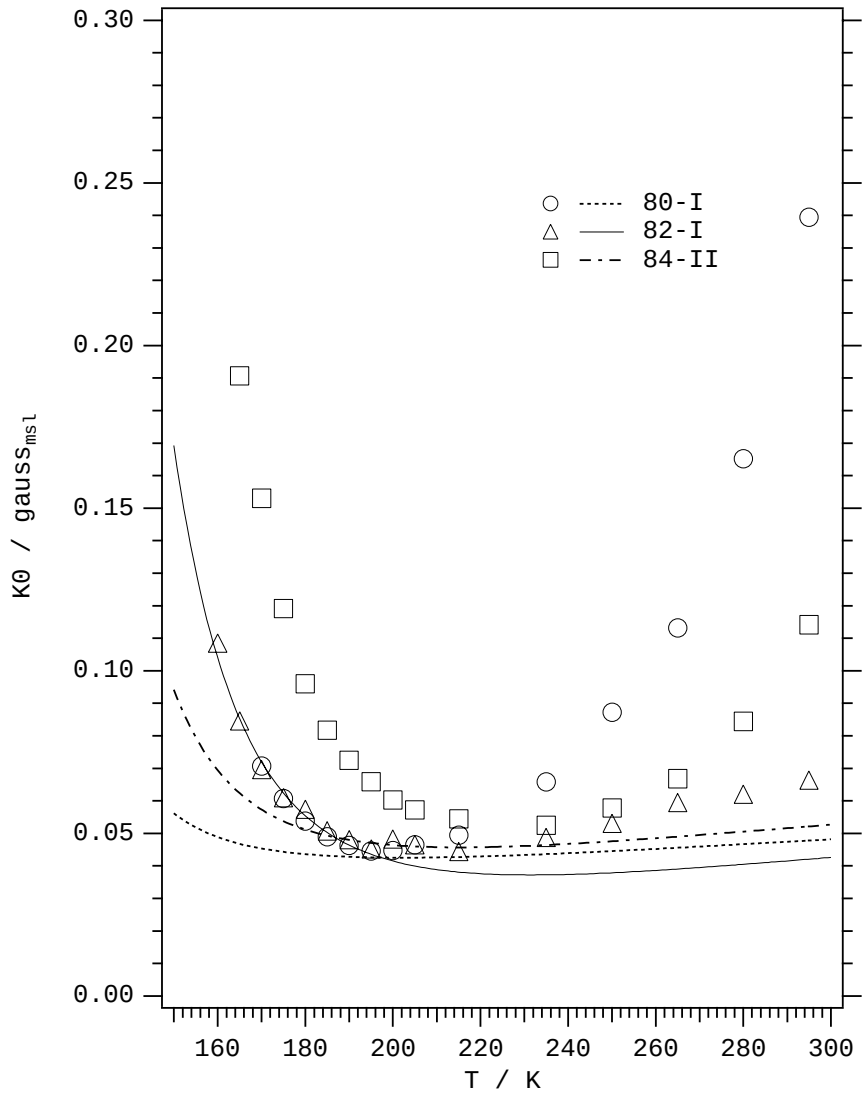

Figure 4-4. Linewidth coefficient K_0 versus temperature for (a) La@C_{82}-I, (b) La@C_{80}-I, and (C) La@C_{84}-II. Lines indicate the theoretical curve.

Figure 4-5 shows the Arrhenius plot of the high temperature region of the residual linewidth contributions to coefficient K_0, which is not expressed by the theory discussed above. The large and linear 1/T dependences of this additional contribution for La@C_{80}-I and La@C_{84}-II, relative to that of La@C_{82}-I, indicated the presence of the unspecified thermally accessible process for above two metallofullerenes. The energy gaps of this unknown process were roughly estimated as 1750 cm^{-1} and 1740 cm^{-1} for La@C_{80}-I and La@C_{84}-II, respectively. The same treatment of the ESR linewidth at high temperature region was performed for Lu@C_{82}, and the origin of the relaxation process with the activation energy of 2280 cm^{-1} was also unspecified. [29]

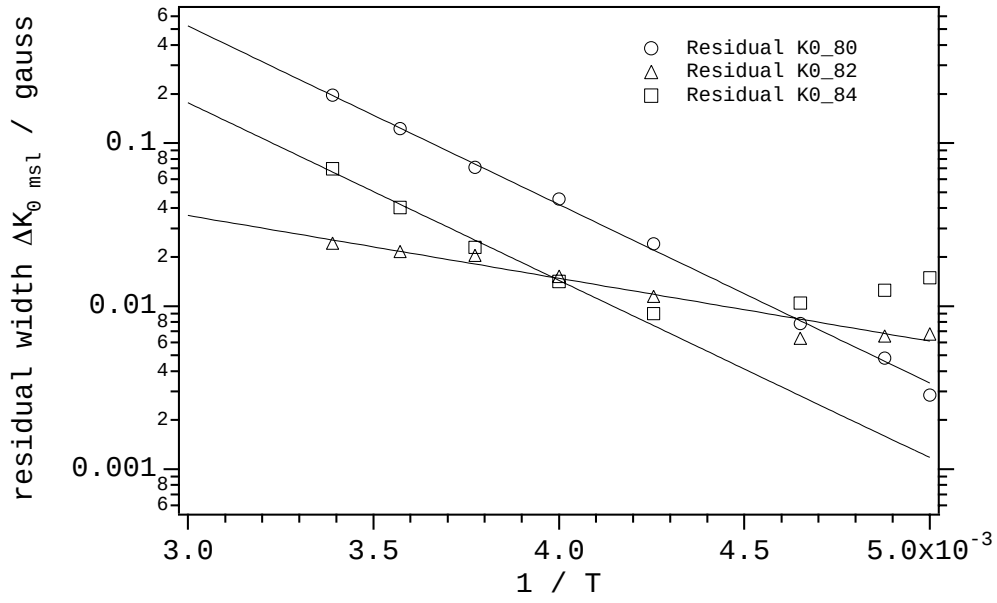

Figure 4-5. Residual linewidth coefficient ΔK_0 versus 1nverse of temperature for La@C_{82}-I, La@C_{80}-I, and La@C_{84}-II. Lines indicate the curve fitting by the equation: $\Delta K_0 = a + b \exp(-c/kT)$.

The origin of this thermally accessible process for above two metallofullernes would be attributed to the follwing mechanisms. One might be originated to the jumping motion of the internal La atom among some local potential minima inside the tri-negative fullerene cage. The energy barriers of the hopping process were small enough for La@C_{80}-I and La@C_{84}-II. The internal motion of the internal atom was suggested by the NMR study of La_2@C_{80}, and the similar value of the activation energy of the internal rotation of La_2 of about 5 k cal/mol (1750 cm^{-1}) was estimated.[2]

The other possibility is the Jumping among the Jahn-Teller distorted structures of the cage. According to the isolated pentagon rule (IPR), 7 ($2C_{2v}$, D_2, D_3, D_{5d}, D_{5h} and I_h) cage isomers of C_{80}, and 24 (C_1, $5C_s$, $5C_2$, $4C_{2v}$, $4D_2$, $2D_{2d}$, D_{3d}, D_{6h} and T_d) cage isomers of C_{84} are plausible.[30] In the IPR-allowed isomers, the cage structure of D_3, D_{5d}, D_{5h} and I_h could be suggested for La@C_{80}-I, and in the same way, the cage structure of D_{2d}, D_{3d}, D_{6h} and T_d could be suggested for La@C_{84}-II. Figure 4-6 shows the simple MO diagrams of C_{84} with D_{2d} and T_d symmetry. The LUMO of the D_{2d} structure is doubly degenerated. And the resultant electronic structure after the intramolecular charge transfer of La@C_{84} attains to the degeneracy and the open shell nature. The similar case can be expected for the T_d structure. We have to note here, the off-center position of the endohedral metal can break the high symmetry of hte total molecular system. However, pseud Jahn-Teller effect could be expected. The estimated values of the activation energies for La@C_{80}-I and La@C_{84}-II should be compared with that the theoretical calculation of the energy potential.

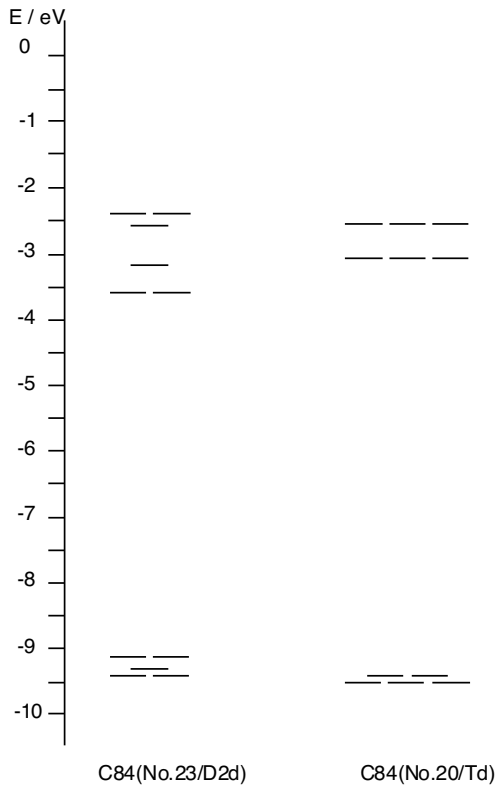

Figure 4-6. MO diagrams of C_{84}.

4. 3. Electronic structures of metallofullerene ions

4. 3. 1. Experimentals

An endohedral metallofullerene samples were prepared and separated according to the method reported before[25]. The sample purity of more than 95 % was confirmed by laser desorption time of flight mass (LD-TOF MASS, Kratos Kompact MALDI IV) and X-band ESR (Bruker ESP300E) measurements. Pyridine, *o*-dichlorobenzene (ODCB), 1, 2, 4-trichlorobenzene (TCB), and carbon disulfide (CS_2) were used as purchased. Electrochemical-grade tetra-*n*-butylammonium perchlorate (TBAP), purchased from Wako, was recrystallized from absolute ethanol and dried under vacuum at 313 K prior to use. Or tetra-*n*-butylammonium perfluorate (TBAF) was used as purchased. Bulk controlled-potential electrolysis of $M@C_{82}$ was used to prepare the corresponding anion and cation using a potentiostat/galvanostat (BAS CW-50). Solutions containing $[Gd@C_{82}]^-$, $[Gd@C_{82}]^+$, and $[La_2@C_{80}]^-$ were obtained in ODCB containing 0.2 M TBAP by setting the applied potential at 150 - 250 mV more negative or more positive than $E_{1/2}$ for the $Gd@C_{82}/[Gd@C_{82}]^-$, $[Gd@C_{82}]^+/Gd@C_{82}$, and $La_2@C_{80}/[La_2@C_{80}]^-$ redox couple, respectively. [23 31 32] Chemical reduction was performed by dissolving in pyridine (DMF) or by mixing with DBU (1,8-diazabicycro[5,4,0]-7-undecene, Wako) in ODCB, which were used as purchased. [33] Chemical oxidation was performed by mixing with MB (tris-(4-bromophenyl)aminium hexachloroantimonate, Aldrich) in ODCB. [34] Vis-NIR spectra were recorded on Hitachi U-3500 spectrophotometer. The W-band ESR measurement was carried out by Bruker E680 spectrometer.

3. 3. 2. Results and discussions

[Anion and cation of $Gd@C_{82}$-I]

$Gd@C_{82}$-I in CS_2 solution gave a Vis-NIR spectrum similar to that of $La@C_{82}$-I, which indicates the identical valence electronic structure of two metallofullerenes. [35] A comparable solvation effect on $Gd@C_{82}$-I by pyridine (DMF) was also observed. The specific absorption band at 980 nm in CS_2 was blue-shifted to the band at 900 nm in pyridine, and the spectrum in pyridine was again identical with that of the anion as shown in Figure 4-7(c). The X-band ESR spectrum of $Gd@C_{82}$-I in pyridine was equivalent with that of the anion (Figure 4-8).

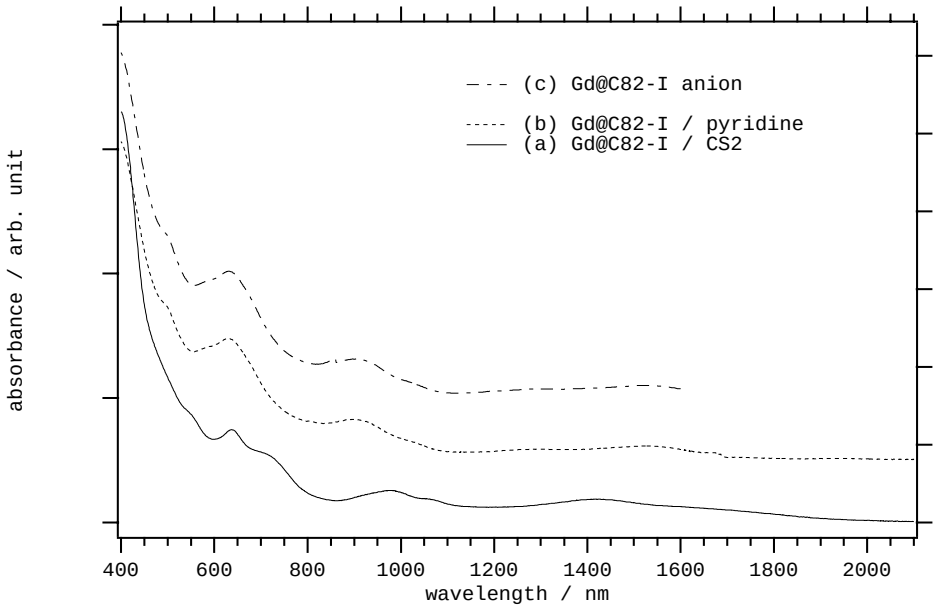

Figure 4-7. Vis-NIR spectra of Gd@C_{82}-I in (a) CS_2, (b) pyridine, and (c) electrochemically generated Gd@C_{82}-I anion in ODCB.

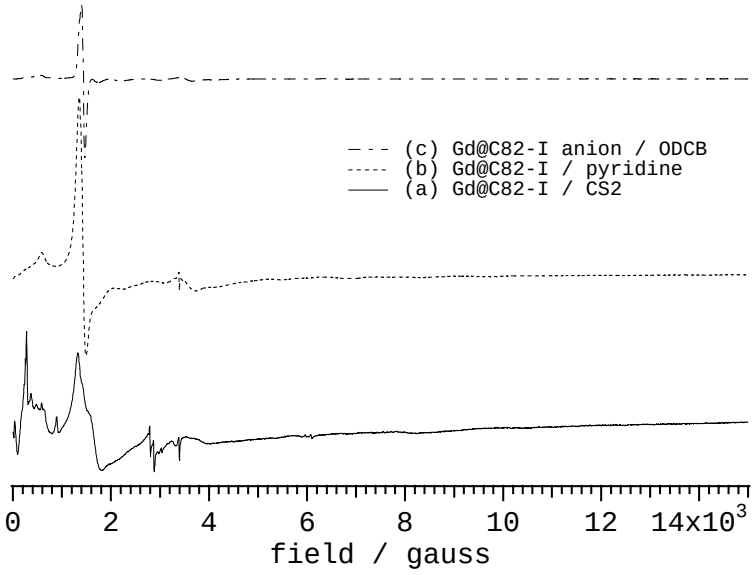

Figure 4-8. X-band ESR spectra of Gd@C_{82}-I in (a) CS_2, (b) pyridine, and (c) electrochemically generated Gd@C_{82}-I anion in CS_2 and acetone. All spectra are obtained at 3 K.

Addition of the electrolyte of TBAF, which act as a phase transfer cataryst, played an important role to stabilize the Gd@C_{82}-I anion. The ESR signal of Gd@C_{82}-I became sharper by adding TBAF and the spectrum was unchanged when the solvent was exchanged to ODCB, as in Figure 4-9. The same trend was observed in the Vis-NIR spectrum (Figure 4-10(b)).

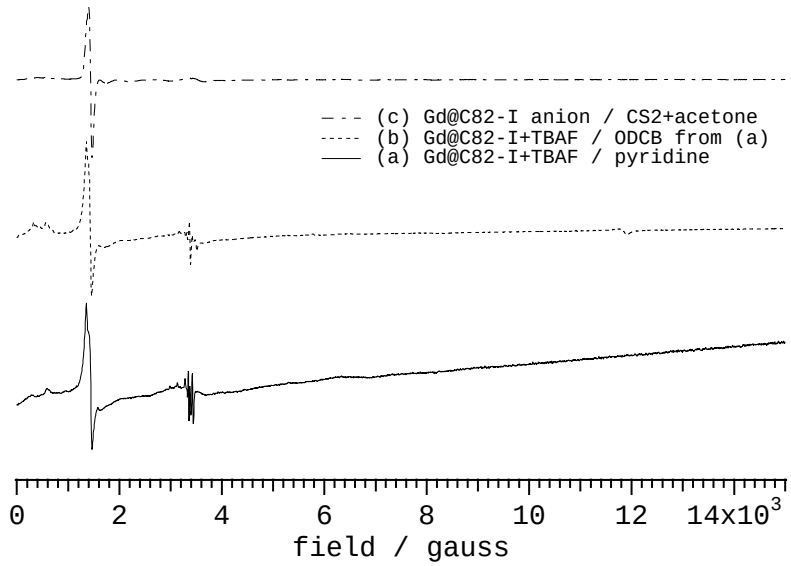

Figure 4-9. X- band ESR spectra of Gd@C_{82}-I with TBAF in (a) pyridine and (b) ODCB obtained from (a). Line (c) shows the electrochemically generated Gd@C_{82}-I anion in CS_2 and acetone. All spectra are obtained at 3 K.

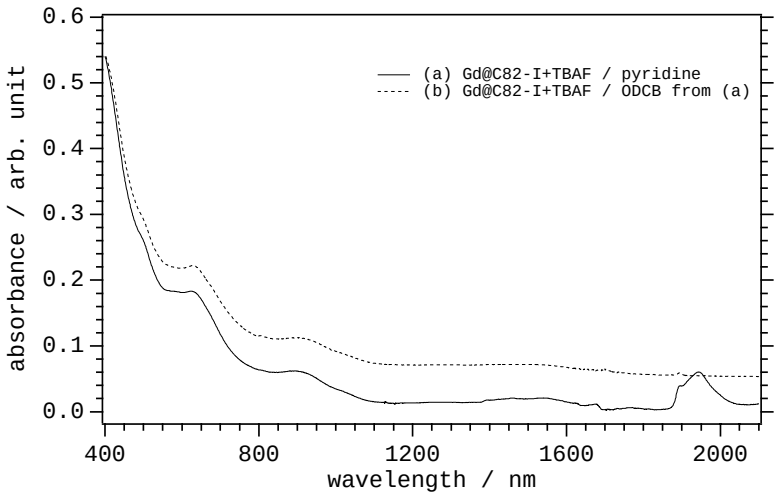

Figure 4-10. Vis-NIR spectra of Gd@C_{82}-I with TBAF in (a) pyridine and (b) ODCB obtained from (a).

The chemical oxidation of Gd@C_{82}-I was investigated. As shown in Figure 4-11, the spectrum of Gd@C_{82}-I (line (a)) was changed to its cation by adding the oxidant of MB (line (b)), which is similar to that of an electrochemically generated La@C_{82}-I cation (line (c)). The spectral change of Gd@C_{82}-I was also observed in the ESR measurement (Figure 4-12). The spectral feature of Gd@C_{82}-I cation was slightly different, but the outline was similar to that of the neutral form. The comparison of the ESR spectra of the anion and cation of Gd@C_{82}-I with that of neutral one suggest that the electronic structure of an endohedral Gd ion unchanged from that of the neutral one through reduction or oxidation process.

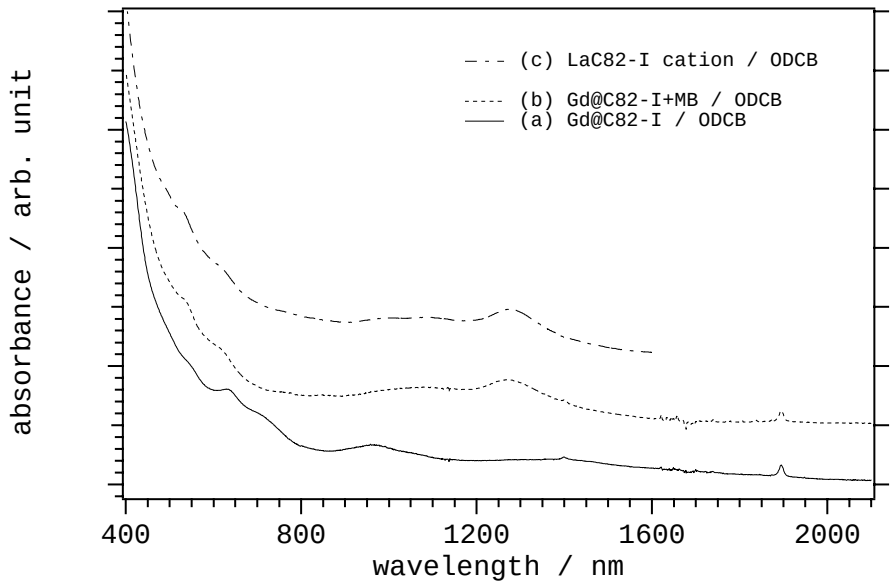

Figure 4-11. Vis-NIR spectra of Gd@C_{82}-I (a) in ODCB, (b) with MB in ODCB. Line (c) shows the electrochemically generated La@C_{82}-I anion in ODCB for comparison.

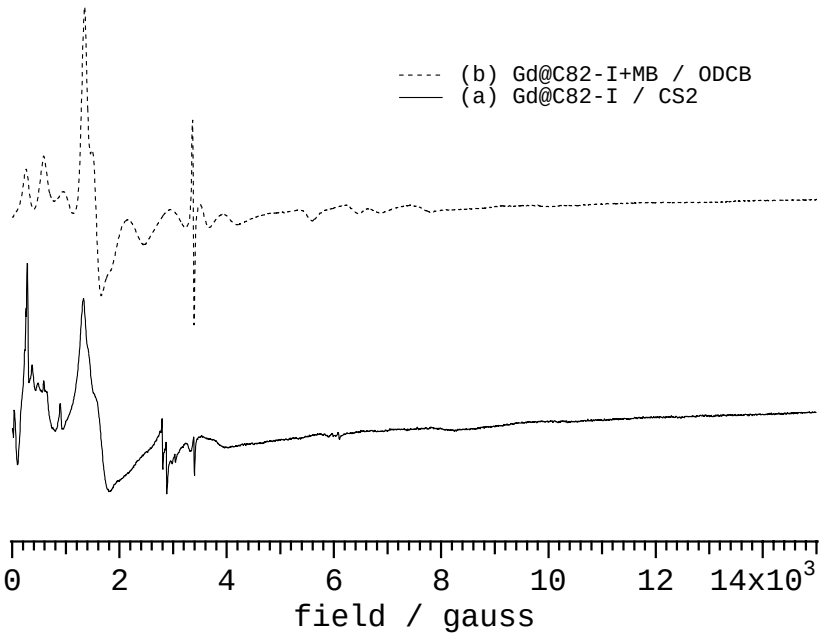

Figure 4-12. X- band ESR spectra of Gd@C_{82}-I (a) with MB in ODCB, and (b) in CS_2. All spectra are measured at 3 K.

The X-band ESR measurement on Gd@C_{82}-I ions suggest the invariant spin state (electronic structure) of Gd^{3+} ion, However, in the X-band experiment, zero-field splitting, which arise from the interaction between two or more numbers of unpaired electrons, were relatively large compared to the electron Zeeman interaction and the simple perturbation theory could not be applied to determine these spectroscopic parameters. Further confirmation of the electronic structure of the anion and cation of Gd@C_{82}-I were performed by the W-band (95 GHz) ESR measurement. Figure 4-13 shows the W-band ESR spectra of Gd@C_{82}-I ions with their simulated spectra. Experimental spectra of Gd@C_{82}-I ions were in good agreement with those of simulated ones with the parameters in table 4-2. W-band ESR spectra were simulated with the spin state of 7/2 for both the anion and the cation of Gd@C_{82}-I, and we straightly concluded the invariant electronic configuration of $4f^7$ of internal Gd^{3+} ion.

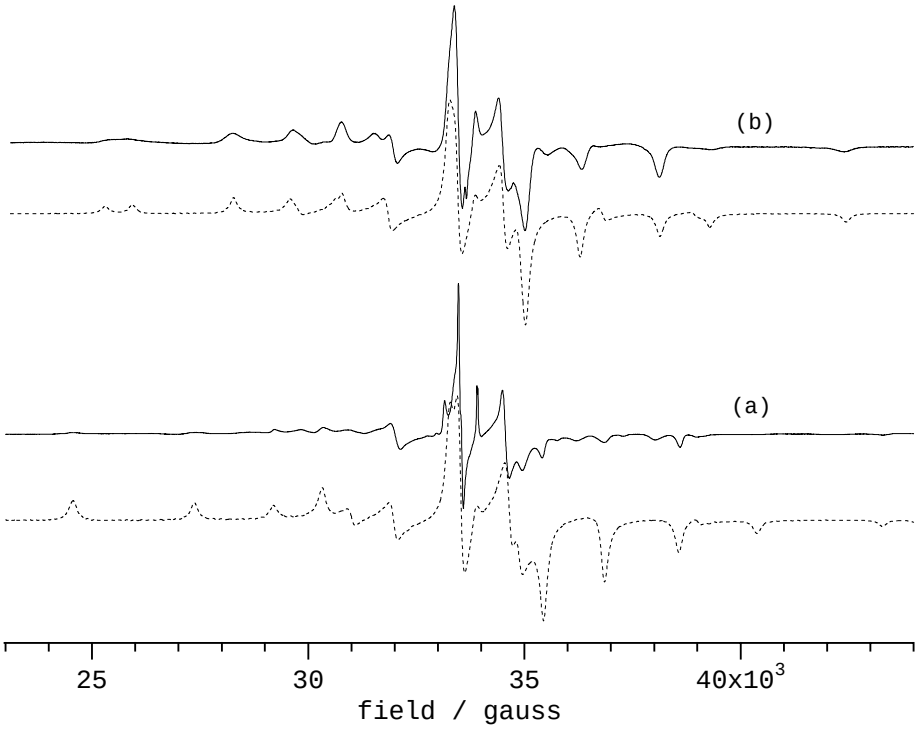

Figure 4-13. W-band ESR spectrum of (a) anion, (b) cation, of Gd@C_{82}-I at 20 K. Broken lines are corresponding simulations.

Table 4-2: ESR parameters of Gd@C_{82}-I ions

parameter	Gd@C_{82}-I anion	Gd@C_{82}-I cation
S	7/2	7/2
g_1	1.985	1.992
g_2	1.990	1.992
g_3	1.993	1.992
D / cm^{-1}	0.218	0.199
E / cm^{-1}	0.019	0.019

Our conclusion of the electronic structure of Gd@C_{82}-I was depicted in Figure 4-14. The valence state of an internal Gd ion was unchanged to +3 toward the reduction and the oxidation of Gd@C_{82}-I. In other word, the SOMO of Gd@C_{82}-I is derived from a π-orbital of C_{82}, and the reduction and the oxidation also occur on the C_{82} cage. This was in good agreement with the previous theoretical calculations of La@C_{82}-I, which has the same electronic configuration to that of Gd@C_{82}-I.[23] Theory predicted the almost invariable charge density on La atom by the reduction and the oxidation of La@C_{82}-I.

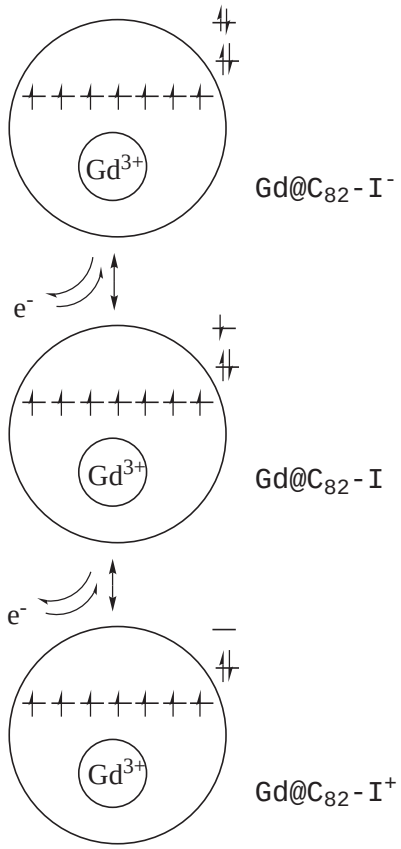

Figure 4-14. Proposed electronic structure of Gd@C_{82}-I ion

[Anion of $La_2@C_{80}$]

The formation of the $La_2@C_{80}$ anion by the solvation of pyridine was proved in previous chapter, by comparing the absorption and the ESR spectrum with that of electrochemically or chemically generated anion.

Figure 4-15 shows the X-band ESR spectra of $La_2@C_{80}$ in mixed solvent (TCB: CS_2: pyridine = 1:3:2, vv) at the temperature range from 295 to 180 K. The linewidth of the signal decreased with decreasing the temperature from 295 to 215 K, and the signal again broadened with decreasing the temperature to the freezing point of the solution. Such a temperature dependence of the linewidth was observed for $La@C_n$s, reported in previous section. At the high temperature region the narrowing of the linewidth was due to the spin-rotation interaction, and the broadening of the linewidth at low temperature region was due to the anisotropic ESR parameters, such as Δg, Δa, and the quadrupole interaction. Figure 4-16 shows the ESR (X-band) spectra of $La_2@C_{80}$ in mixed solvent (TCB: CS_2: pyridine = 2:3:2, vv) at the temperature range from 180 to 80 K. The sample solution was still frozen, but the further spectral change was observed by lowering the temperature. Such a spectral change in the frozen solution might be attributed to the internal motion of the La dimmer. And the threshold energy of c. a. 0.2 k cal / mol (~120 K) was estimated. The spectral feature was not changed at the temperature bellow 100 K, which may be attributed to the increase of the longitudinal relaxation time, T_1.

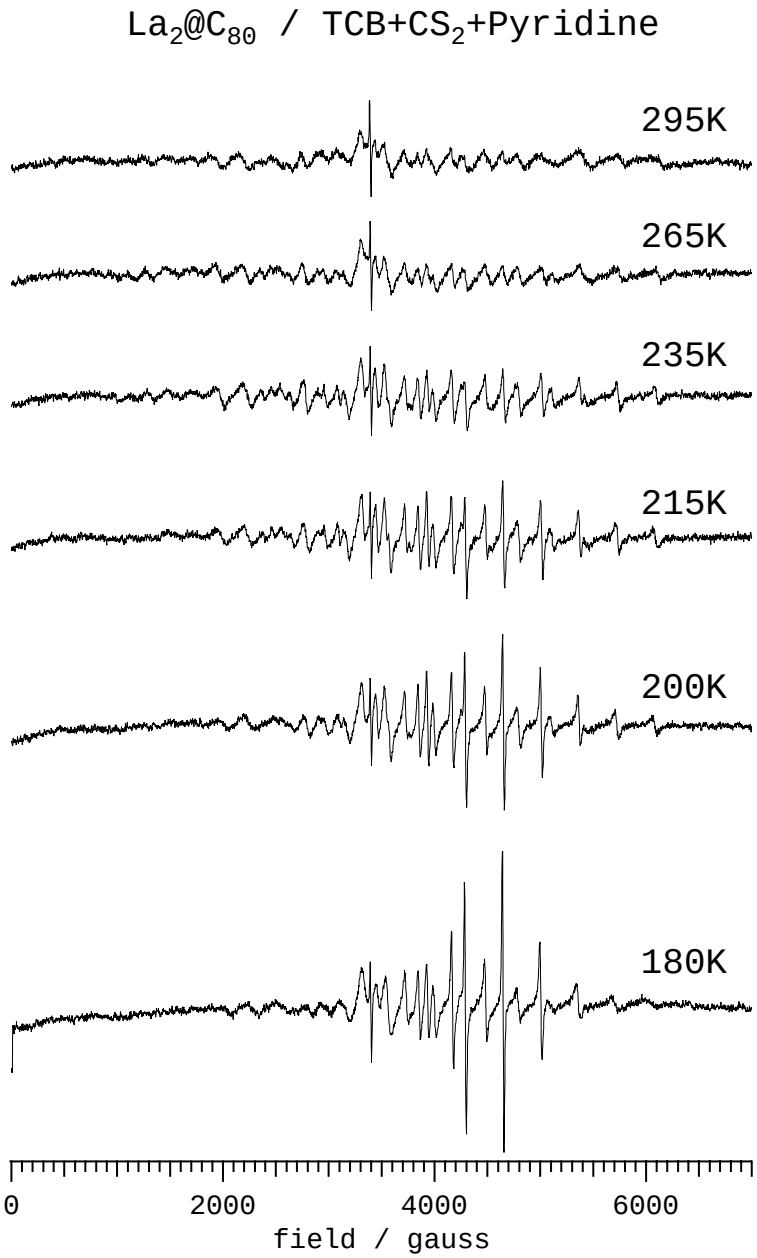

Figure 4-15. X- band ESR spectra of $La_2@C_{80}$ in TCB: CS_2: pyridine (1:3:2, vv) at the temperature range from 295 K to 180 K

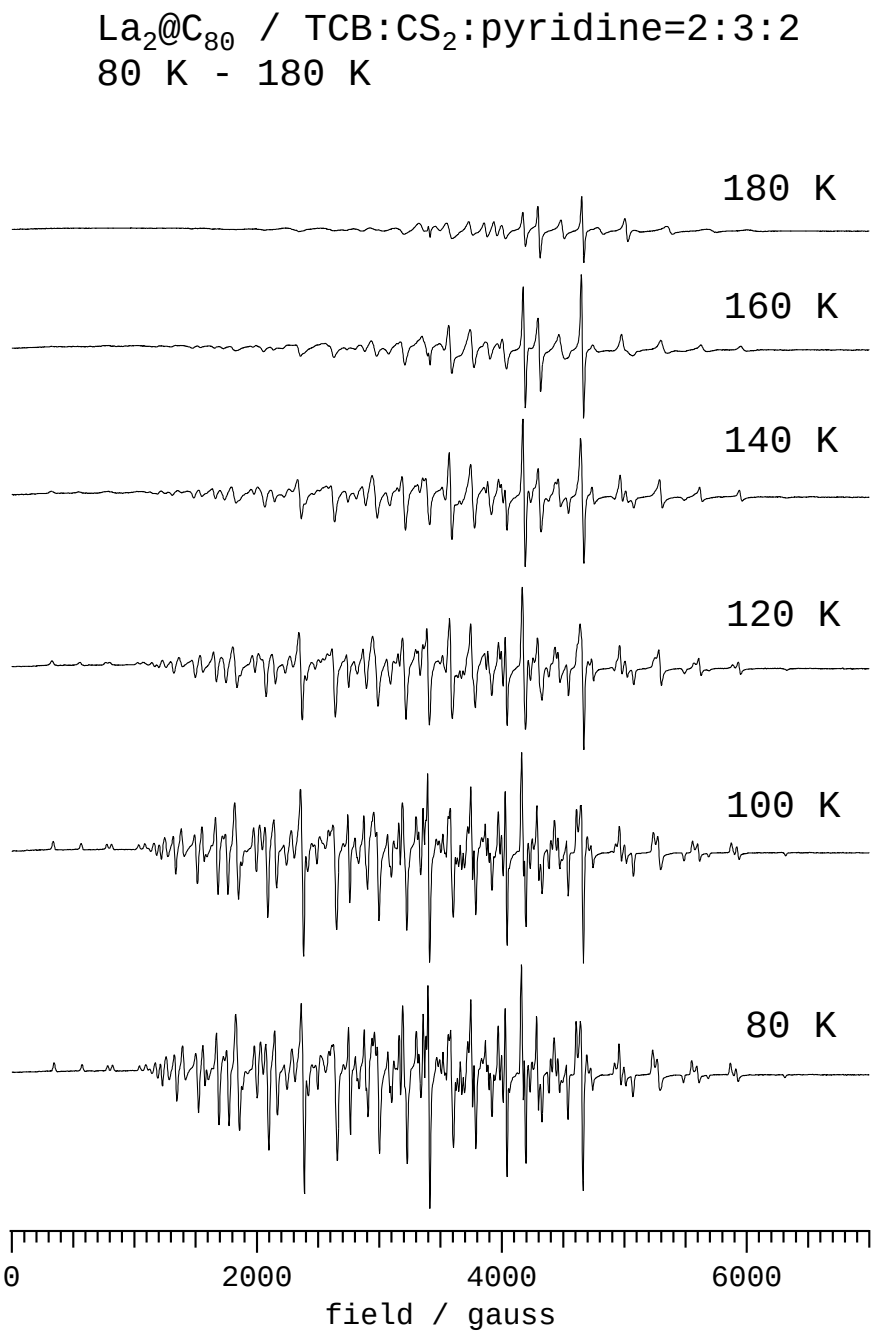

Figure 4-16. X- band ESR spectra of $La_2@C_{80}$ in TCB: CS_2: pyridine (1:3:2, vv) at the temperature range from 180 K to 80 K.

As shown in Figure 4-15, the spectrum appeared more than 15 lines, which was expected from the simple relation (= 2I+1 lines). This would be originated from the presence of the large hyperfine interaction respect to the Zeeman interaction, and the forbidden transition might be observed. The W-band (95 GHz) ESR experiment could simplified the ESR spectrum. Figure 4-17 shows the W-band ESR spectrum of the $La_2@C_{80}$, which was cocrystallized with TBAF from that of the pyridine solution, in CS_2 and acetone at 20K. At W-band, the Zeeman interaction increased about one order of magnitude than that at X-band, and the W-band spectrum can easily simulated by the perturbation theory. The g factor smaller than 2.0023, which is the value for free electron, suggested the presence of spin-orbit interaction of unpaired electron to internal La ion.

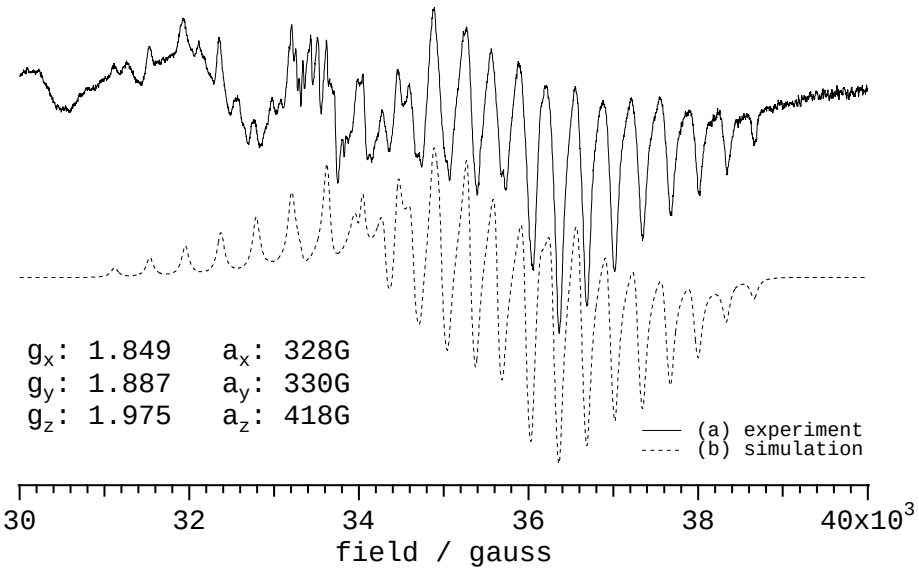

Figure 4-17. W- band ESR spectrum of $La_2@C_{80}$ with TBAF, co-crystallized from pyridine solution, in CS_2 and acetone at 20 K. Simulated spectrum is also shown.

Theoretical calculation of $La_2@C_{80}$ anion predicted that the excess electron would be lying on the $6s\sigma_g$ orbital of the internal La dimmer, as in Figure 4-18. [32] And the group theory requires the mixing of higher lying $5d\sigma_g$ and $5d\delta_g$ orbital with $6s\sigma_g$ orbital. The spin densities on the 6s and the $5d_z^2$ orbital of the La atom were estimated by comparing

the isotropic and the anisotropic hfc with those of atomic ones. [27] The estimated spin densities on the 6s and the $5d_z^2$ orbital of one La were 0.17 and 1.23, respectively. The spin density on the $5d_z^2$-orbital was overestimated, because we used the atomic data as a reference. The reference values of hfc should be taken from that of the La dimmer. We could be originated to the anisotropy of hfc to the non-spherical $6s\sigma_g$ orbital of the La dimmer. However, the result of the ESR measurement strongly suggested that the excess electron was on the internal La dimmer of $La_2@C_{80}$. This is in contrast to the electronic state of $M@C_{82}$ anion, in which the excess electron is lying on the C_{82} cage. As in the case of $La_2@C_{80}$ anion, the model of reduction-induced valency change of the encapsulated ion was reported for the case of $Sc_3N@C_{80}$ anion. [36]

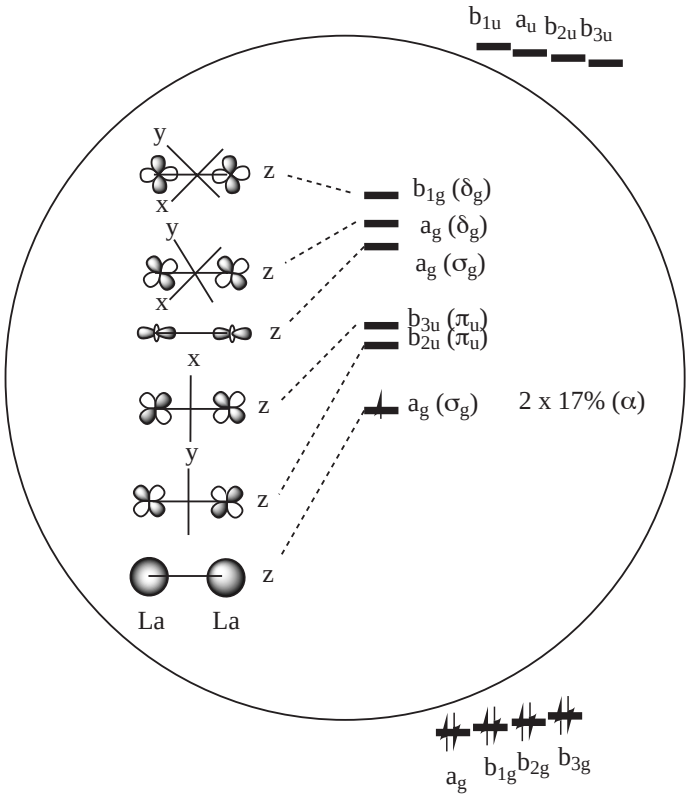

Figure 4-18. Proposed electronic structure of $La_2@C_{80}$ anion

4. 4. Conclusion

The temperature dependent ESR study of La@C_n isomers in CS_2 solution revealed the influence of the cage structure on the electronic structure of endohedral La atom. The anisotropic ESR parameters, such as Δg, Δa, and the quadrupole interaction, were determined. The quantitative discussion of these parameters indicated that the electronic structure of all La@C_n could be described as $La^{3+}@C_n^{3-}$. The various values of g close to g_e reflected the relative position of the low-lying La-derived orbital to that of the π orbital of the cage. And the discussion on the NQI suggested the distance between the lanthanum to cage decreased with increasing the size of the fullerene cage. Interesting feature such as the internal motion of the endohedral atom, or the jumping among the Jahn-Teller distorted structures of fullerene cage was suggested for La@C_{80}-I and La@C_{84}-II.

The electronic structures of metallofullerene ions were investigated by ESR spectroscopy. Reductions of Gd@C_{82}-I and La_2@C_{80} were performed by the reductive solvation of pyridine (DMF). And the chemical oxidation of Gd@C_{82}-I was carried out by the reaction with MB. The oxidation state of endohedral Gd^{3+} ion in Gd@C_{82}-I is unchanged towards the reduction and the oxidation process, which was suggested by X-band ESR measurements, and then was confirmed by W-band ESR measurements. The analysis of ESR spectra of La_2@C_{80} anion suggested that the excess electron was on the internal La_2 dimmer. This is in contrast to the anion of M@C_{82}-I, the excess electron placed on the C_{82} cage.

4. 5. Appendix

Appendix 4A

Temperature dependent ESR spectra of La@C_ns in CS_2.

Figure 4A-1. Temperature dependent ESR spectra of La@C_ns (n=76-78) in CS_2.
Figure 4A-2. Temperature dependent ESR spectra of La@C_{80} in CS_2.
Figure 4A-3. Temperature dependent ESR spectra of La@C_{82} in CS_2.
Figure 4A-4. Temperature dependent ESR spectra of La@C_{86} in CS_2.
Figure 4A-5. Temperature dependent ESR spectra of La@C_{88} in CS_2.
Figure 4A-6. Temperature dependent ESR spectra of La@C_{90} in CS_2.

Appendix 4B

Temperature dependence of the linewidth coefficients of La@C_ns in CS_2.

Figure 4B-1. Temperature dependence of the linewidth coefficient of La@C_ns (n=76-78) in CS_2.
Figure 4B-2. Temperature dependence of the linewidth coefficient of La@C_{80} in CS_2.
Figure 4B-3. Temperature dependence of the linewidth coefficient of La@C_{82} in CS_2.
Figure 4B-4. Temperature dependence of the linewidth coefficient of La@C_{84} in CS_2.
Figure 4B-5. Temperature dependence of the linewidth coefficient of La@C_{86} in CS_2.
Figure 4B-6. Temperature dependence of the linewidth coefficient of La@C_{88} in CS_2.
Figure 4B-7. Temperature dependence of the linewidth coefficient of La@C_{90} in CS_2.

Appendix 4C

Experimental (full line) and simulated (dotted line) ESR spectra of La@C_ns in toluene at 80K.

Figure 4C-1. Experimental (full line) and simulated (dotted line) ESR spectra of La@C_ns (n=76-78) in toluene at 80K.
Figure 4C-2. Experimental (full line) and simulated (dotted line) ESR spectra of La@C_{80} in toluene at 80K.

Figure 4C-3. Experimental (full line) and simulated (dotted line) ESR spectra of La@C_{82} in toluene at 80K.

Figure 4C-4. Experimental (full line) and simulated (dotted line) ESR spectra of La@C_{84} in toluene at 80K.

Figure 4C-5. Experimental (full line) and simulated (dotted line) ESR spectra of La@C_{86} in toluene at 80K.

Figure 4C-6. Experimental (full line) and simulated (dotted line) ESR spectra of La@C_{88} in toluene at 80K.

Figure 4C-7. Experimental (full line) and simulated (dotted line) ESR spectra of La@C_{90} in toluene at 80K.

Figure 4A-1

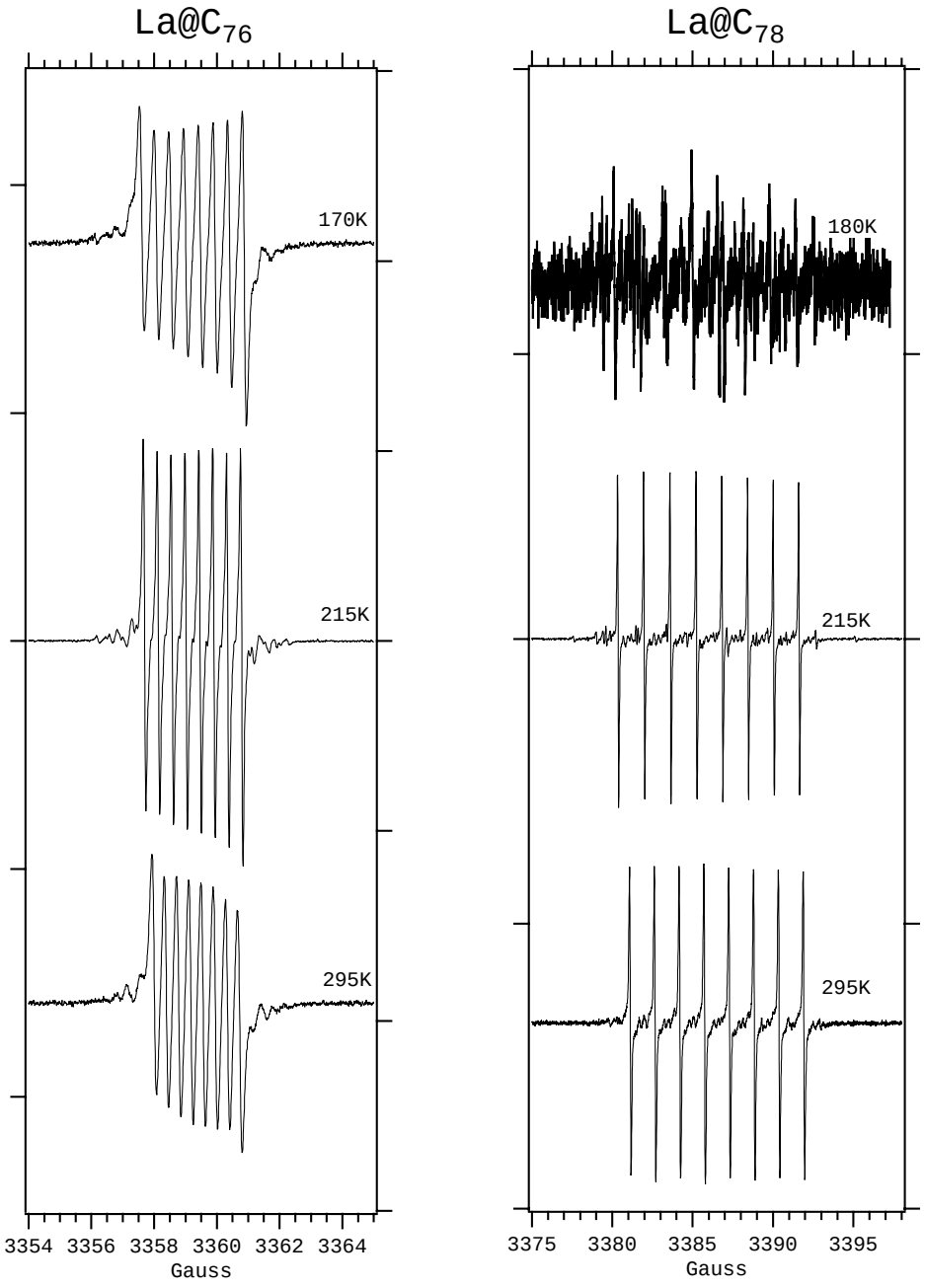

Figure 4A-1. Temperature dependent ESR spectra of La@C_ns (n=76-78) in CS_2.

Figure 4A-2

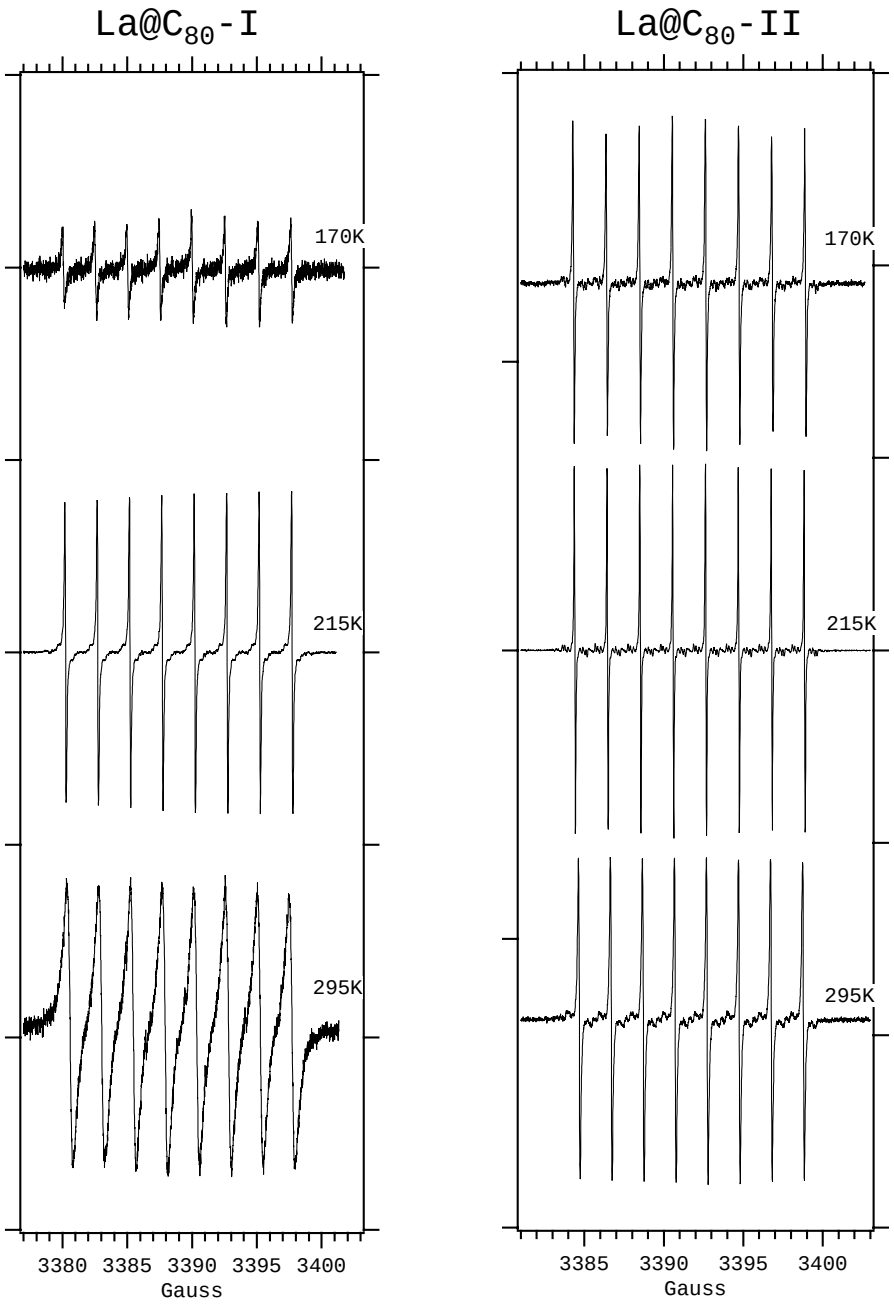

Figure 4A-2. Temperature dependent ESR spectra of La@C_{80} in CS_2.

Figure 4A-3

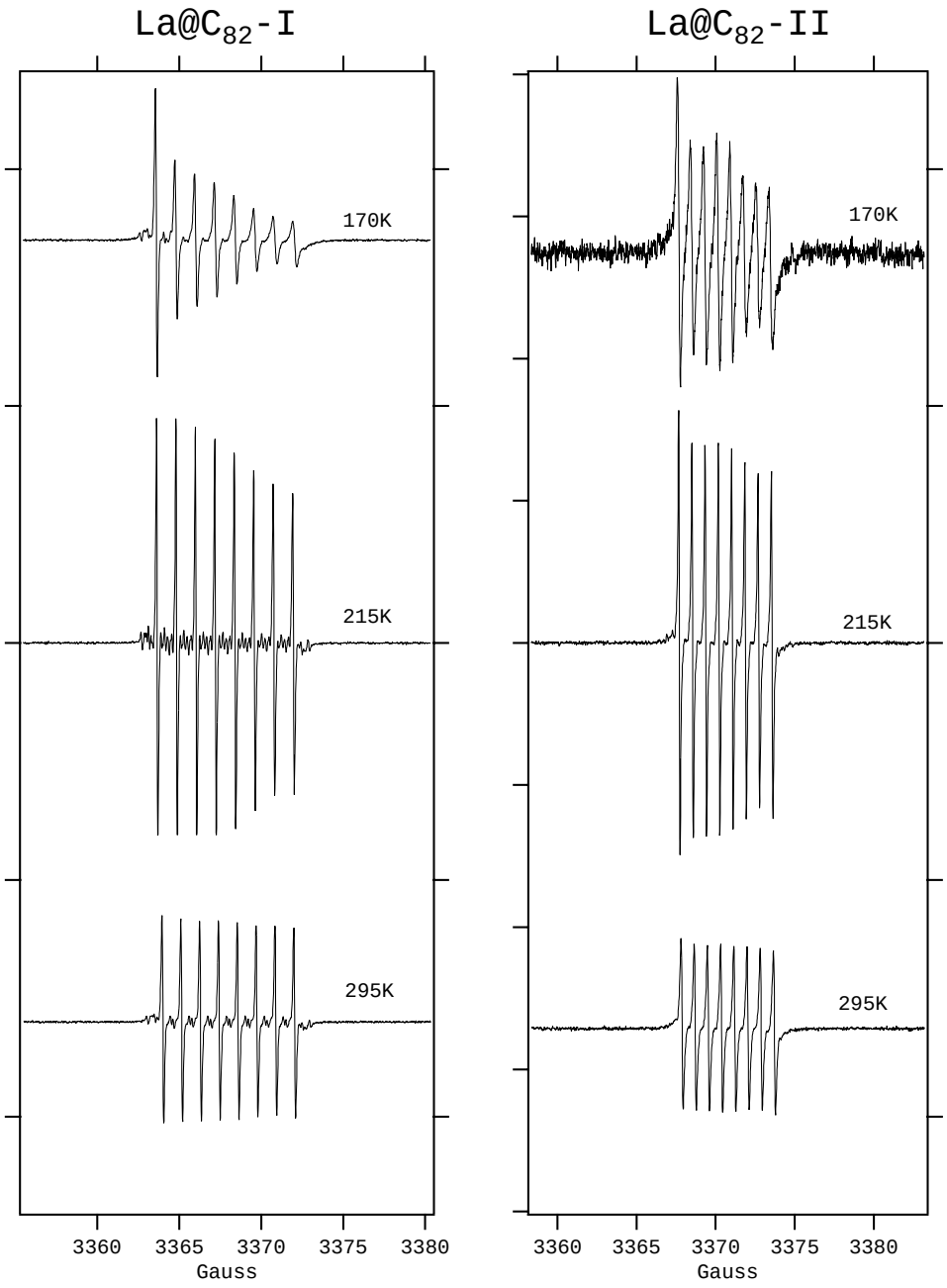

Figure 4A-3. Temperature dependent ESR spectra of $La@C_{82}$ in CS_2.

Figure 4A-4

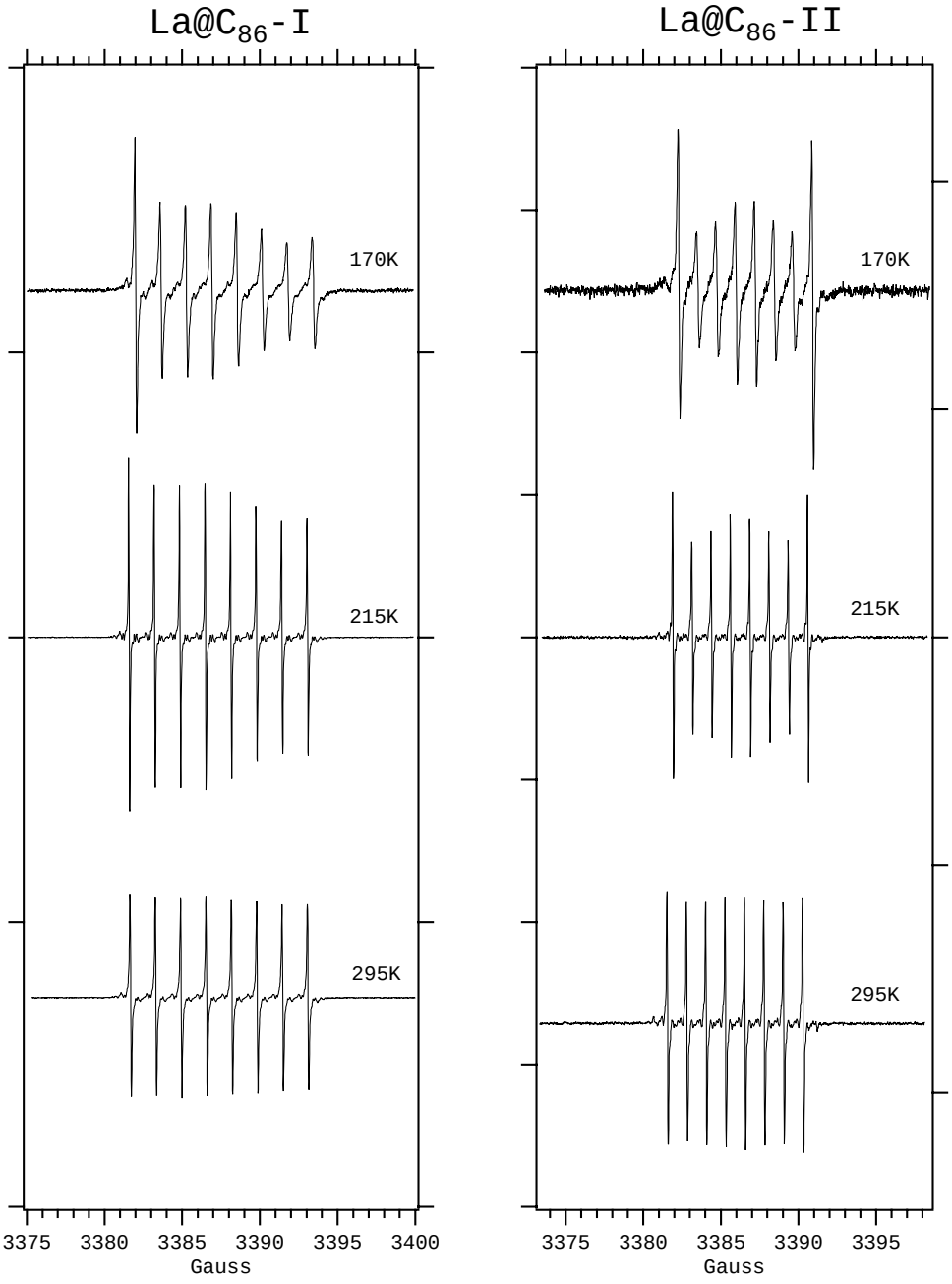

Figure 4A-4. Temperature dependent ESR spectra of La@C_{86} in CS_2.

Figure 4A-5

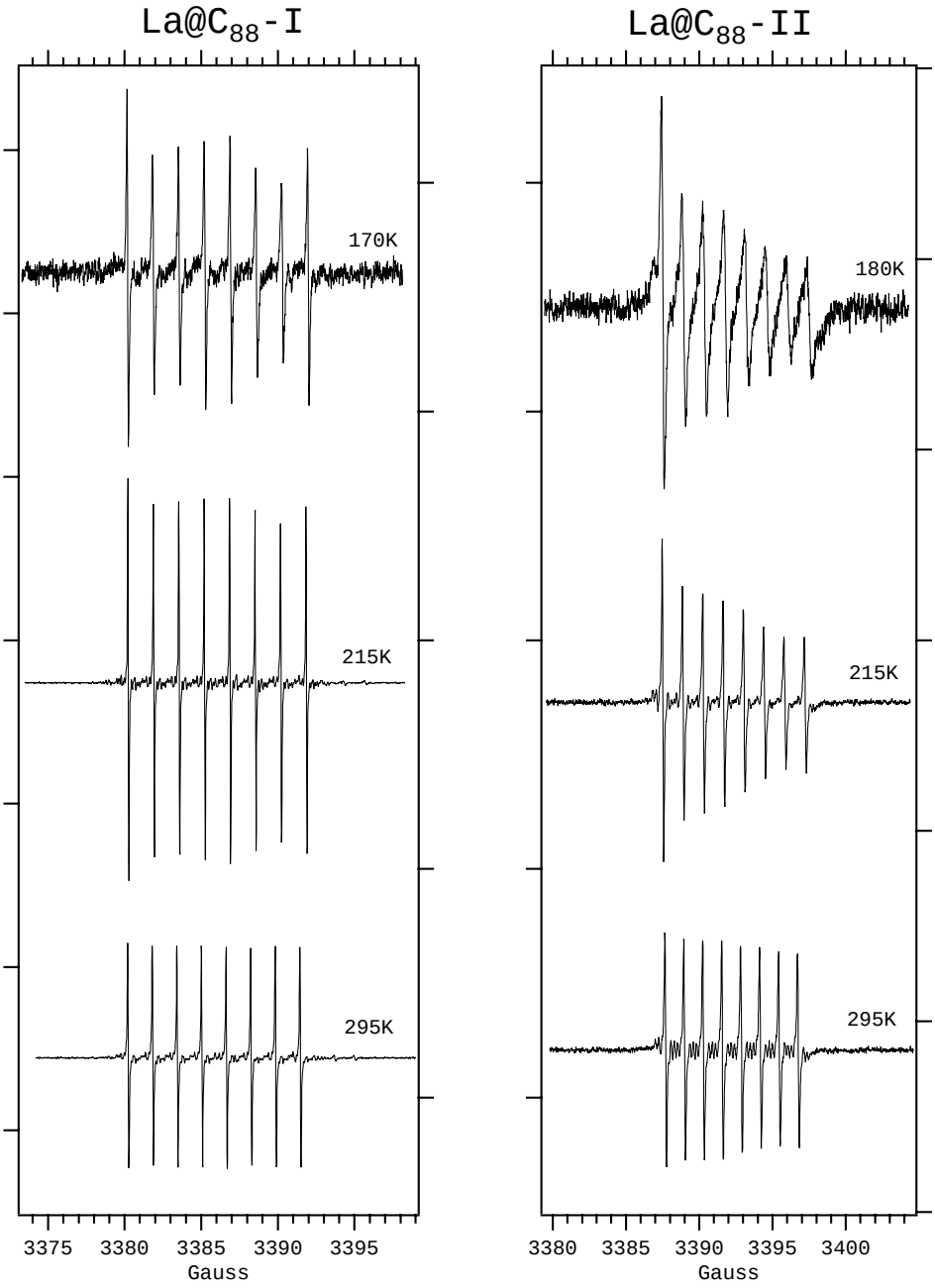

Figure 4A-5. Temperature dependent ESR spectra of La@C_{88} in CS_2.

Figure 4A-5, continued

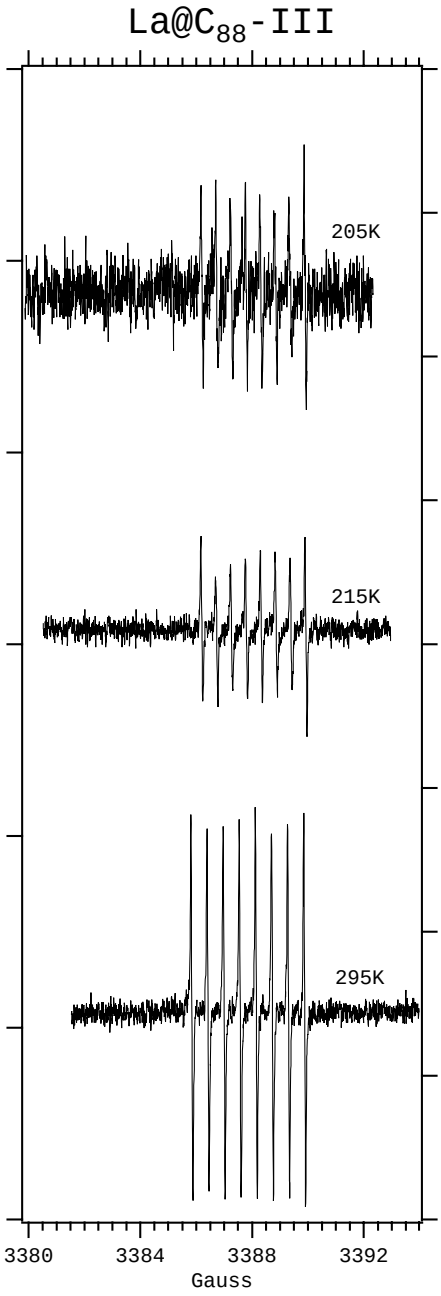

Figure 4A-5. Temperature dependent ESR spectra of La@C_{88} in CS_2.

Figure 4A-6

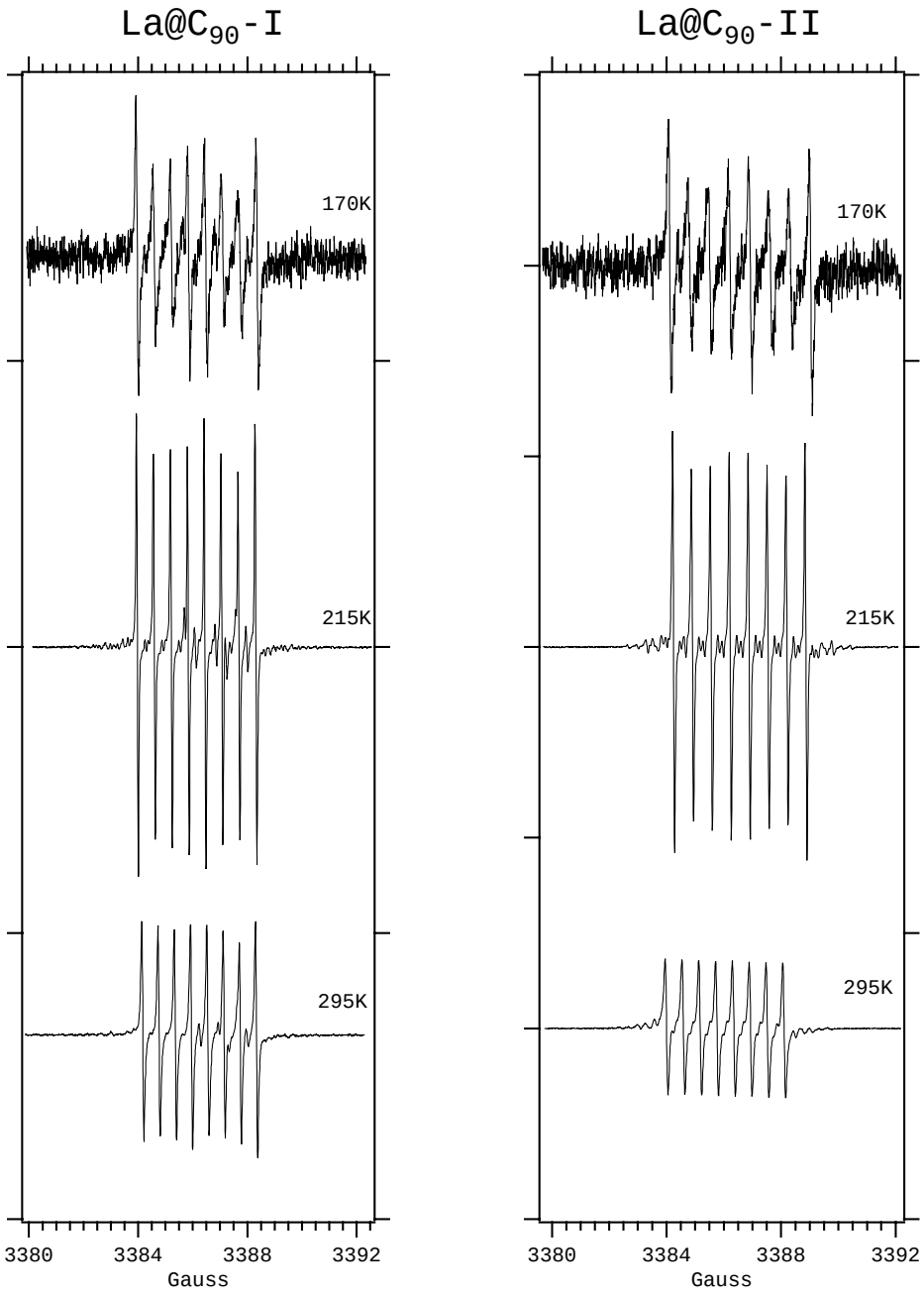

Figure 4A-6. Temperature dependent ESR spectra of La@C_{90} in CS_2.

Figure 4A-6, continued

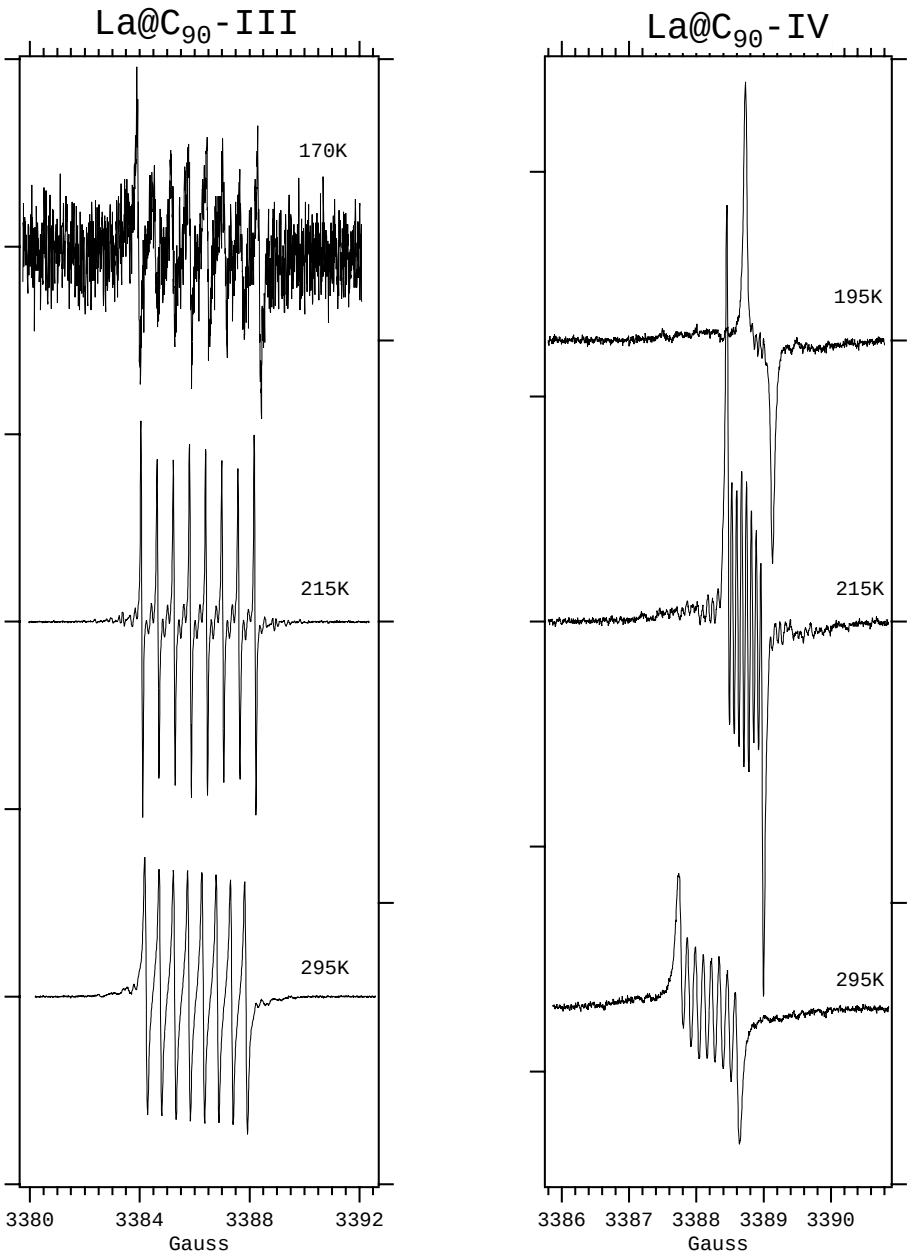

Figure 4A-6. Temperature dependent ESR spectra of La@C_{90} in CS_2.

Figure 4B-1.

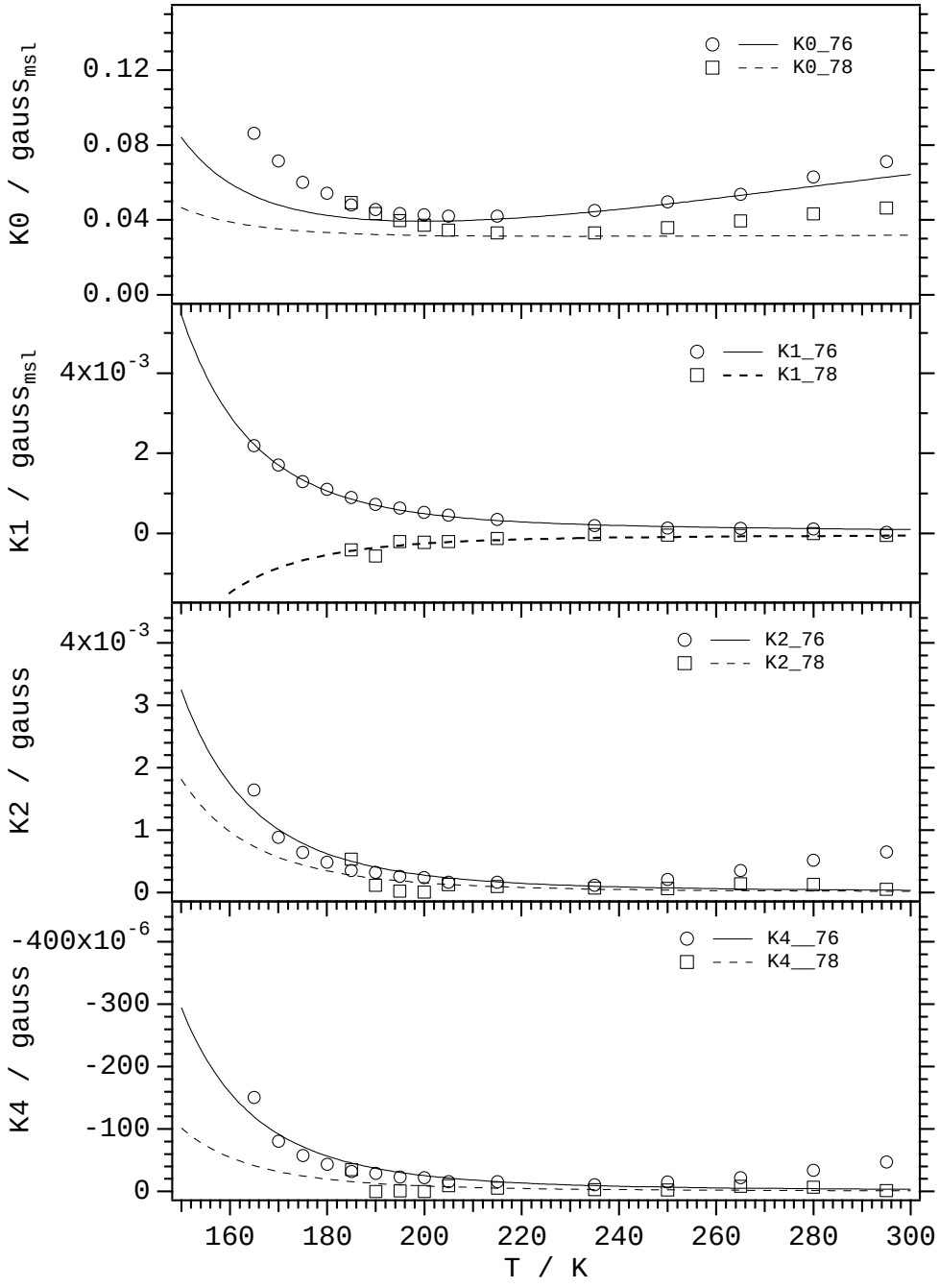

Figure 4B-1. Temperature dependence of the linewidth coefficient of La@C_ns (n=76-78) in CS_2.

Figure 4B-2.

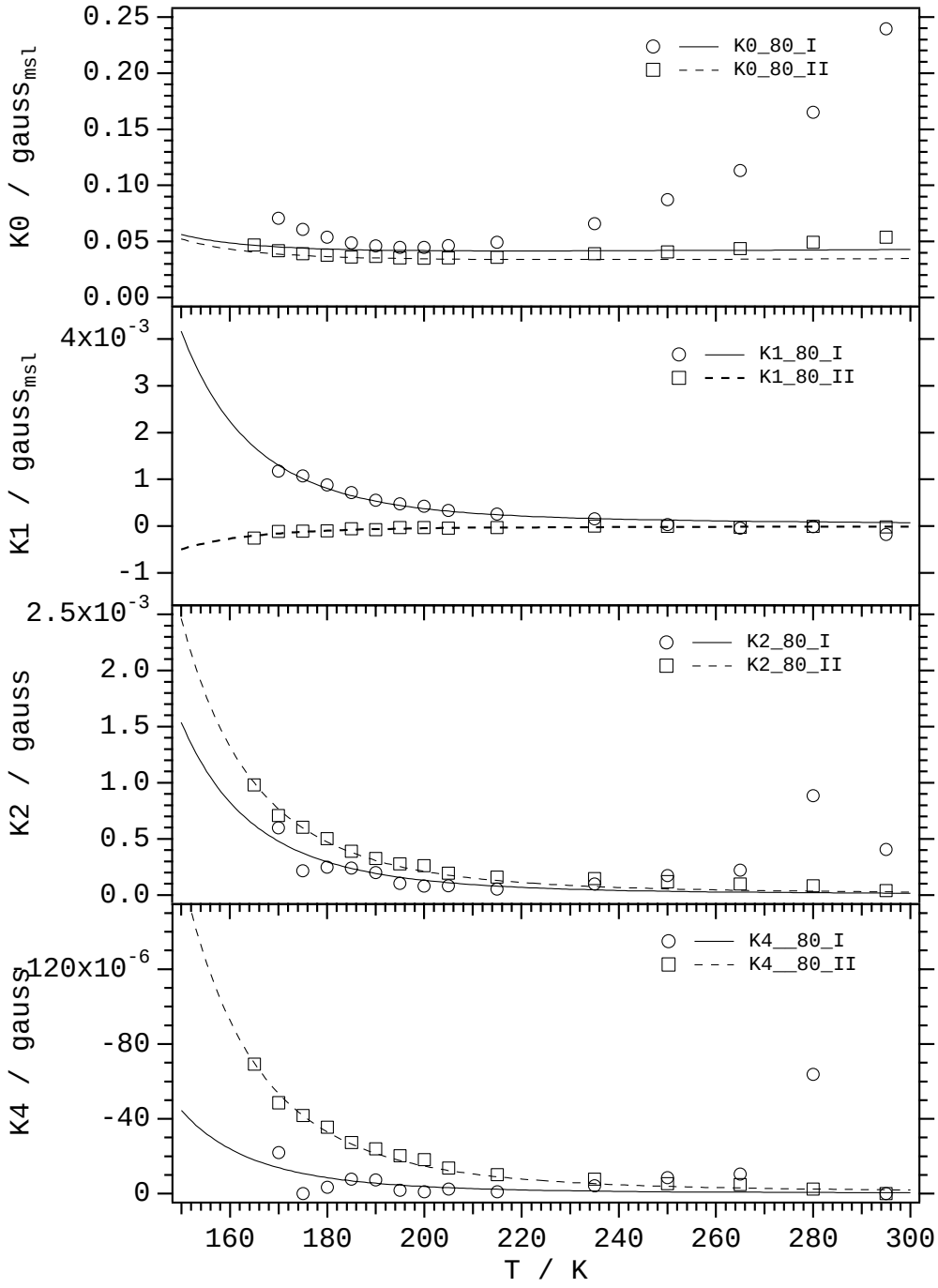

Figure 4B-2. Temperature dependence of the linewidth coefficient of La@C_{80} in CS_2.

Figure 4B-3

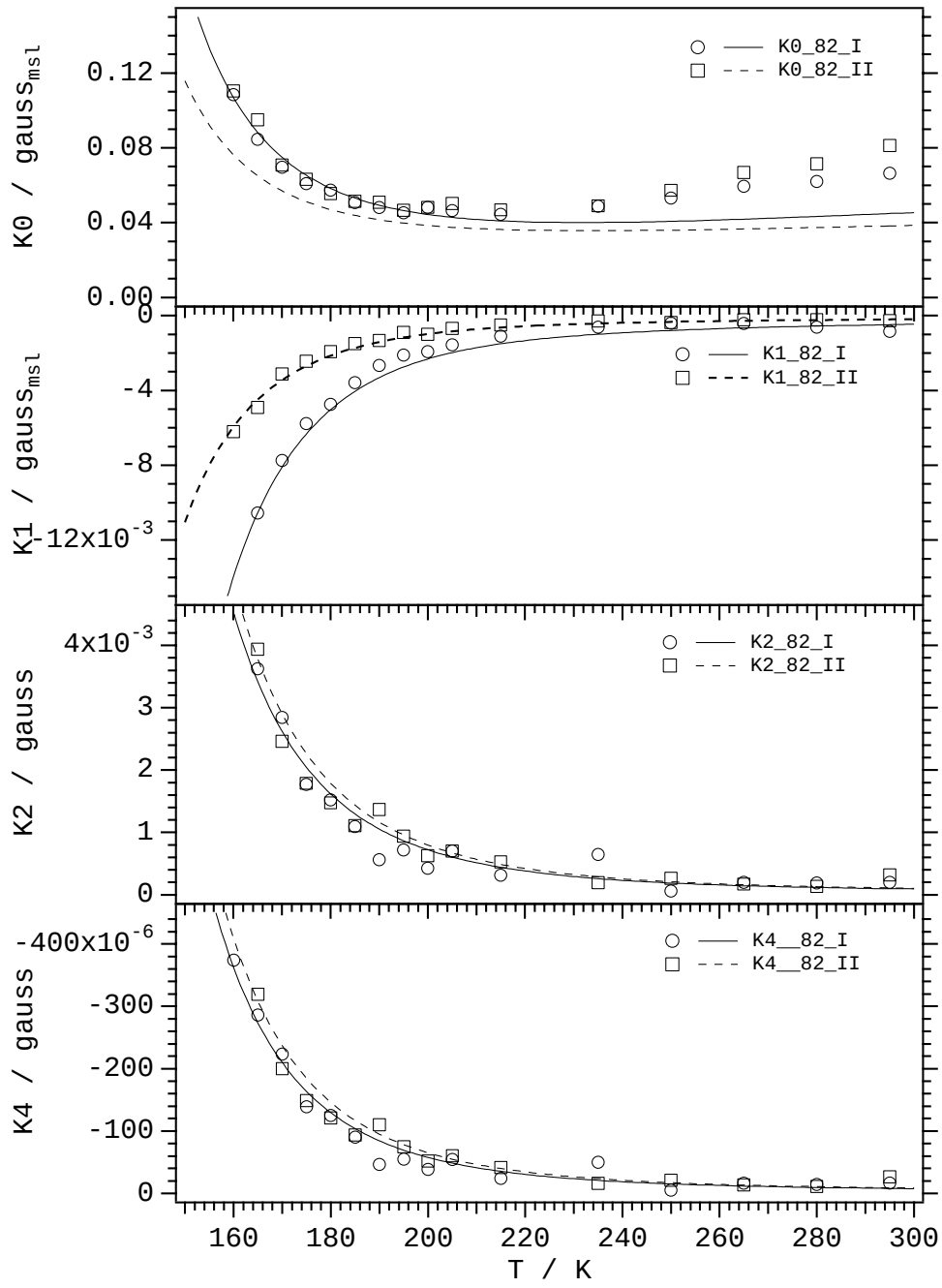

Figure 4B-3. Temperature dependence of the linewidth coefficient of La@C_{82} in CS_2.

Figure 4B-4

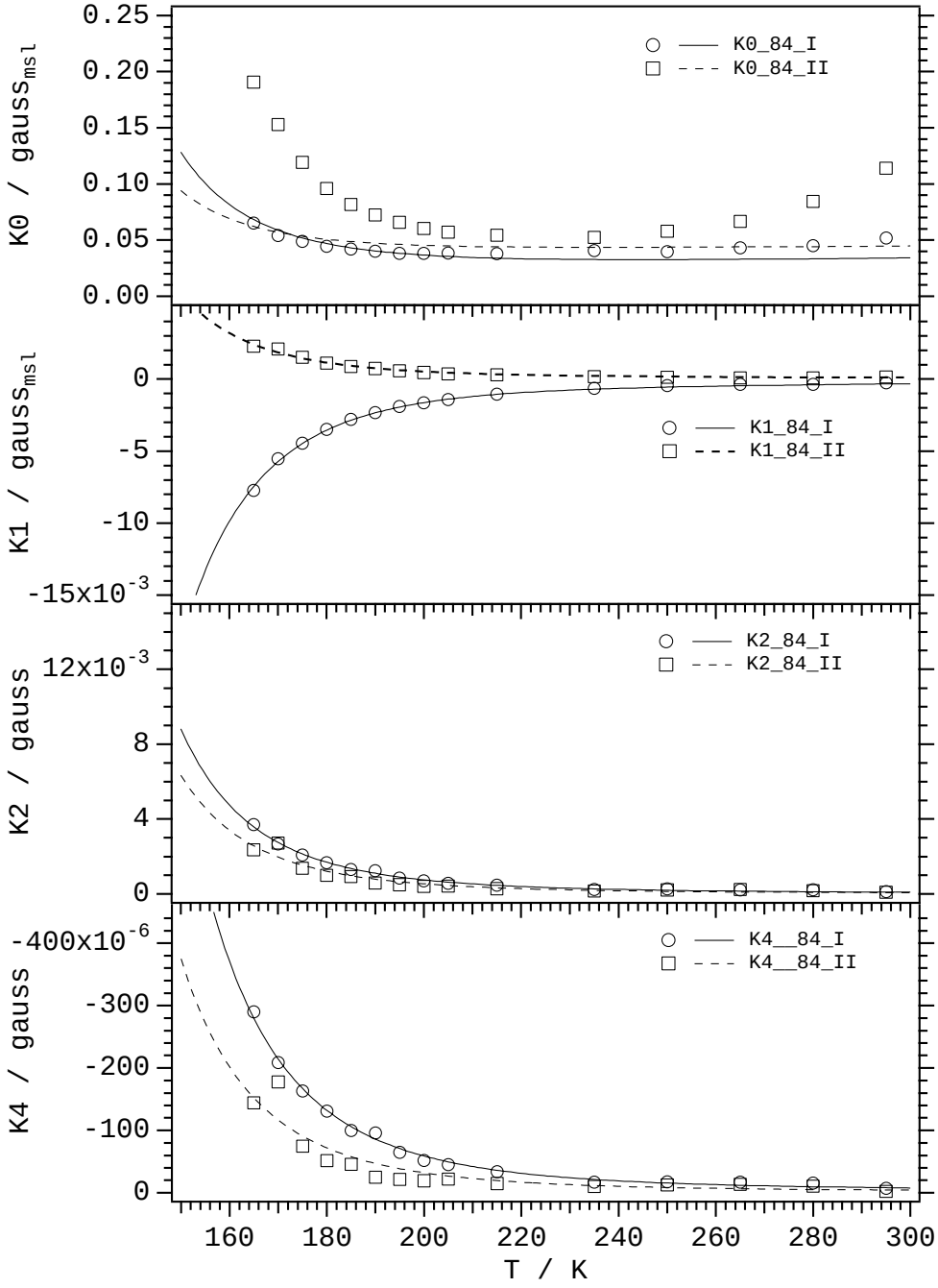

Figure 4B-4. Temperature dependence of the linewidth coefficient of La@C_{84} in CS_2.

Figure 4B-5

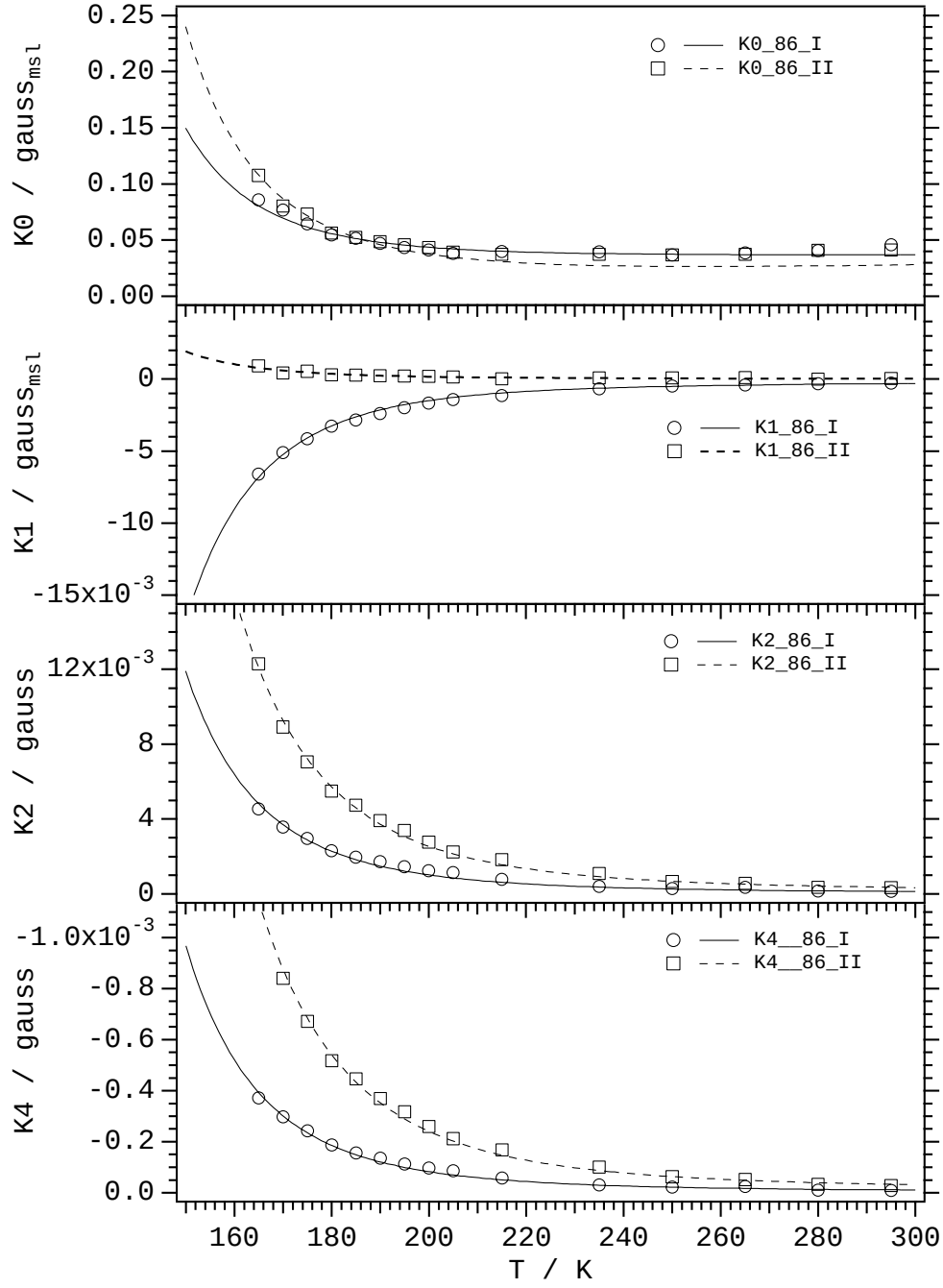

Figure 4B-5. Temperature dependence of the linewidth coefficient of La@C_{86} in CS_2.

Figure 4B-6

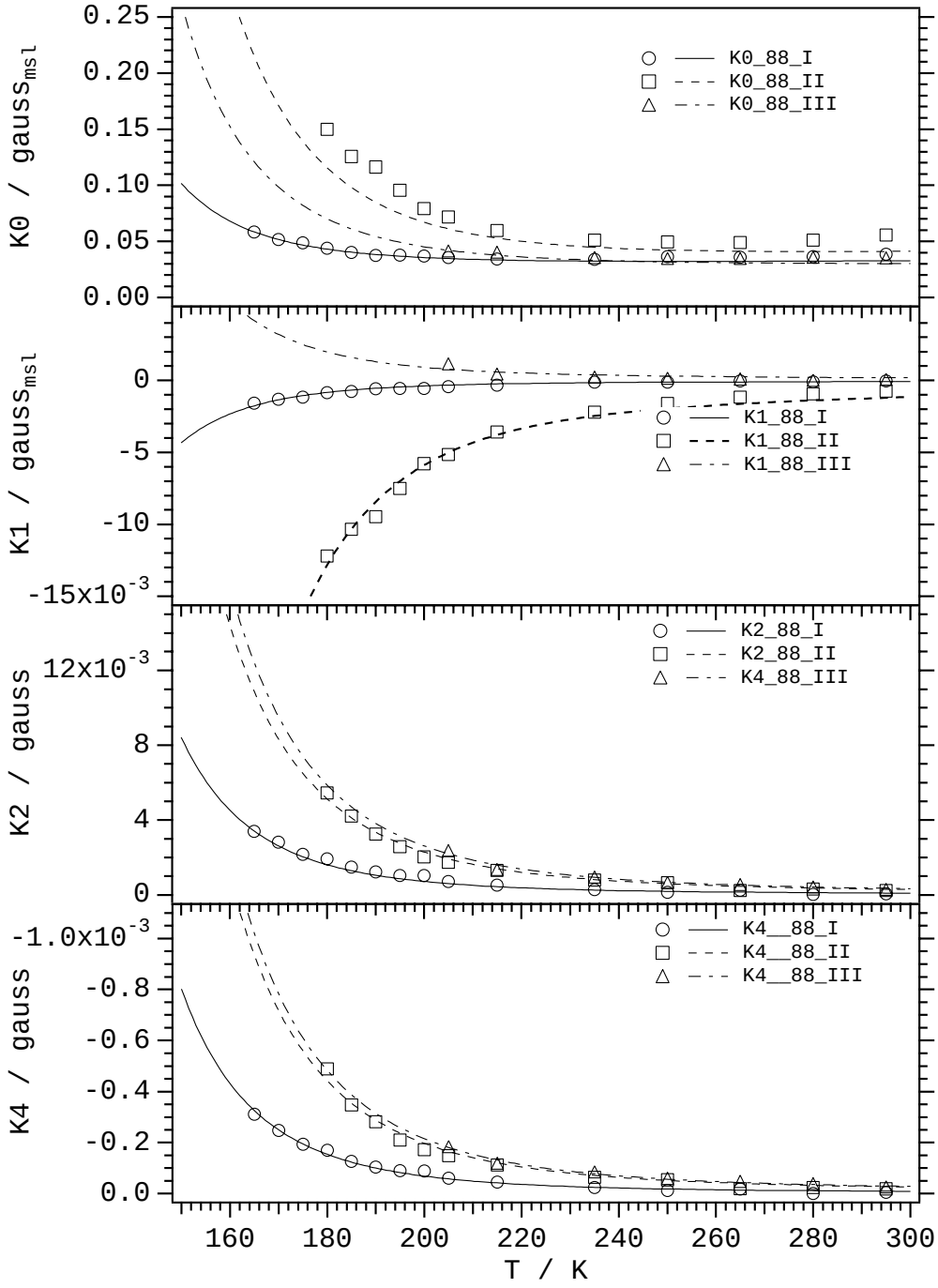

Figure 4B-6. Temperature dependence of the linewidth coefficient of La@C_{88} in CS_2.

Figure 4B-7

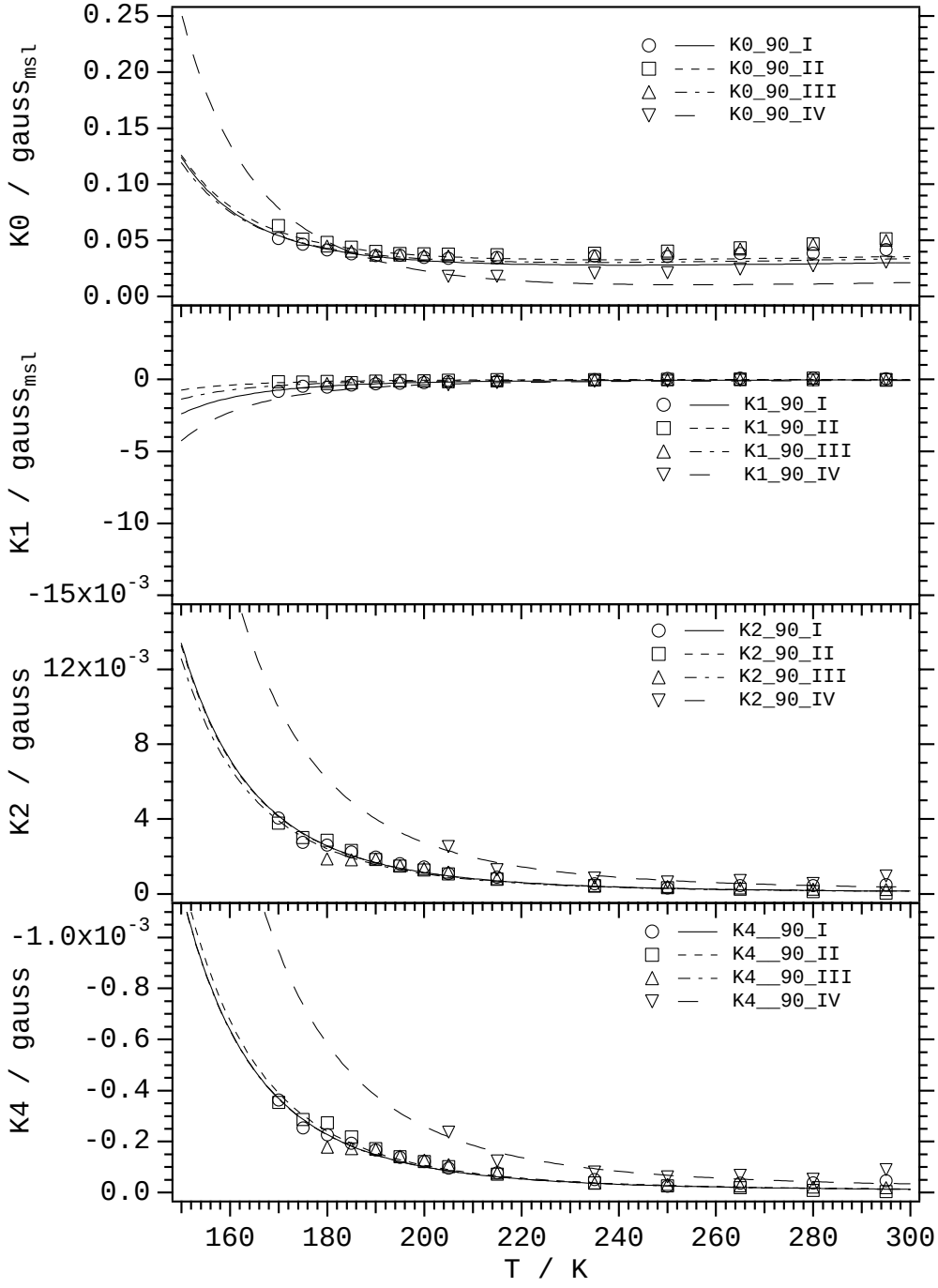

Figure 4B-7. Temperature dependence of the linewidth coefficient of La@C_{90} in CS_2.

Figure 4C-1

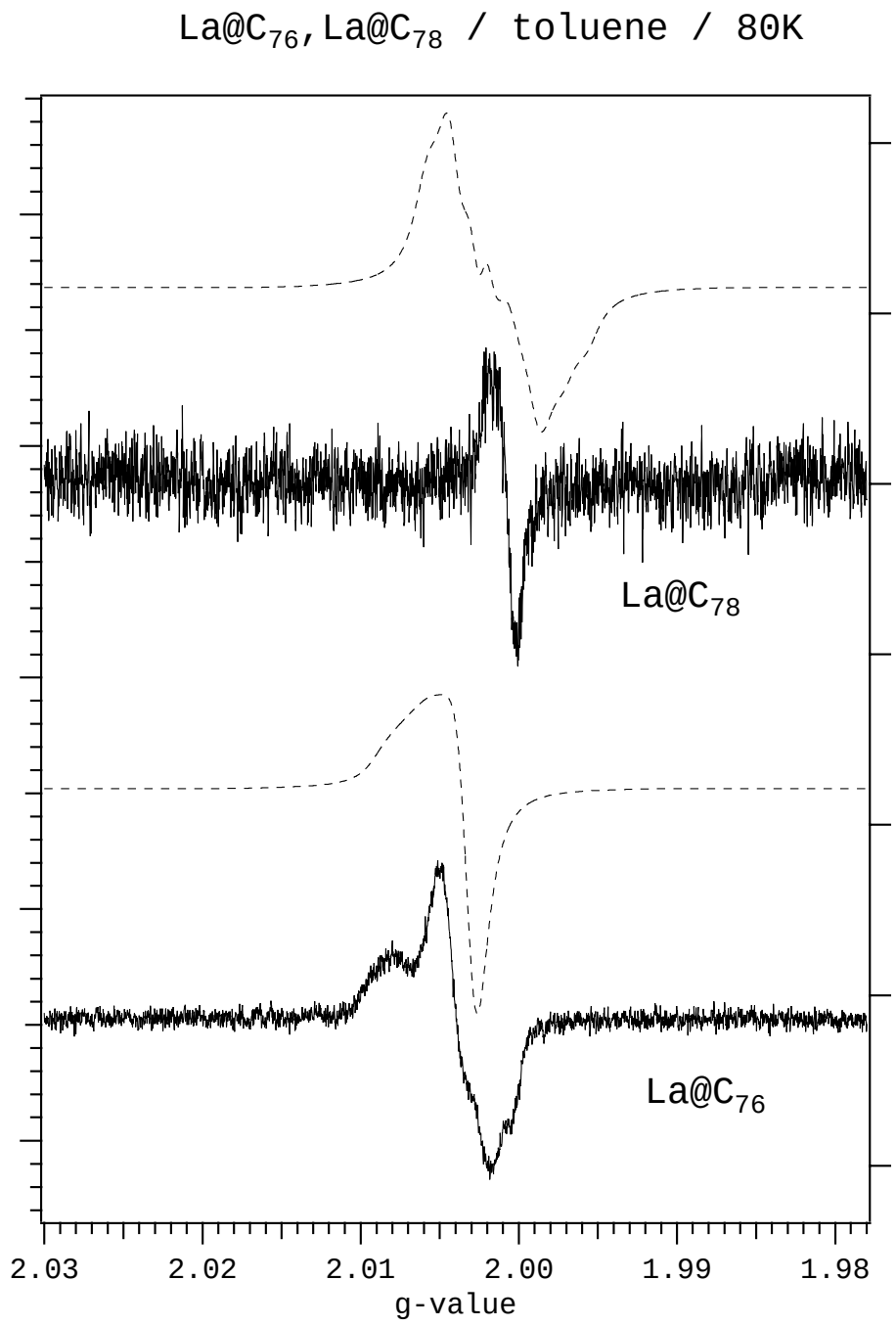

Figure 4C-1. Experimental (full line) and simulated (dotted line) ESR spectra of La@C_ns (n=76-78) in toluene at 80K.

Figure 4C-2

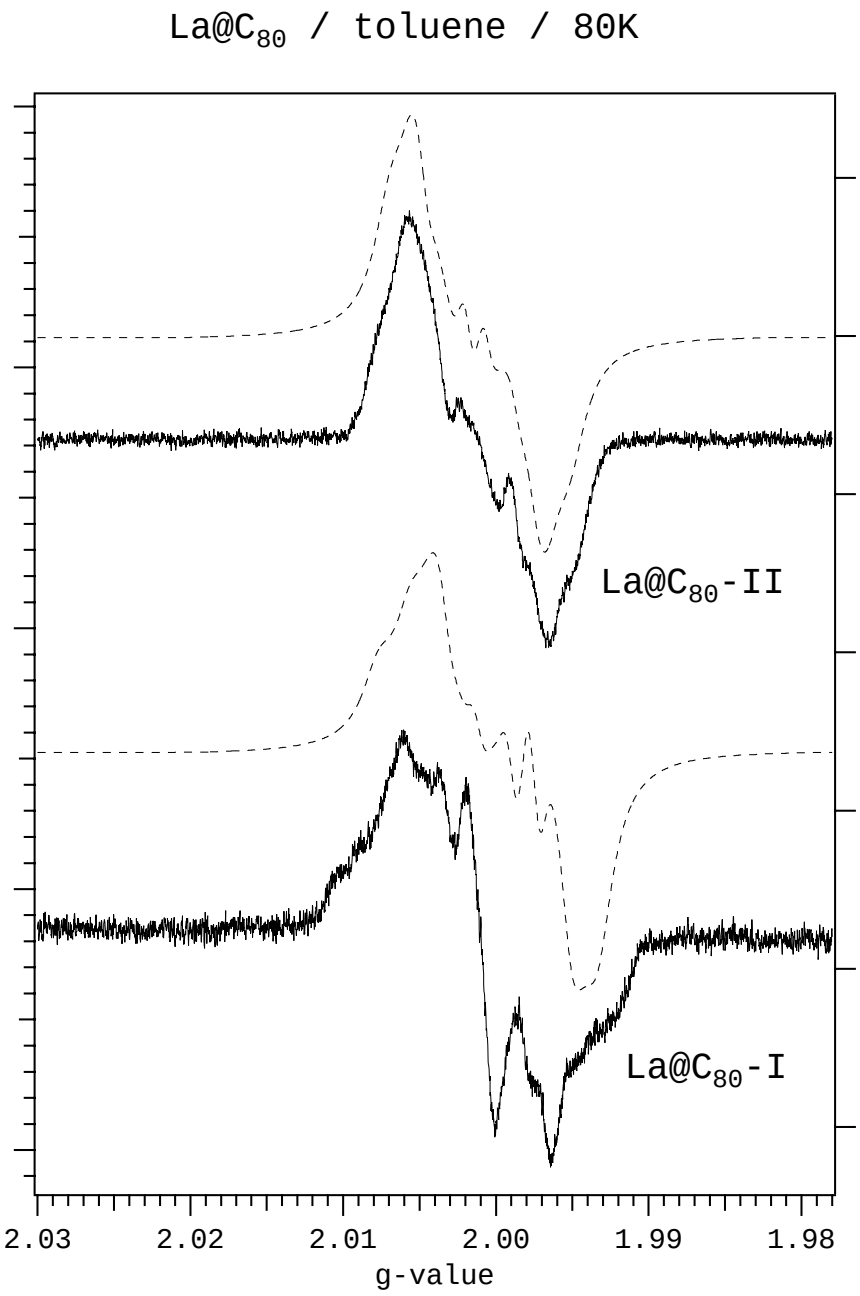

Figure 4C-2. Experimental (full line) and simulated (dotted line) ESR spectra of La@C_{80} in toluene at 80K.

Figure 4C-3

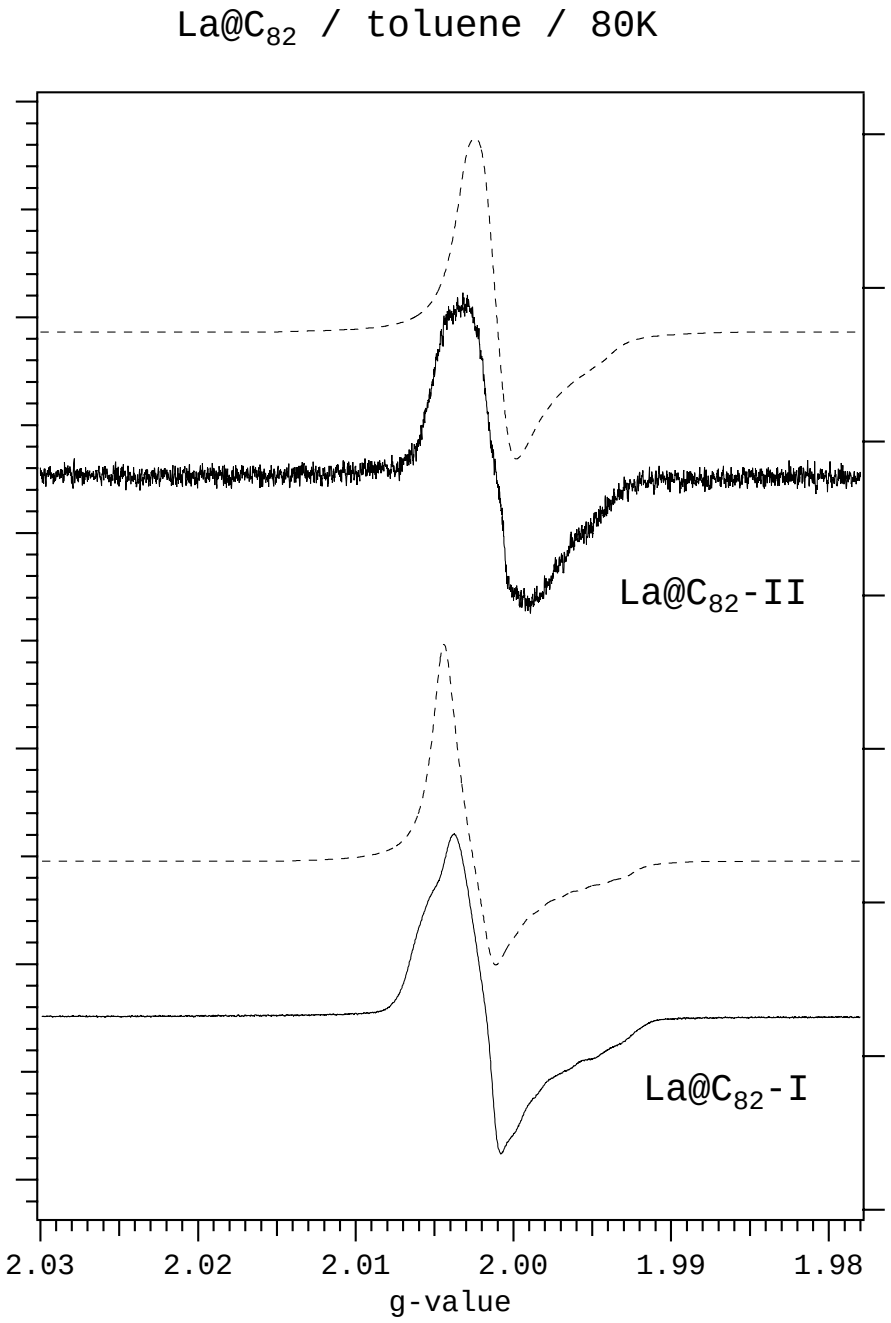

Figure 4C-3. Experimental (full line) and simulated (dotted line) ESR spectra of La@C_{82} in toluene at 80K.

Figure 4C-4

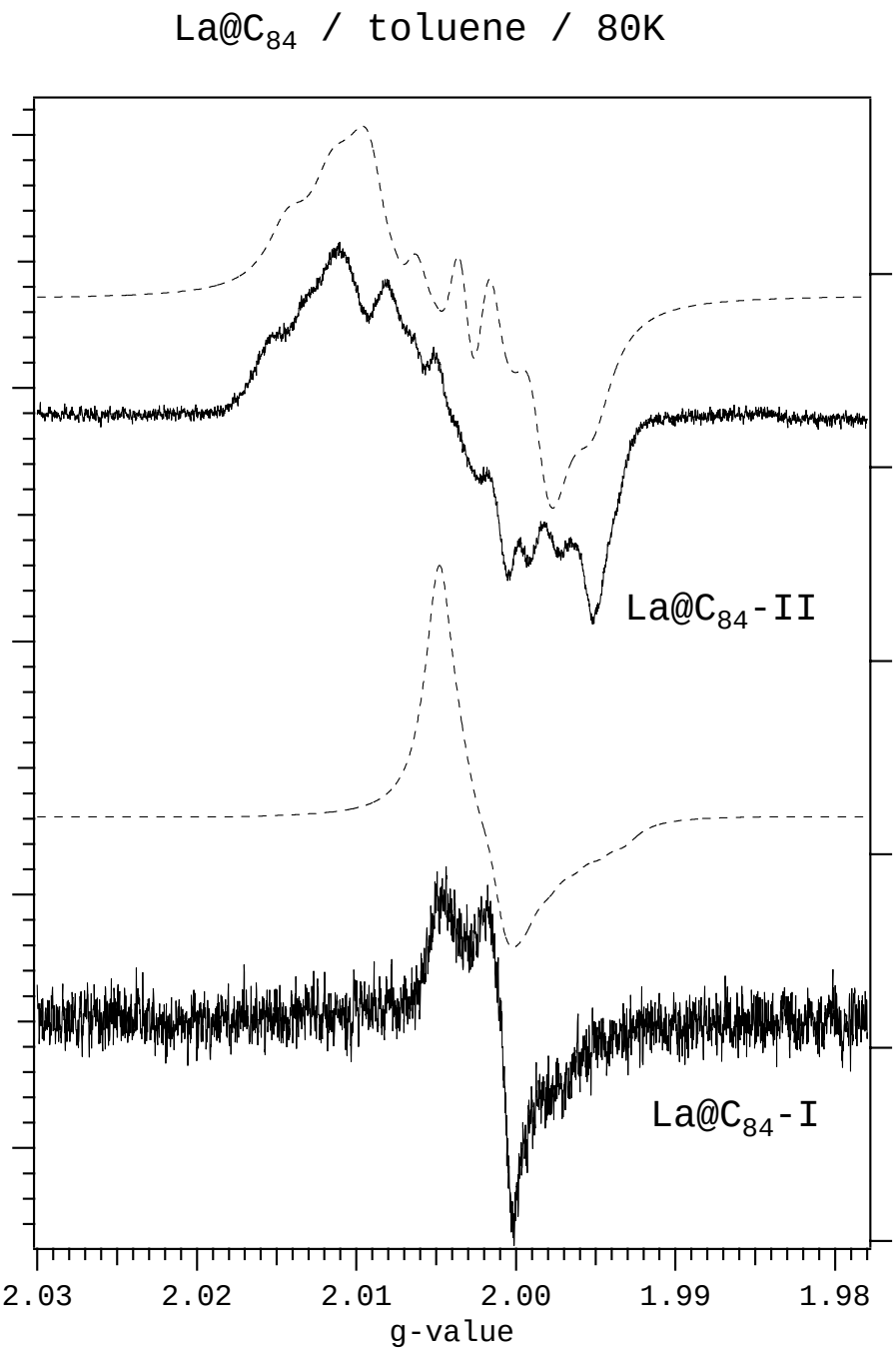

Figure 4C-4. Experimental (full line) and simulated (dotted line) ESR spectra of La@C_{84} in toluene at 80K.

Figure 4C-5

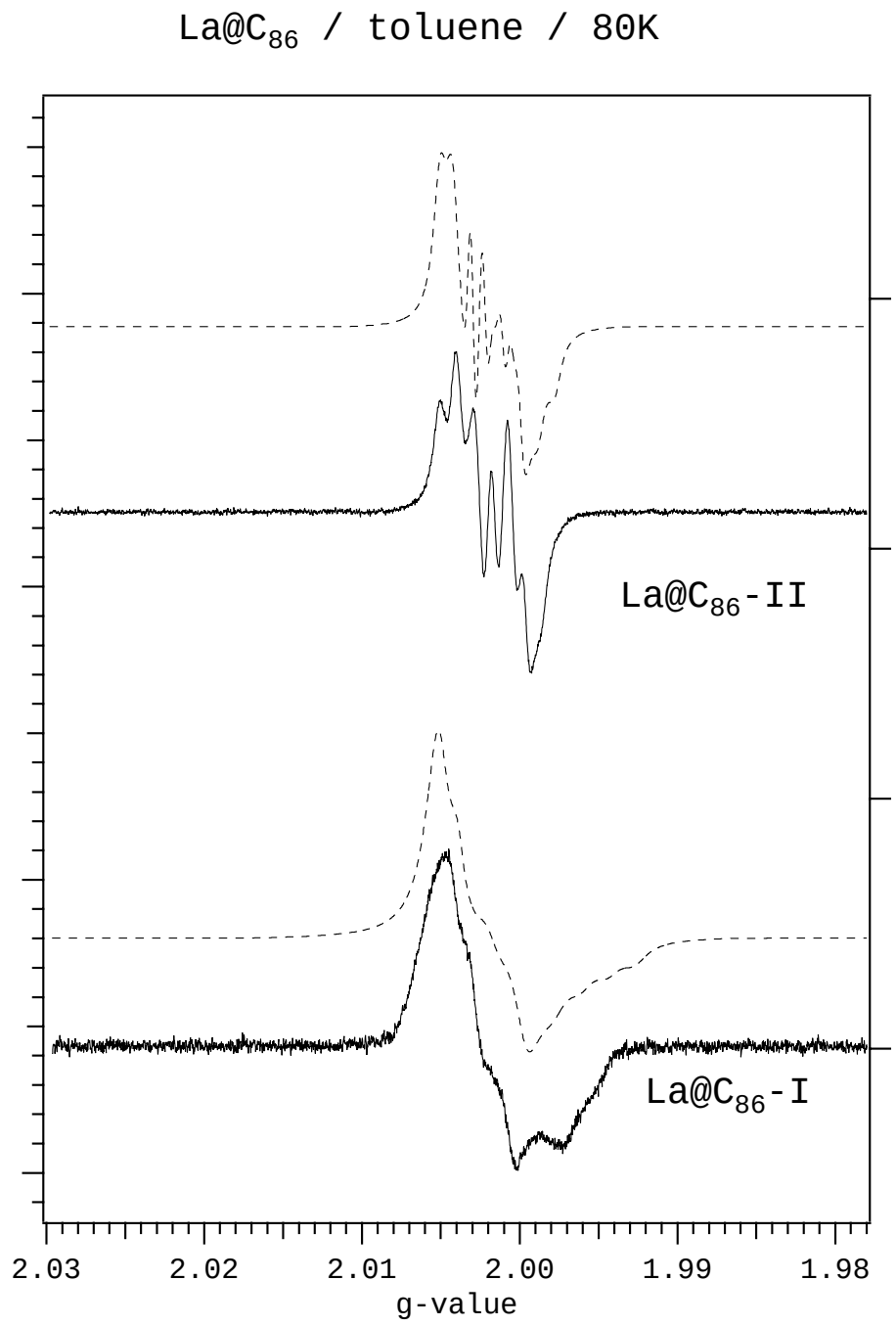

Figure 4C-5. Experimental (full line) and simulated (dotted line) ESR spectra of La@C_{86} in toluene at 80K.

Figure 4C-6

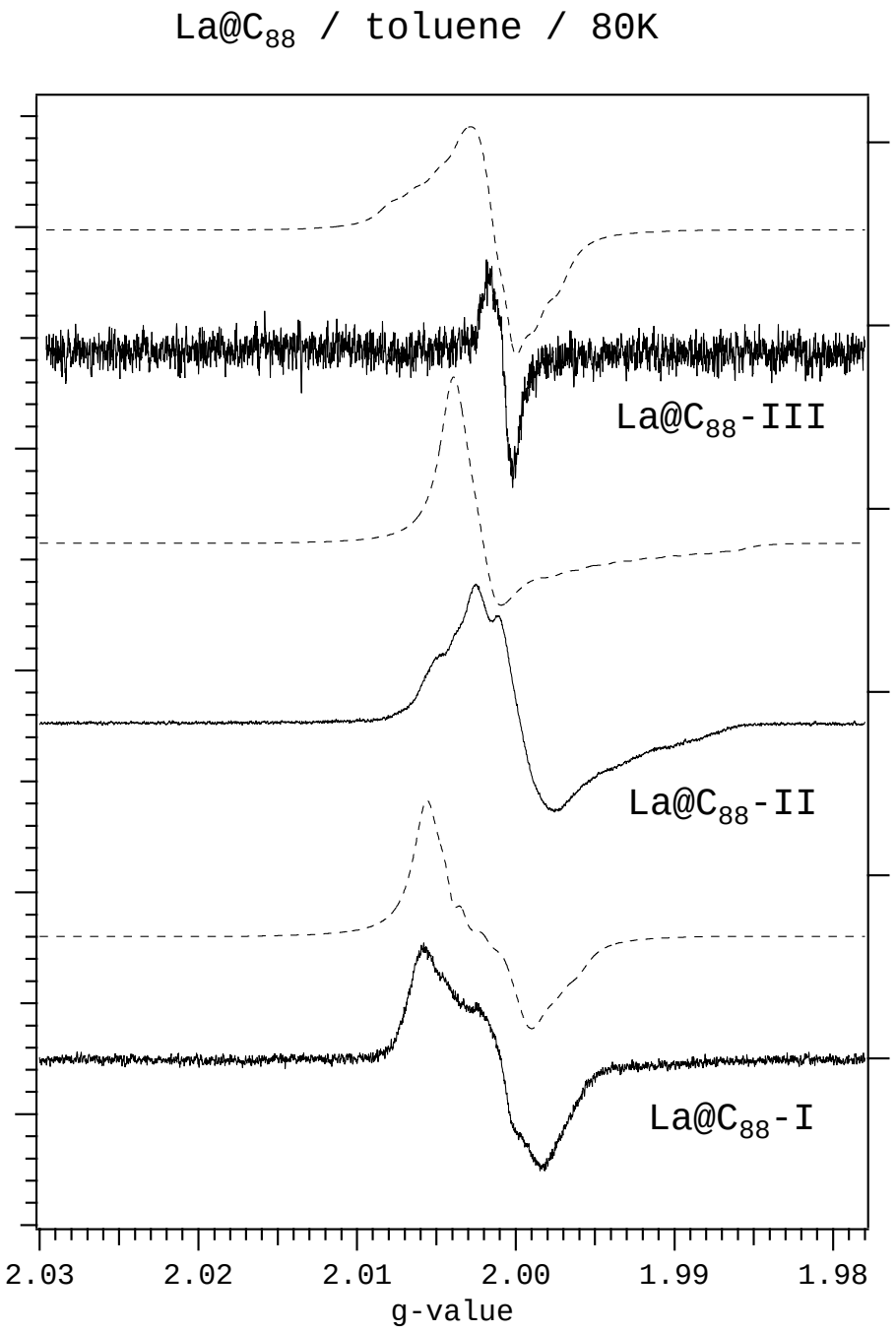

Figure 4C-6. Experimental (full line) and simulated (dotted line) ESR spectra of La@C_{88} in toluene at 80K.

Figure 4C-7

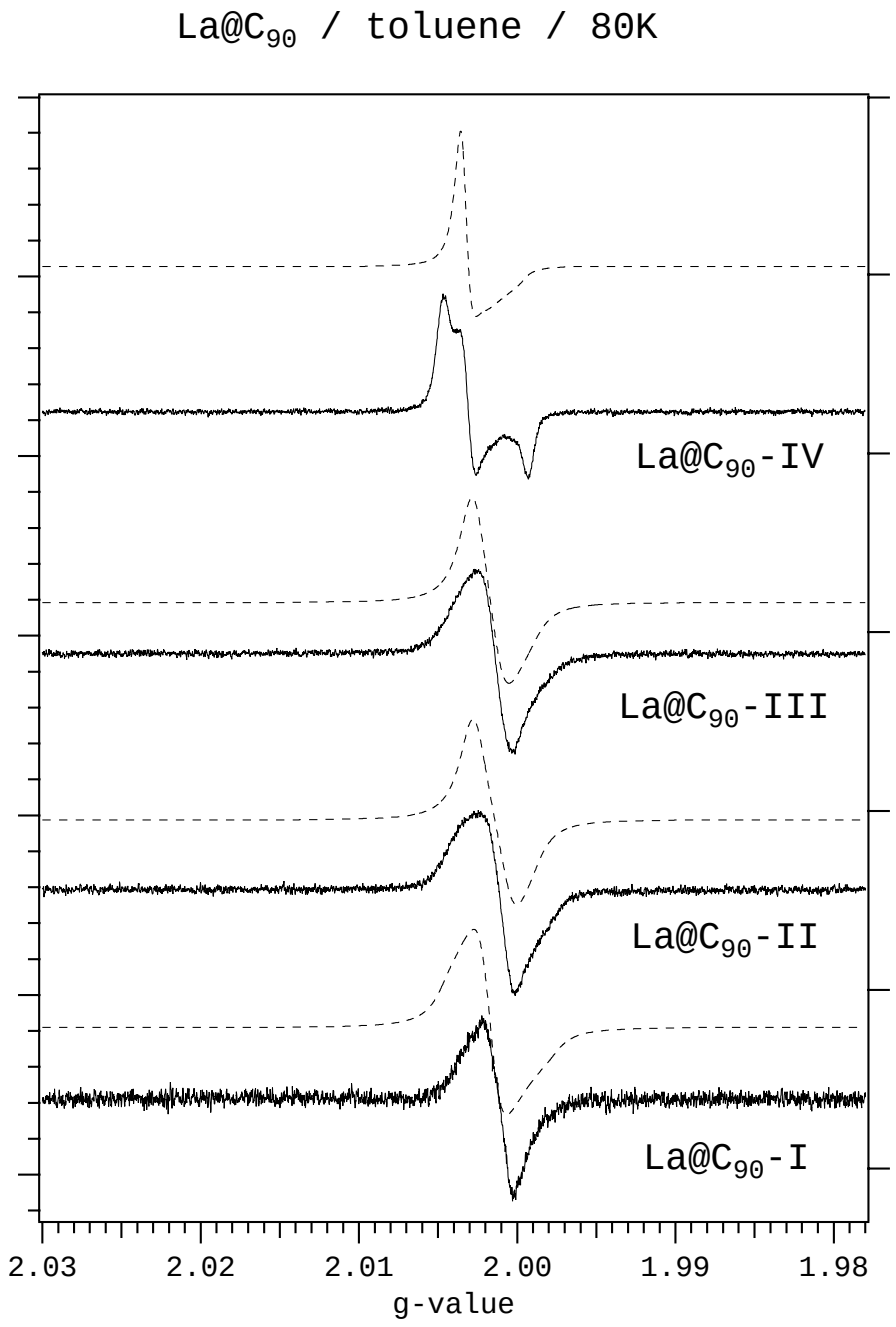

Figure 4C-7. Experimental (full line) and simulated (dotted line) ESR spectra of La@C_{90} in toluene at 80K.

Chapter 5.
Summary

This thesis discussed about the separation and the electronic structure of lanthanum endohedral fullerenes, as a prototype of lanthanoid metallofullerenes. Furthermore, the chemical property of endohedral metallofullerenes, such as solvent effect, was investigated.

The chemical property of metallofullerenes, such as the solvent effect, was investigated in chapter 2. The efficient reduction of metallofullerenes, La@C_{82}-I, II, and La_2@C_{80}, by solvation of pyridine and DMF was confirmed by the spectroscopic measurements, such as ESR, Vis-NIR, and NMR spectroscopy. The reduction of metallofullerenes by solvation is reversible process with almost 100 % yield, which was in contrast to that of C_{60}. The difference of the reduction efficiency between metallofullerenes and C_{60} could be explained by the discussion with previously reported electrochemical investigations. The finding of the reduction by solvation of pyridine (DMF) gave the plausible explanation of the remarkable extraction behavior of these solvents to metallofullerenes with the +3 type metal(s) inside. The next interest is about the +2 type metallofullerenes, which have closed shell electronic structure on these cages. Investigations of the solvent effect on the +2 type metallofullerenes, such as Ca@C_{82} and Eu@C_{82}, will give more information about the electronic structure of these molecules. And more, the use of these solvents will open a door for further applications, such as the isolation of new type of fullerene molecule, which have not been obtained to date.

In chapter 3, the separation and basic characterization of mono-lanthanum endohedral fullerene isomers with the cage size of 76 to 90 were investigated. The lanthanum endohedral fullerenes were produced by an arc discharge of La-carbon composite rod and extracted by CS_2 and pyridine. The two-stage HPLC technique was improved by replacing commonly used toluene with chlorobenzene as an eluent, to obtain less stable La@C_n samples in high purity. The new mono-lanthanum endohedral fullerene isomers with the cage size of 76, 78, 80 (2 isomers), 84 (2 isomers), 86 (another isomer), and 88 (3 isomers) were obtained. The purity of samples was confirmed by LD-TOF mass,

ESR, and Vis-NIR absorption spectroscopy. The number of available La@C_n isomer was determined as in table 3-1. Furthermore, an analysis of HPLC retention behavior suggested the electronic structure of $La^{3+}@C_n^{3-}$. The construction of the separation protocol may open a new direction of the studies on the metallofullerenes. Further experiments such as the determination of the molecular structure and the systematic characterization of each La@C_n isomer will play an important role to explain the formation mechanism of metallofullerenes. On the other hand, we can suggest that this separation protocol can be applied to the M3+ type mono-lanthanoid endohedral fullerenes with small change, and the comparison of the Vis-NIR spectrum of the structural isomer of M@C_n with that of La@C_ns will give an important contribution for the determination of the molecular structure. The validity of above suggestions was confirmed by our recent experiment on the separation of Gd@C_n. The separation of the Gd@C_{76} and Gd@C_{82}-II were performed by the same separation protocol, and the Vis-NIR spectra were similar to that of corresponding La@C_{76} and La@C_{82}-II.

In chapter 4, the detailed electronic structures of the series of mono-lanthanum fullerene were discussed in the first section. The temperature and the M_I dependence of ESR line width of La@C_n (n=76-90) in CS_2 solution was analyzed in terms of the rotational diffusion of a radical molecule in solution. The anisotropic ESR parameters, such as Δg, Δa and the nuclear quadrupole coupling constant, were determined. The validity of this analysis was confirmed by comparison of the spectra in frozen solution with those from the simulation. The quantitative treatment of these parameters revealed the formal electronic structure of $La^{3+}@C_n^{3-}$. The cage size dependence was crudely observed for the quadrupole interaction. Furthermore, the high symmetry of the cage structure was suggested for La@C_{80}-I and La@C_{84}-II. Further experimental and theoretical investigations should be needed. This ESR study of the series of La@C_ns could not explain the reason of the Magic Number of 82.

In the latter section of chapter 4, the electronic structures of endohedral metallofullerene ions were investigated. The analysis of the ESR spectra of the anion and the cation of Gd@C_{82}-I suggested that the reduction and oxidation occur on the π-orbital of C_{82}, and the oxidation state of an endohedral Gd atom remain unchanged from +3. The interesting case is that of $La_2@C_{80}$ anion. The reduction induced valency change was suggested for $La_2@C_{80}$ anion, because the large spin density on the internal

La dimmer was observed. Recently, a similar ESR spectrum was observed for $La_2@C_{76}$ in pyridine. This suggested that the reduction induced valency change is a general character of di-lanthanum metallofullerenes.

This research work gave some basic information, which is useful for further experimental and theoretical research works of endohedral metallofulllerenes. The author hopes that further investigations of these exotic molecules will open a new direction in chemistry and physics.

References

Chapter 1.

(1) Kratschmer, W.; Lamb, L. D.; Fostiropoulos, K.; Huffman, D. R. *Nature* **1990**, *347*, 354-358.

(2) Chai, Y.; Guo, T.; Jin, C. M.; Haufler, R. E.; Chibante, L. P. F.; Fure, J.; Wang, L. H.; Alford, J. M.; Smalley, R. E. *J. Phys. Chem.* **1991**, *95*, 7564-7568.

(3) Johnson, R. D.; Devries, M. S.; Salem, J.; Bethune, D. S.; Yannoni, C. S. *Nature* **1992**, *355*, 239-240.

(4) Shinohara, H. *Rep. Prog. Phys.* **2000**, *63*, 843-892.

(5) Shinohara, H. In *Fullerenes; Chemistry, Physics, and Technology*; Kadish, K. M., Ruoff, R. S., Eds.; John Wiley & Sons, Inc, 2000.

(6) Nagase, S.; Kobayashi, K.; Akasaka, T. In *Fullerenes; Chemistry, Physics, and Technology*; Kadish, K. M., Ruoff, R. S., Eds.; John Wiley & Sons, Inc, 2000.

(7) Liu, S. Y.; Sun, S. Q. *J. Organomet. Chem.* **2000**, *599*, 74-86.

(8) Kikuchi, K.; Suzuki, S.; Nakao, Y.; Nakahara, N.; Wakabayashi, T.; Shiromaru, H.; Saito, K.; Ikemoto, I.; Achiba, Y. *Chem. Phys. Lett.* **1993**, *216*, 67-71.

(9) Yamamoto, K.; Funasaka, H.; Takahashi, T.; Akasaka, T. *J. Phys. Chem.* **1994**, *98*, 2008-2011.

(10) Gromov, A.; Kratschmer, W.; Krawez, N.; Tellgmann, R.; Campbell, E. E. B. *Chem. Commun.* **1997**, 2003-2004.

(11) Weidinger, A.; Waiblinger, M.; Pietzak, B.; Murphy, T. A. *Appl. Phys. A-Mater. Sci. Process.* **1998**, *66*, 287-292.

(12) Knapp, C.; Weiden, N.; Kass, K.; Dinse, K. P.; Pietzak, B.; Waiblinger, M.; Weidinger, A. *Mol. Phys.* **1998**, *95*, 999-1004.

(13) Dinse, K. P.; Kass, H.; Knapp, C.; Weiden, N. *Carbon* **2000**, *38*, 1635-1640.

(14) Heath, J. R.; Obrien, S. C.; Zhang, Q.; Liu, Y.; Curl, R. F.; Kroto, H. W.; Tittel, F. K.; Smalley, R. E. *J. Am. Chem. Soc.* **1985**, *107*, 7779-7780.

(15) Saunders, M.; Jimenezvazquez, H. A.; Cross, R. J.; Poreda, R. J. *Science* **1993**, *259*, 1428-1430.

(16) Bandow, S.; Kitagawa, H.; Mitani, T.; Inokuchi, H.; Saito, Y.; Yamaguchi, H.; Hayashi, N.; Sato, H.; Shinohara, H. *J. Phys. Chem.* **1992**, *96*, 9609-9612.

(17) Fuchs, D.; Rietschel, H.; Michel, R. H.; Fischer, A.; Weis, P.; Kappes, M. M. *J. Phys. Chem.* **1996**, *100*, 725-729.

(18) Yamamoto, K.; Funasaka, H. In *Recent Advances in the Chemistry and Physics of Fullerenes and Related Materials*; Kadish, K. M., Ruoff, R. S., Eds.; Electrochemical Society, Pennington, NJ, 1996; p 593.

(19) Sivaraman, N.; Dhamodaran, R.; Kaliappan, I.; Srinivasan, T. G.; Rao, P. R. V.; Mathews, C. K. *J. Org. Chem.* **1992**, *57*, 6077-6079.

(20) Ruoff, R. S.; Tse, D. S.; Malhotra, R.; Lorents, D. C. *J. Phys. Chem.* **1993**, *97*, 3379-3383.

(21) Scrivens, W. A.; Tour, J. M. *J. Chem. Soc.-Chem. Commun.* **1993**, 1207-1209.

(22) Sun, D. Y.; Liu, Z. Y.; Guo, S. H.; Xu, W. G.; Liu, S. Y. *Fullerene Sci. Technol.* **1997**, *5*, 137-147.

(23) Sun, D. Y.; Liu, Z. Y.; Guo, X. H.; Xu, W. G.; Liu, S. Y. *J. Phys. Chem. B* **1997**, *101*, 3927-3930.

(24) Tso, T. S. C.; Wan, T. S. M.; Zhang, H. W.; Kwong, K. P.; Wong, T.; Shinohara, H.; Inakuma, M. *Tetrahedron Lett.* **1996**, *37*, 9249-9252.

(25) Ding, J. Q.; Yang, S. H. *Chem. Mat.* **1996**, *8*, 2824-2827.

(26) Ding, J. Q.; Yang, S. H. *J. Phys. Chem. Solids* **1997**, *58*, 1661-1667.

(27) Laukhina, E. E.; Bubnov, V. P.; Estrin, Y. I.; Golod, Y. A.; Khodorkovskii, M. A.; Koltover, V. K.; Yagubskii, E. B. *J. Mater. Chem.* **1998**, *8*, 893-895.

(28) Kanbara, T.; Kubozono, Y.; Takabayashi, Y.; Fujiki, S.; Iida, S.; Haruyama, Y.; Kashino, S.; Emura, S.; Akasaka, T. *Phys. Rev. B* **2001**, *6411*, 3403-+.

(29) Kubozono, Y.; Maeda, H.; Takabayashi, Y.; Hiraoka, K.; Nakai, T.; Kashino, S.; Emura, S.; Ukita, S.; Sogabe, T. *J. Am. Chem. Soc.* **1996**, *118*, 6998-6999.

(30) Kubozono, Y.; Noto, T.; Ohta, T.; Maeda, H.; Kashino, S.; Emura, S.; Ukita, S.; Sogabe, T. *Chem. Lett.* **1996**, 453-454.

(31) Kubozono, Y.; Ohta, T.; Hayashibara, T.; Maeda, H.; Ishida, H.; Kashino, S.; Oshima, K.; Yamazaki, H.; Ukita, S.; Sogabe, T. *Chem. Lett.* **1995**, 457-458.

(32) Yeretzian, C.; Wiley, J. B.; Holczer, K.; Su, T.; Nguyen, S.; Kaner, R. B.; Whetten, R. L. *J. Phys. Chem.* **1993**, *97*, 10097-10101.

(33) Diener, M. D.; Alford, J. M. *Nature* **1998**, *393*, 668-671.

(34) Welch, C. J.; Pirkle, W. H. *Journal of Chromatography* **1992**, *609*, 89-101.

(35) Kimata, K.; Hosoya, K.; Araki, T.; Tanaka, N. *J. Org. Chem.* **1993**, *58*, 282-283.

(36) Jinno, K.; Saito, Y.; Chen, Y. L.; Luehr, G.; Archer, J.; Fetzer, J. C.; Biggs, W. R. *J. Microcolumn Sep.* **1993**, *5*, 135-140.

(37) Xiao, J.; Savina, M. R.; Martin, G. B.; Francis, A. H.; Meyerhoff, M. E. *J. Am. Chem. Soc.* **1994**, *116*, 9341-9342.

(38) Saito, Y.; Ohta, H.; Nagashima, H.; Itoh, K.; Jinno, K.; Pesek, J. J. *J. Microcolumn Sep.* **1995**, *7*, 41-49.

(39) Kimata, K.; Hirose, T.; Moriuchi, K.; Hosoya, K.; Araki, T.; Tanaka, N. *Anal. Chem.* **1995**, *67*, 2556-2561.

(40) Fowler, P. W.; Manolopoulos, D. E. *An Atras of Fullerenes*; Cleandon Press: Oxford, 1995.

(41) Yamamoto, K.; Funasaka, H.; Takahashi, T.; Akasaka, T.; Suzuki, T.; Maruyama, Y. *J. Phys. Chem.* **1994**, *98*, 12831-12833.

(42) John, T.; Dennis, S.; Shinohara, H. *Appl. Phys. A-Mater. Sci. Process.* **1998**, *66*, 243-247.

(43) Okazaki, T.; Lian, Y. F.; Gu, Z. N.; Suenaga, K.; Shinohara, H. *Chem. Phys. Lett.* **2000**, *320*, 435-440.

(44) Akiyama, K.; Sueki, K.; Kodama, T.; Kikuchi, K.; Ikemoto, I.; Katada, M.; Nakahara, H. *J. Phys. Chem. A* **2000**, *104*, 7224-7226.

(45) Sueki, K.; Akiyama, K.; Kikuchi, K.; Nakahara, H. *J. Phys. Chem. B* **1999**, *103*, 1390-1392.

(46) Akiyama, K.; Sueki, K.; Kodama, T.; Kikuchi, K.; Takigawa, Y.; Nakahara, H.; Ikemoto, I.; Katada, M. *Chem. Phys. Lett.* **2000**, *317*, 490-496.

(47) Cao, B. P.; Hasegawa, M.; Okada, K.; Tomiyama, T.; Okazaki, T.; Suenaga, K.; Shinohara, H. *J. Am. Chem. Soc.* **2001**, *123*, 9679-9680.

(48) Sueki, K.; Kikuchi, K.; Akiyama, K.; Sawa, T.; Katada, M.; Ambe, S.; Ambe, F.; Nakahara, H. *Chem. Phys. Lett.* **1999**, *300*, 140-144.

(49) Yannoni, C. S.; Hoinkis, M.; Devries, M. S.; Bethune, D. S.; Salem, J. R.; Crowder, M. S.; Johnson, R. D. *Science* **1992**, *256*, 1191-1192.

(50) Shinohara, H.; Sato, H.; Saito, Y.; Ohkohchi, M.; Ando, Y. *J. Phys. Chem.* **1992**, *96*, 3571-3573.

(51) Shinohara, H.; Inakuma, M.; Hayashi, N.; Sato, H.; Saito, Y.; Kato, T.; Bandow, S. *J. Phys. Chem.* **1994**, *98*, 8597-8599.

(52) Hoinkis, M.; Yannoni, C. S.; Bethune, D. S.; Salem, J. R.; Johnson, R. D.; Crowder, M. S.; Devries, M. S. *Chem. Phys. Lett.* **1992**, *198*, 461-465.

(53) Suzuki, S.; Kawata, S.; Shiromaru, H.; Yamauchi, K.; Kikuchi, K.; Kato, T.; Achiba, Y. *J. Phys. Chem.* **1992**, *96*, 7159-7161.

(54) Suzuki, S.; Kojima, Y.; Nakao, Y.; Wakabayashi, T.; Kawata, S.; Kikuchi, K.; Achiba, Y.; Kato, T. *Chem. Phys. Lett.* **1994**, *229*, 512-516.

(55) Bartl, A.; Dunsch, L.; Kirbach, U. *Solid State Commun.* **1995**, *94*, 827-831.

(56) Bartl, A.; Dunsch, L.; Frohner, J.; Kirbach, U. *Chem. Phys. Lett.* **1994**, *229*, 115-121.

(57) Bartl, A.; Dunsch, L.; Kirbach, U. *Appl. Magn. Reson.* **1996**, *11*, 301-314.

(58) Bartl, A.; Dunsch, L.; Kirbach, U.; Schandert, B. *Synth. Met.* **1995**, *70*, 1365-1368.

(59) Saito, Y.; Yokoyama, S.; Inakuma, M.; Shinohara, H. *Chem. Phys. Lett.* **1996**, *250*, 80-84.

(60) Kato, T.; Suzuki, S.; Kikuchi, K.; Achiba, Y. *J. Phys. Chem.* **1993**, *97*, 13425-13428.

(61) Rubsam, M.; Pluschau, M.; Schweitzer, P.; Dinse, K. P.; Fuchs, D.; Rietschel, H.; Michel, R. H.; Benz, M.; Kappes, M. M. *Chem. Phys. Lett.* **1995**, *240*, 615-621.

(62) Rubsam, M.; Schweitzer, P.; Dinse, K. P. *Chem. Phys. Lett.* **1996**, *263*, 540-544.

(63) Rubsam, M.; Schweitzer, P.; Dinse, K. P. *J. Phys. Chem.* **1996**, *100*, 19310-19314.

(64) Schweitzer, P.; Dinse, K. P. *Appl. Magn. Reson.* **1997**, *13*, 365-374.

(65) Seifert, G.; Bartl, A.; Dunsch, L.; Ayuela, A.; Rockenbauer, A. *Appl. Phys. A-Mater. Sci. Process.* **1998**, *66*, 265-271.

(66) Inakuma, M.; Shinohara, H. *J. Phys. Chem. B* **2000**, *104*, 7595-7599.

(67) Weiden, N.; Kass, H.; Dinse, K. P. *J. Phys. Chem. B* **1999**, *103*, 9826-9830.

(68) Knapp, C.; Weiden, N.; Dinse, K. P. *Appl. Phys. A-Mater. Sci. Process.* **1998**, *66*, 249-255.

(69) Knorr, S.; Grupp, A.; Mehring, M.; Kirbach, U.; Bartl, A.; Dunsch, L. *Appl. Phys. A-Mater. Sci. Process.* **1998**, *66*, 257-264.

(70) Kato, T.; Bandou, S.; Inakuma, M.; Shinohara, H. *J. Phys. Chem.* **1995**, *99*, 856-858.

(71) Vanloosdrecht, P. H. M.; Johnson, R. D.; Devries, M. S.; Kiang, C. H.; Bethune, D. S.; Dorn, H. C.; Burbank, P.; Stevenson, S. *Phys. Rev. Lett.* **1994**, *73*, 3415-3418.

(72) Sanakis, Y.; Tagmatarchis, N.; Aslanis, E.; Ioannidis, N.; Petrouleas, V.; Shinohara, H.; Prassides, K. *J. Am. Chem. Soc.* **2001**, *123*, 9924-9925.

(73) Jakes, P.; Dinse, K. P. *J. Am. Chem. Soc.* **2001**, *123*, 8854-8855.

(74) Lebedkin, S.; Renker, B.; Heid, R.; Schober, H.; Rietschel, H. *Appl. Phys. A-Mater. Sci. Process.* **1998**, *66*, 273-280.

(75) Krause, M.; Kuran, P.; Kirbach, U.; Dunsch, L. *Carbon* **1999**, *37*, 113-115.

(76) Inakuma, M.; Yamamoto, E.; Kai, T.; Wang, C. R.; Tomiyama, T.; Shinohara, H.; Dennis, T. J. S.; Hulman, M.; Krause, M.; Kuzmany, H. *J. Phys. Chem. B* **2000**, *104*, 5072-5077.

(77) Hino, S.; Takahashi, H.; Iwasaki, K.; Matsumoto, K.; Miyazaki, T.; Hasegawa, S.; Kikuchi, K.; Achiba, Y. *Phys. Rev. Lett.* **1993**, *71*, 4261-4263.

(78) Hino, S.; Umishita, K.; Iwasaki, K.; Miyamae, T.; Inakuma, M.; Shinohara, H. *Chem. Phys. Lett.* **1999**, *300*, 145-151.

(79) Hino, S.; Umishita, K.; Iwasaki, K.; Miyazaki, T.; Miyamae, T.; Kikuchi, K.; Achiba, Y. *Chem. Phys. Lett.* **1997**, *281*, 115-122.

(80) Kessler, B.; Bringer, A.; Cramm, S.; Schlebusch, C.; Eberhardt, W.; Suzuki, S.; Achiba, Y.; Esch, F.; Barnaba, M.; Cocco, D. *Phys. Rev. Lett.* **1997**, *79*, 2289-2292.

(81) Iwasaki, K.; Umishita, K.; Hino, S.; Kikuchi, K.; Achiba, Y.; Shinohara, H. *Mol. Cryst. Liquid Cryst.* **2000**, *340*, 643-648.

(82) Pichler, T.; Hu, Z.; Grazioli, C.; Legner, S.; Knupfer, M.; Golden, M. S.; Fink, J.; de Groot, F. M. F.; Hunt, M. R. C.; Rudolf, P.; Follath, R.; Jung, C.; Kjeldgaard, L.; Bruhwiler, P.; Inakuma, M.; Shinohara, H. *Phys. Rev. B* **2000**, *62*, 13196-13201.

(83) Pichler, T.; Knupfer, M.; Golden, M. S.; Boske, T.; Fink, J.; Kirbach, U.; Kuran, P.; Dunsch, L.; Jung, C. *Appl. Phys. A-Mater. Sci. Process.* **1998**, *66*, 281-285.

(84) Park, C. H.; Wells, B. O.; Dicarlo, J.; Shen, Z. X.; Salem, J. R.; Bethune, D. S.; Yannoni, C. S.; Johnson, R. D.; Devries, M. S.; Booth, C.; Bridges, F.; Pianetta, P. *Chem. Phys. Lett.* **1993**, *213*, 196-201.

(85) Kajiyama, H.; Tomioka, Y.; Ishibashi, M.; Taniguchi, Y. *Abstr. Pap. Am. Chem. Soc.* **1994**, *207*, 314-PHYS.

(86) Kubozono, Y.; Takabayashi, Y.; Kashino, S.; Kondo, M.; Wakahara, T.; Akasaka, T.; Kobayashi, K.; Nagase, S.; Emura, S.; Yamamoto, K. *Chem. Phys. Lett.* **2001**, *335*, 163-169.

(87) Suenaga, K.; Iijima, S.; Kato, H.; Shinohara, H. *Phys. Rev. B* **2000**, *62*, 1627-1630.

(88) Suenaga, K.; Tence, T.; Mory, C.; Colliex, C.; Kato, H.; Okazaki, T.; Shinohara, H.; Hirahara, K.; Bandow, S.; Iijima, S. *Science* **2000**, *290*, 2280-+.

(89) Kato, H.; Suenaga, K.; Mikawa, W.; Okumura, M.; Miwa, N.; Yashiro, A.; Fujimura, H.; Mizuno, A.; Nishida, Y.; Kobayashi, K.; Shinohara, H. *Chem. Phys. Lett.* **2000**, *324*, 255-259.

(90) Okazaki, T.; Suenaga, K.; Lian, Y. F.; Gu, Z. N.; Shinohara, H. *J. Chem. Phys.* **2000**, *113*, 9593-9597.

(91) Sato, W.; Sueki, K.; Achiba, Y.; Nakahara, H.; Ohkubo, Y.; Asai, K. *Phys. Rev. B* **2001**, *6302*, 4405-U4174.

(92) Sato, W.; Sueki, K.; Kikuchi, K.; Kobayashi, K.; Suzuki, S.; Achiba, Y.; Nakahara, H.; Ohkubo, Y.; Ambe, F.; Asai, K. *Phys. Rev. Lett.* **1998**, *80*, 133-136.

(93) Sato, W.; Sueki, K.; Kikuchi, K.; Suzuki, S.; Achiba, Y.; Nakahara, H.; Ohkubo, Y.; Asai, K.; Ambe, F. *Phys. Rev. B* **1998**, *58*, 10850-10856.

(94) Takata, M.; Nishibori, E.; Umeda, B.; Sakata, M.; Yamamoto, E.; Shinohara, H. *Phys. Rev. Lett.* **1997**, *78*, 3330-3333.

(95) Takata, M.; Umeda, B.; Nishibori, E.; Sakata, M.; Saito, Y.; Ohno, M.; Shinohara, H. *Nature* **1995**, *377*, 46-49.

(96) Nishibori, E.; Takata, M.; Sakata, M.; Inakuma, M.; Shinohara, H. *Chem. Phys. Lett.* **1998**, *298*, 79-84.

(97) Nishibori, E.; Takata, M.; Sakata, M.; Shinohara, H. *J. Synchrot. Radiat.* **1998**, *5*, 977-979.

(98) Nishibori, E.; Takata, M.; Sakata, M.; Tanaka, H.; Hasegawa, M.; Shinohara, H. *Chem. Phys. Lett.* **2000**, *330*, 497-502.

(99) Nishibori, E.; Takata, M.; Sakata, M.; Taninaka, A.; Shinohara, H. *Angew. Chem.-Int. Edit.* **2001**, *40*, 2998-2999.

(100) Watanuki, T.; Fujiwara, A.; Ishii, K.; Matuoka, Y.; Suematsu, H.; Ohwada, K.; Nakao, H.; Fujii, Y.; Kodama, T.; Kikuchi, K.; Achiba, Y. *Mol. Cryst. Liquid Cryst.* **2000**, *340*, 639-642.

(101) Nagase, S.; Kobayashi, K.; Akasaka, T. *Bull. Chem. Soc. Jpn.* **1996**, *69*, 2131-2142.

(102) Nagase, S.; Kobayashi, K.; Akasaka, T. *Theochem-J. Mol. Struct.* **1997**, *398*, 221-227.

(103) Nagase, S.; Kobayashi, K.; Akasaka, T. *J. Comput. Chem.* **1998**, *19*, 232-239.

(104) Nagase, S.; Kobayashi, K.; Akasaka, T. *Journal of Molecular Structure-Theochem* **1999**, *462*, 97-104.

(105) Kobayashi, K.; Nagase, S.; Yoshida, M.; Osawa, E. *J. Am. Chem. Soc.* **1997**, *119*, 12693-12694.

(106) Poirier, D. M.; Knupfer, M.; Weaver, J. H.; Andreoni, W.; Laasonen, K.; Parrinello, M.; Bethune, D. S.; Kikuchi, K.; Achiba, Y. *Phys. Rev. B* **1994**, *49*, 17403-17412.

(107) Schulte, J.; Bohm, M. C.; Dinse, K. P. *Chem. Phys. Lett.* **1996**, *259*, 48-54.

(108) Schulte, J.; Bohm, M. C.; Dinse, K. P. *Theochem-J. Mol. Struct.* **1998**, *427*, 279-292.

(109) Nagase, S.; Kobayashi, K.; Kato, T.; Achiba, Y. *Chem. Phys. Lett.* **1993**, *201*, 475-480.

(110) Nagase, S.; Kobayashi, K. *Chem. Phys. Lett.* **1993**, *214*, 57-63.

(111) Nagase, S.; Kobayashi, K. *Chem. Phys. Lett.* **1994**, *228*, 106-110.

(112) Nagase, S.; Kobayashi, K. *J. Chem. Soc.-Chem. Commun.* **1994**, 1837-1838.

(113) Kobayashi, K.; Nagase, S. *Chem. Phys. Lett.* **1997**, *274*, 226-230.

(114) Kobayashi, K.; Nagase, S. *Chem. Phys. Lett.* **1998**, *282*, 325-329.

(115) Kobayashi, K.; Nagase, S.; Akasaka, T. *Chem. Phys. Lett.* **1995**, *245*, 230-236.

(116) Kobayashi, K.; Nagase, S. *Chem. Phys. Lett.* **1996**, *262*, 227-232.

(117) Kobayashi, K.; Nagase, S.; Akasaka, T. *Chem. Phys. Lett.* **1996**, *261*, 502-506.

(118) Nagase, S.; Kobayashi, K. *Chem. Phys. Lett.* **1994**, *231*, 319-324.

(119) Nagase, S.; Kobayashi, K. *Chem. Phys. Lett.* **1997**, *276*, 55-61.

(120) Kobayashi, K.; Nagase, S. *Chem. Phys. Lett.* **1999**, *302*, 312-316.

(121) Kobayashi, K.; Nagase, S. *Chem. Phys. Lett.* **1999**, *313*, 45-51.

(122) Akasaka, T.; Kato, T.; Kobayashi, K.; Nagase, S.; Yamamoto, K.; Funasaka, H.; Takahashi, T. *Nature* **1995**, *374*, 600-601.

(123) Suzuki, T.; Maruyama, Y.; Kato, T.; Akasaka, T.; Kobayashi, K.; Nagase, S.; Yamamoto, K.; Funasaka, H.; Takahashi, T. *J. Am. Chem. Soc.* **1995**, *117*, 9606-9607.

(124) Akasaka, T.; Kato, T.; Nagase, S.; Kobayashi, K.; Yamamoto, K.; Funasaka, H.; Takahashi, T. *Tetrahedron* **1996**, *52*, 5015-5020.

(125) Akasaka, T.; Nagase, S.; Kobayashi, K. *J. Synth. Org. Chem. Jpn.* **1996**, *54*, 580-585.

(126) Akasaka, T.; Nagase, S.; Kobayashi, K.; Suzuki, T.; Kato, T.; Kikuchi, K.; Achiba, Y.; Yamamoto, K.; Funasaka, H.; Takahashi, T. *Angew. Chem.-Int. Edit. Engl.* **1995**, *34*, 2139-2141.

(127) Akasaka, T.; Nagase, S.; Kobayashi, K.; Suzuki, T.; Kato, T.; Yamamoto, K.; Funasaka, H.; Takahashi, T. *J. Chem. Soc.-Chem. Commun.* **1995**, 1343-1344.

(128) Kato, T.; Akasaka, T.; Kobayashi, K.; Nagase, S.; Yamamoto, K.; Funasaka, H.; Takahashi, T. *Appl. Magn. Reson.* **1996**, *11*, 293-300.

(129) Kato, T.; Akasaka, T.; Kobayashi, K.; Nagase, S.; Kikuchi, K.; Achiba, Y.; Suzuki, T.; Yamamoto, K. *J. Phys. Chem. Solids* **1997**, *58*, 1779-1783.

(130) Akasaka, T.; Okubo, S.; Wakahara, T.; Yamamoto, K.; Kobayashi, K.; Nagase, S.; Kato, T.; Kako, M.; Nakadaira, Y.; Kitayama, Y.; Matsuura, K. *Chem. Lett.* **1999**, 945-946.

(131) Suzuki, T.; Maruyama, Y.; Kato, T.; Kikuchi, K.; Nakao, Y.; Achiba, Y.; Kobayashi, K.; Nagase, S. *Angew. Chem.-Int. Edit. Engl.* **1995**, *34*, 1094-1096.

(132) Suzuki, T.; Maruyama, Y.; Kato, T.; Kikuchi, K.; Nakao, Y.; Suzuki, S.; Achiba, Y.; Yamamoto, K.; Funasaka, H.; Takahashi, T. *Synth. Met.* **1995**, *70*, 1443-1446.

(133) Akasaka, T.; Nagase, S.; Kobayashi, K.; Walchli, M.; Yamamoto, K.; Funasaka, H.; Kako, M.; Hoshino, T.; Erata, T. *Angew. Chem.-Int. Edit. Engl.* **1997**, *36*, 1643-1645.

(134) Yamamoto, E.; Tansho, M.; Tomiyama, T.; Shinohara, H.; Kawahara, H.; Kobayashi, Y. *J. Am. Chem. Soc.* **1996**, *118*, 2293-2294.

(135) Wang, C. R.; Kai, T.; Tomiyama, T.; Yoshida, T.; Kobayashi, Y.; Nishibori, E.; Takata, M.; Sakata, M.; Shinohara, H. *Angew. Chem.-Int. Edit.* **2001**, *40*, 397-399.

(136) Wang, C. R.; Kai, T.; Tomiyama, T.; Yoshida, T.; Kobayashi, Y.; Nishibori, E.; Takata, M.; Sakata, M.; Shinohara, H. *Nature* **2000**, *408*, 426-427.

(137) Xu, Z. D.; Nakane, T.; Shinohara, H. *J. Am. Chem. Soc.* **1996**, *118*, 11309-11310.

(138) Stevenson, S.; Rice, G.; Glass, T.; Harich, K.; Cromer, F.; Jordan, M. R.; Craft, J.; Hadju, E.; Bible, R.; Olmstead, M. M.; Maitra, K.; Fisher, A. J.; Balch, A. L.; Dorn, H. C. *Nature* **1999**, *401*, 55-57.

(139) Stevenson, S.; Fowler, P. W.; Heine, T.; Duchamp, J. C.; Rice, G.; Glass, T.; Harich, K.; Hajdu, E.; Bible, R.; Dorn, H. C. *Nature* **2000**, *408*, 427-428.

(140) Kodama, T.; Ozawa, N.; Miyake, Y.; Sakaguchi, K.; Nishikawa, H.; Ikemoto, I.; Kikuchi, K.; Achiba, Y. *J. Am. Chem. Soc.* **2002**, *124*, 1452-1455.

(141) Akasaka, T.; Wakahara, T.; Nagase, S.; Kobayashi, K.; Waelchli, M.; Yamamoto, K.; Kondo, M.; Shirakura, S.; Okubo, S.; Maeda, Y.; Kato, T.; Kako, M.; Nakadaira, Y.; Nagahata, R.; Gao, X.; Van Caemelbecke, E.; Kadish, K. M. *J. Am. Chem. Soc.* **2000**, *122*, 9316-9317.

(142) Akasaka, T.; Wakahara, T.; Nagase, S.; Kobayashi, K.; Waelchli, M.; Yamamoto, K.; Kondo, M.; Shirakura, S.; Maeda, Y.; Kato, T.; Kako, M.; Nakadaira, Y.; Gao, X.; Van Caemelbecke, E.; Kadish, K. M. *J. Phys. Chem. B* **2001**, *105*, 2971-2974.

(143) Vonhelden, G.; Hsu, M. T.; Gotts, N.; Bowers, M. T. *J. Phys. Chem.* **1993**, *97*, 8182-8192.

(144) Clemmer, D. E.; Hunter, J. M.; Shelimov, K. B.; Jarrold, M. F. *Nature* **1994**, *372*, 248-250.

(145) Clemmer, D. E.; Shelimov, K. B.; Jarrold, M. F. *J. Am. Chem. Soc.* **1994**, *116*, 5971-5972.

(146) Shelimov, K. B.; Clemmer, D. E.; Jarrold, M. F. *J. Phys. Chem.* **1994**, *98*, 12819-12821.

(147) Shelimov, K. B.; Clemmer, D. E.; Jarrold, M. F. *J. Phys. Chem.* **1995**, *99*, 11376-11386.

(148) Shelimov, K. B.; Jarrold, M. F. *J. Am. Chem. Soc.* **1995**, *117*, 6404-6405.

(149) Shelimov, K. B.; Jarrold, M. F. *J. Am. Chem. Soc.* **1996**, *118*, 1139-1147.

(150) Ettl, R.; Chao, I.; Diederich, F.; Whetten, R. L. *Nature* **1991**, *353*, 149-153.

(151) Diederich, F.; Whetten, R. L.; Thilgen, C.; Ettl, R.; Chao, I.; Alvarez, M. M. *Science* **1991**, *254*, 1768-1770.

(152) Kikuchi, K.; Nakahara, N.; Wakabayashi, T.; Suzuki, S.; Shiromaru, H.; Miyake, Y.; Saito, K.; Ikemoto, I.; Kainosho, M.; Achiba, Y. *Nature* **1992**, *357*, 142-145.

(153) Dennis, T. J. S.; Kai, T.; Asato, K.; Tomiyama, T.; Shinohara, H.; Yoshida, T.; Kobayashi, Y.; Ishiwatari, H.; Miyake, Y.; Kikuchi, K.; Achiba, Y. *J. Phys. Chem. A* **1999**, *103*, 8747-8752.

(154) Smalley, R. E. *Accounts Chem. Res.* **1992**, *25*, 98-105.

(155) Wakabayashi, T.; Achiba, Y. *Chem. Phys. Lett.* **1992**, *190*, 465-468.

(156) Wakabayashi, T.; Kikuchi, K.; Shiromaru, H.; Suzuki, S.; Achiba, Y. *Z. Phys. D-Atoms Mol. Clusters* **1993**, *26*, S258-S260.

(157) Saito, S.; Sawada, S. *Chem. Phys. Lett.* **1992**, *198*, 466-471.

(158) Maruyama, S.; Yamaguchi, Y. *Chem. Phys. Lett.* **1998**, *286*, 343-349.

(159) Yamamoto, K.; Funasaka, H.; Takahashi, T.; Akasaka, T. In *Recent Advances in the Chemistry and Physics of Fullerenes and Related Materials*; Kadish, K. M., Ruoff, R. S., Eds.; Electrochemical Society, Pennington, NJ, 1997; p 375.

(160) Tagmatarchis, N.; Aslanis, E.; Prassides, K.; Shinohara, H. *Chem. Mat.* **2001**, *13*, 2374-2379.

(161) Tagmatarchis, N.; Aslanis, E.; Shinohara, H.; Prassides, K. *J. Phys. Chem. B* **2000**, *104*, 11010-11012.

(162) Kubozono, Y.; Hiraoka, K.; Takabayashi, Y.; Nakai, T.; Ohta, T.; Maeda, H.; Ishida, H. *Chem. Lett.* **1996**, 1061-1062.

(163) Ding, J. Q.; Yang, S. H. *J. Am. Chem. Soc.* **1996**, *118*, 11254-11257.

(164) Ding, J. Q.; Lin, N.; Weng, L. T.; Cue, N.; Yang, S. H. *Chem. Phys. Lett.* **1996**, *261*, 92-97.

(165) Ding, J. Q.; Yang, S. H. *Angew. Chem.-Int. Edit. Engl.* **1996**, *35*, 2234-2235.

(166) Yamamoto, K. In *The 16th Fullerene General Sympojium*: Okazaki, Japan, 1999; p 156.

(167) Maeda, Y. In *Ph. D. Thesis*; Niiigata University: Niigata, Japan, 2001.

Chapter 2.

(1) Bandow, S.; Kitagawa, H.; Mitani, T.; Inokuchi, H.; Saito, Y.; Yamaguchi, H.; Hayashi, N.; Sato, H.; Shinohara, H. *J. Phys. Chem.* **1992**, *96*, 9609-9612.

(2) Yamamoto, K.; Funasaka, H.; Takahashi, T.; Akasaka, T. *J. Phys. Chem.* **1994**, *98*, 2008-2011.

(3) Liu, B. B.; Lin, Z. Y.; Xu, W. G.; Yang, H. B.; Gao, C. X.; Lu, J. S.; Liu, S. Y.; Zou, G. T. *Tetrahedron* **1998**, *54*, 11123-11128.

(4) Xiao, J.; Savina, M. R.; Martin, G. B.; Francis, A. H.; Meyerhoff, M. E. *J. Am. Chem. Soc.* **1994**, *116*, 9341-9342.

(5) Kubozono, Y.; Maeda, H.; Takabayashi, Y.; Hiraoka, K.; Nakai, T.; Kashino, S.; Emura, S.; Ukita, S.; Sogabe, T. *J. Am. Chem. Soc.* **1996**, *118*, 6998-6999.

(6) Akasaka, T.; Wakahara, T.; Nagase, S.; Kobayashi, K.; Waelchli, M.; Yamamoto, K.; Kondo, M.; Shirakura, S.; Okubo, S.; Maeda, Y.; Kato, T.; Kako, M.; Nakadaira, Y.; Nagahata, R.; Gao, X.; Van Caemelbecke, E.; Kadish, K. M. *J. Am. Chem. Soc.* **2000**, *122*, 9316-9317.

(7) Akasaka, T.; Wakahara, T.; Nagase, S.; Kobayashi, K.; Waelchli, M.; Yamamoto, K.; Kondo, M.; Shirakura, S.; Maeda, Y.; Kato, T.; Kako, M.; Nakadaira, Y.; Gao, X.; Van Caemelbecke, E.; Kadish, K. M. *J. Phys. Chem. B* **2001**, *105*, 2971-2974.

(8) Okubo, S.; Kato, T.; Inakuma, M.; Shinohara, H. *New Diam. Front. Carbon Technol.* **2001**, *11*, 285-294.

(9) Suzuki, T.; Kikuchi, K.; Oguri, F.; Nakao, Y.; Suzuki, S.; Achiba, Y.; Yamamoto, K.; Funasaka, H.; Takahashi, T. *Tetrahedron* **1996**, *52*, 4973-4982.

(10) Suzuki, T.; Maruyama, Y.; Kato, T.; Kikuchi, K.; Nakao, Y.; Achiba, Y.; Kobayashi, K.; Nagase, S. *Angew. Chem.-Int. Edit. Engl.* **1995**, *34*, 1094-1096.

(11) Skiebe, A.; Hirsch, A.; Klos, H.; Gotschy, B. *Chem. Phys. Lett.* **1994**, *220*, 138-140.

(12) Reed, C. A.; Bolskar, R. D. *Chem. Rev.* **2000**, *100*, 1075-1119.

(13) Kato, T.; Kodama, T.; Shida, T. *Chem. Phys. Lett.* **1993**, *205*, 405-409.

(14) Kato, T. *Laser Chem.* **1994**, *14*, 155-160.

(15) Cheng, J. X.; Fang, Y.; Huang, Q. J.; Yan, Y. J.; Li, X. Y. *Chem. Phys. Lett.* **2000**, *330*, 262-266.

(16) Yoshizawa, K.; Sato, T.; Tanaka, K.; Yamabe, T. *Chem. Phys. Lett.* **1993**, *213*, 498-502.

(17) Dubois, D.; Moninot, G.; Kutner, W.; Jones, M. T.; Kadish, K. M. *J. Phys. Chem.* **1992**, *96*, 7137-7145.

(18) Noviandri, I.; Bolskar, R. D.; Lay, P. A.; Reed, C. A. *J. Phys. Chem. B* **1997**, *101*, 6350-6358.

(19) Wohlfarth, C. In *Handbook of Chemistry and Physics*; CRC Press Inc: Florida, 2000-2001; Vol. 81, pp 6-149.

(20) Tsuji, K.; Yoshida, H.; HAayashi, K. *J. Chem. Phys.* **1966**, *45*, 2894-2897.

(21) Bower, H. J.; McRac, J. A.; Symons, M. C. R. *J. Chem. Soc. A* **1968**, 2696-2699.

(22) Shida, T.; Hamill, W. *J. Chem. Phys.* **1966**, *44*, 2369-2374.

(23) Shida, T.; Kato, T. *Chem. Phys. Lett.* **1979**, *68*, 106-110.

(24) Diener, M. D.; Alford, J. M. *Nature* **1998**, *393*, 668-671.

Chapter 3.

(1) Johnson, R. D.; Devries, M. S.; Salem, J.; Bethune, D. S.; Yannoni, C. S. *Nature* **1992**, *355*, 239-240.

(2) Hoinkis, M.; Yannoni, C. S.; Bethune, D. S.; Salem, J. R.; Johnson, R. D.; Crowder, M. S.; Devries, M. S. *Chem. Phys. Lett.* **1992**, *198*, 461-465.

(3) Suzuki, S.; Kawata, S.; Shiromaru, H.; Yamauchi, K.; Kikuchi, K.; Kato, T.; Achiba, Y. *J. Phys. Chem.* **1992**, *96*, 7159-7161.

(4) Bandow, S.; Kitagawa, H.; Mitani, T.; Inokuchi, H.; Saito, Y.; Yamaguchi, H.; Hayashi, N.; Sato, H.; Shinohara, H. *J. Phys. Chem.* **1992**, *96*, 9609-9612.

(5) Kikuchi, K.; Suzuki, S.; Nakao, Y.; Nakahara, N.; Wakabayashi, T.; Shiromaru, H.; Saito, K.; Ikemoto, I.; Achiba, Y. *Chem. Phys. Lett.* **1993**, *216*, 67-71.

(6) Yamamoto, K.; Funasaka, H.; Takahashi, T.; Akasaka, T. *J. Phys. Chem.* **1994**, *98*, 2008-2011.

(7) Yamamoto, K.; Funasaka, H.; Takahashi, T.; Akasaka, T.; Suzuki, T.; Maruyama, Y. *J. Phys. Chem.* **1994**, *98*, 12831-12833.

(8) Yamamoto, K.; Funasaka, H.; Takahashi, T.; Akasaka, T. In *Recent Advances in the Chemistry and Physics of Fullerenes and Related Materials*; Kadish, K. M., Ruoff, R. S., Eds.; Electrochemical Society, Pennington, NJ, 1997, p 375.

(9) Yamamoto, K. In *The 16th Fullerene General Sympojium*: Okazaki, Japan, 1999, p 156.

(10) Kimata, K.; Hirose, T.; Moriuchi, K.; Hosoya, K.; Araki, T.; Tanaka, N. *Anal. Chem.* **1995**, *67*, 2556-2561.

(11) Yamamoto, K.; Funasaka, H. In *Recent Advances in the Chemistry and Physics of Fullerenes and Related Materials*; Kadish, K. M., Ruoff, R. S., Eds.; Electrochemical Society, Pennington, NJ, 1996, p 593.

(12) Schweitzer, P.; Dinse, K. P. *Appl. Magn. Reson.* **1997**, *13*, 365-374.

(13) Stevenson, S.; Burbank, P.; Harich, K.; Sun, Z.; Dorn, H. C.; van Loosdrecht, P. H. M.; deVries, M. S.; Salem, J. R.; Kiang, C. H.; Johnson, R. D.; Bethune, D. S. *J. Phys. Chem. A* **1998**, *102*, 2833-2837.

(14) Fuchs, D.; Rietschel, H.; Michel, R. H.; Fischer, A.; Weis, P.; Kappes, M. M. *J. Phys. Chem.* **1996**, *100*, 725-729.

(15) Kikuchi, K.; Sueki, K.; Akiyama, K.; Kodama, T.; Katada, M.; Nakahara, H.; Ikemoto, I.; Akasaka, T. In *Recent Advances in the Chemistry and Physics of Fullerenes and Related Materials*; Kadish, K. M., Ruoff, R. S., Eds.; Electrochemical Society, Pennington, NJ, 1997, p 408.

(16) Ding, J. Q.; Yang, S. H. *J. Phys. Chem. Solids* **1997**, *58*, 1661-1667.

(17) Akiyama, K.; Sueki, K.; Kodama, T.; Kikuchi, K.; Ikemoto, I.; Katada, M.; Nakahara, H. *J. Phys. Chem. A* **2000**, *104*, 7224-7226.

(18) Akasaka, T.; Okubo, S.; Kondo, M.; Maeda, Y.; Wakahara, T.; Kato, T.; Suzuki, T.; Yamamoto, K.; Kobayashi, K.; Nagase, S. *Chem. Phys. Lett.* **2000**, *319*, 153-156.

Chapter 4.

(1) Johnson, R. D.; Devries, M. S.; Salem, J.; Bethune, D. S.; Yannoni, C. S. *Nature* **1992**, *355*, 239-240.

(2) Akasaka, T.; Nagase, S.; Kobayashi, K.; Walchli, M.; Yamamoto, K.; Funasaka, H.; Kako, M.; Hoshino, T.; Erata, T. *Angew. Chem.-Int. Edit. Engl.* **1997**, *36*, 1643-1645.

(3) Nishibori, E.; Takata, M.; Sakata, M.; Taninaka, A.; Shinohara, H. *Angew. Chem.-Int. Edit.* **2001**, *40*, 2998-2999.

(4) Kato, T.; Bandou, S.; Inakuma, M.; Shinohara, H. *J. Phys. Chem.* **1995**, *99*, 856-858.

(5) Takata, M.; Nishibori, E.; Sakata, M.; Inakuma, M.; Yamamoto, E.; Shinohara, H. *Phys. Rev. Lett.* **1999**, *83*, 2214-2217.

(6) Hoinkis, M.; Yannoni, C. S.; Bethune, D. S.; Salem, J. R.; Johnson, R. D.; Crowder, M. S.; Devries, M. S. *Chem. Phys. Lett.* **1992**, *198*, 461-465.

(7) Suzuki, S.; Kawata, S.; Shiromaru, H.; Yamauchi, K.; Kikuchi, K.; Kato, T.; Achiba, Y. *J. Phys. Chem.* **1992**, *96*, 7159-7161.

(8) Bandow, S.; Kitagawa, H.; Mitani, T.; Inokuchi, H.; Saito, Y.; Yamaguchi, H.; Hayashi, N.; Sato, H.; Shinohara, H. *J. Phys. Chem.* **1992**, *96*, 9609-9612.

(9) Yamamoto, K.; Funasaka, H.; Takahashi, T.; Akasaka, T. *J. Phys. Chem.* **1994**, *98*, 2008-2011.

(10) Shinohara, H.; Sato, H.; Ohkohchi, M.; Ando, Y.; Kodama, T.; Shida, T.; Kato, T.; Saito, Y. *Nature* **1992**, *357*, 52-54.

(11) Kato, T.; Suzuki, S.; Kikuchi, K.; Achiba, Y. *J. Phys. Chem.* **1993**, *97*, 13425-13428.

(12) Okabe, N.; Ohba, Y.; Suzuki, S.; Kawata, S.; Kikuchi, K.; Achiba, Y.; Iwaizumi, M. *Chem. Phys. Lett.* **1995**, *235*, 564-569.

(13) Rubsam, M.; Schweitzer, P.; Dinse, K. P. *J. Phys. Chem.* **1996**, *100*, 19310-19314.

(14) Rubsam, M.; Schweitzer, P.; Dinse, K. P. *Chem. Phys. Lett.* **1996**, *263*, 540-544.

(15) Rubsam, M.; Pluschau, M.; Schweitzer, P.; Dinse, K. P.; Fuchs, D.; Rietschel, H.; Michel, R. H.; Benz, M.; Kappes, M. M. *Chem. Phys. Lett.* **1995**, *240*, 615-621.

(16) Knorr, S.; Grupp, A.; Mehring, M.; Kirbach, U.; Bartl, A.; Dunsch, L. *Appl. Phys. A-Mater. Sci. Process.* **1998**, *66*, 257-264.

(17) Seifert, G.; Bartl, A.; Dunsch, L.; Ayuela, A.; Rockenbauer, A. *Appl. Phys. A-Mater. Sci. Process.* **1998**, *66*, 265-271.

(18) Yamamoto, K.; Funasaka, H.; Takahashi, T.; Akasaka, T.; Suzuki, T.; Maruyama, Y. *J. Phys. Chem.* **1994**, *98*, 12831-12833.

(19) Inakuma, M.; Shinohara, H. *J. Phys. Chem. B* **2000**, *104*, 7595-7599.

(20) Inakuma, M. O., M.; Shinohara, H. In *"Fullerenes" Recent Advances in Chemistry and Physics of Fullerenes and Related Materials*; Kadish, K. M., Ruoff, R. S., Eds.; ECS: Pennington, NJ, 1995; pp 330-342.

(21) Schweitzer, P.; Dinse, K. P. *Appl. Magn. Reson.* **1997**, *13*, 365-374.

(22) Yamamoto, K. I., T; Sakurai, K; Funasaka,H In *"Fullerenes" Recent Advances in Chemistry and Physics of Fullerenes and Related Materials*; Kadish, K. M., Ruoff, R. S., Eds.; ECS: Pennington, NJ, 1997; Vol. PV97-14, pp 375-389.

(23) Akasaka, T.; Wakahara, T.; Nagase, S.; Kobayashi, K.; Waelchli, M.; Yamamoto, K.; Kondo, M.; Shirakura, S.; Okubo, S.; Maeda, Y.; Kato, T.; Kako, M.; Nakadaira, Y.; Nagahata, R.; Gao, X.; Van Caemelbecke, E.; Kadish, K. M. *J. Am. Chem. Soc.* **2000**, *122*, 9316-9317.

(24) Akasaka, T.; Wakahara, T.; Nagase, S.; Kobayashi, K.; Waelchli, M.; Yamamoto, K.; Kondo, M.; Shirakura, S.; Maeda, Y.; Kato, T.; Kako, M.; Nakadaira, Y.; Gao, X.; Van Caemelbecke, E.; Kadish, K. M. *J. Phys. Chem. B* **2001**, *105*, 2971-2974.

(25) Okubo, S.; Kato, T.; Inakuma, M.; Shinohara, H. *New Diam. Front. Carbon Technol.* **2001**, *11*, 285-294.

(26) Wilson, R.; Kivelson, D. *J. Chem. Phys* **1966**, *44*, 154-168.

(27) Morton, J. R. P., K. F. *Journal of Magnetic Resonance* **1978**, *30*, 577-582.

(28) Nishibori, E.; Takata, M.; Sakata, M.; Tanaka, H.; Hasegawa, M.; Shinohara, H. *Chem. Phys. Lett.* **2000**, *330*, 497-502.

(29) Knapp, C.; Weiden, N.; Dinse, K. P. *Appl. Phys. A-Mater. Sci. Process.* **1998**, *66*, 249-255.

(30) Fowler, P. W.; Manolopoulos, D. E. *An Atras of Fullerenes*; Cleandon Press: Oxford, 1995.

(31) Suzuki, T.; Kikuchi, K.; Oguri, F.; Nakao, Y.; Suzuki, S.; Achiba, Y.; Yamamoto, K.; Funasaka, H.; Takahashi, T. *Tetrahedron* **1996**, *52*, 4973-4982.

(32) Suzuki, T.; Maruyama, Y.; Kato, T.; Kikuchi, K.; Nakao, Y.; Achiba, Y.; Kobayashi, K.; Nagase, S. *Angew. Chem.-Int. Edit. Engl.* **1995**, *34*, 1094-1096.

(33) Skiebe, A.; Hirsch, A.; Klos, H.; Gotschy, B. *Chem. Phys. Lett.* **1994**, *220*, 138-140.

(34) Maeda, Y. In *Ph. D. thesis*; Niiigata University, 2001.

(35) Akiyama, K.; Sueki, K.; Kodama, T.; Kikuchi, K.; Ikemoto, I.; Katada, M.; Nakahara, H. *J. Phys. Chem. A* **2000**, *104*, 7224-7226.

(36) Jakes, P.; Dinse, K. P. *J. Am. Chem. Soc.* **2001**, *123*, 8854-8855.

List of Publications

"Separation and characterization of ESR-active Lanthanum Endohedral Fullerenes,"
Okubo, S.; Kato, T.; Inakuma, M.; Shinohara, H. *New Diam. Front. Carbon Technol.* 2001, *11*, 285-294.
"Efficient Reduction of Metallofullerenes by Solvation of Pyridine and Dimethylformamide,"
Submitted for publication..

Other publications

[Journals]

"Endohedrally metal-doped heterofullerenes": La@C81N and La- 2@C79N,"

Akasaka, T.; Okubo, S.; Wakahara, T.; Yamamoto, K.; Kobayashi, K.; Nagase, S.; Kato, T.; Kako, M.; Nakadaira, Y.; Kitayama, Y.; Matsuura, K. *Chem. Lett.* **1999**, 945-946.
"Isolation and characterization of two Pr@C-82 isomers,"
Akasaka, T.; Okubo, S.; Kondo, M.; Maeda, Y.; Wakahara, T.; Kato, T.; Suzuki, T.; Yamamoto, K.; Kobayashi, K.; Nagase, S. *Chem. Phys. Lett.* **2000**, *319*, 153-156.
"La@C-82 anion. An unusually stable metallofullerene,"
Akasaka, T.; Wakahara, T.; Nagase, S.; Kobayashi, K.; Waelchli, M.; Yamamoto, K.; Kondo, M.; Shirakura, S.; Okubo, S.; Maeda, Y.; Kato, T.; Kako, M.; Nakadaira, Y.; Nagahata, R.; Gao, X.; Van Caemelbecke, E.; Kadish, K. M. *J. Am. Chem. Soc.* **2000**, *122*, 9316-9317.
"Direct resolution of C-76 enantiomers by HPLC using an amylose- based chiral stationary phase,"
Yamamoto, C.; Hayashi, T.; Okamoto, Y.; Ohkubo, S.; Kato, T. *Chem. Commun.* **2001**, 925-926.
"Errata of "Direct resolution of C-76 enantiomers by HPLC using an amylose-based chiral stationary phase,"
Yamamoto, C.; Hayashi, T.; Okamoto, Y.; Ohkubo, S.; Kato, T. *Chem. Commun.* **2001**, 1896-1896.

[Proceedings]

"Endohedrally Metal-Doped Heterofullerenes,"

Akasaka, T.; Okubo, S.; Kobayashi, K.; Nagase, S.; Kato, T.; Yamamoto, K.; Funasaka, H.; Kako, M.; Nakadaira, Y. In *Recent Advances in the Chemistry and Physics of Fullerenes and Related Materials*; Kadish, K. M., Ruoff, R. S., Eds.; Electrochemical Society, Pennington, NJ, **1998**; pp 1003.

"Determination of the Cage Structure of La@C82,"

Kato, T.; Sato, K.; Takui, T.; Hurum, D.; Okubo, S.; Akasaka, T. In *Recent Advances in the Chemistry and Physics of Fullerenes and Related Materials*; Kadish, K. M., Ruoff, R. S., Eds.; Electrochemical Society, Pennington, NJ, **1998**; pp 967.

“Isolation and Characterization of a Pr@C82 isomer,”

Akasaka, T.; Okubo, S.; Wakahara, T.; Yamamoto, K.; Kato, T.; Suzuki, T.; Nagase, S.; Kobayashi, K. In *Recent Advances in the Chemistry and Physics of Fullerenes and Related Materials*; Kadish, K. M., Ruoff, R. S., Eds.; Electrochemical Society, Pennington, NJ, **1999**; pp 771.

“Spin Chemistry of Metallofullerenes,”

Kato, T.; Yamamoto, K.; Okubo, S.; Akasaka, T. In *Recent Advances in the Chemistry and Physics of Fullerenes and Related Materials*; Kadish, K. M., Ruoff, R. S., Eds.; Electrochemical Society, Pennington, NJ, **1999**; pp 756.

“Spin Dynamics of ESR-active Lanthanum Endohedral Fullerenes,”

Okubo, S.; Kato, T.; Inakuma, M.; Shinohara, H. In *Recent Advances in the Chemistry and Physics of Fullerenes and Related Materials*; Kadish, K. M., Ruoff, R. S., Eds.; Electrochemical Society, Pennington, NJ, **2000**; pp 291.

“Spin Dynamics of Lanthanum Metallofullerenes,”

Okubo, S.; Kato, T. In *The International Symposium on Nanonetwork Materials, Fullerenes, Nanotubes, and Realated Systems*; Saito, S., Ed.; AIP, **2001**; pp 469-472.

“Electronic State of Scandium Trimer Encapculated in C82 Cage,”
Kato, T.; Okubo, S.; Inakuma, M.; Shinohara, H. *Physics of the Solid State* **2002**, *44*, 410.

Acknowledgements

The author sincerely wishes to Prof. Tatsuhisa Kato of Institute for Moleccular Science (IMS) for his valuable guidance, helpful suggestions, firm encouragement and large patience through out this work.

The author is very grateful to Dr. Naoki Hayashi, Dr. Kou Furukawa, Dr. Namiki Toyama, Dr. Katsuichi Kanemoto, and Prof. Kraus-Peter Dinse of Kato group for their useful discussions.

The author gratefully acknowledges to Masahiro Sakai, Seiji Makita, Dr. Hajime Ito, Masaaki Nagata of IMS for the assistance of ESR measurement, LD-TOF measurement, and preparation of grass apparatus.

The author gratefully Prof. Takeshi Akasaka and Takatsugu Wakahara of Tsukuba University for his valuable guidance, helpful suggestion, and firm encouragement

The author wishes to thank to Mikiko Ara, Takuya Kondo, Dr. Yasuyuki Niino, Dr. Yutaka, Maeda, Minoru, Itoh, Shingo Shirakura, Ryu Sato, Aminur Rahman, Masahiro Kondo, Takahiro Sato, Satomi Takahashi and the member of Prof. Akasaka's research group for the usefull discussions and warm encouragement.

The author gratefully acknowledges to Dr. Kazunori Yamamoto of Power Reactor and Nuclear Fuel Development Corporation for valuable discussions and important suggestions in HPLC separation of metallofullerenes.

The author gratefully acknowledges to Prof. Hisanori Shinohara, Masayasu Inakuma, Haruhito Kato, and Yasuhiro Ito of Nagoya University for valuable discussions and collaboration in production and extraction of metallofullerenes.

The author gratefully acknowledges to Prof. Yoshio Okamoto, Dr. Chiyo Yamamoto, and Tomoko Hayashi of Nagoya University for the collaboration in the separation of the enantiomer of C_{76}.

The author is grateful to Prof. Toshiyasu Suzuki of IMS for valuable discussions.

The author gratefully acknowledges to Prof. Shigeru Nagase and Dr. Kaoru Kobayashi of IMS for valuable discussion.

The author is very grateful to Prof. Noboru Hirota of Kyoto University for discussion and important suggestions.

The author gratefully acknowledges to Prof. Tomoaki Sasaki and Katumitsu Nakamura of Nihon University for their valuable guidance and firm encouragement. Thanks are also due to Tohru Uzaki, Mitsuro Matsuda, Masahiro Mouri, Yasuaki Suhara, Yasuyuki Kondo, Atsushi Shinozaki, Yasuhiro Ozawa, Takayuki Ohno, Mitsutaka Nakamura, Masayuki Hiruma, Daiji Munakata of Prof Sasaki's research group.

Finally, the author gratefully acknowledges to his parents, Mutsuo Okubo and Kimiko Okubo, for encouragement and financial support.

September, 2002. Shingo Okubo